

An Effective Sphaleron Awakens

Xu-Xiang Li^{a†}, Michael J. Ramsey-Musolf^{b,c,d,e*},
Tuomas V. I. Tenkanen^{b,c,f,g†}, and Yanda Wu^{b,c§}

^a*Department of Physics and Astronomy, University of Utah,
Salt Lake City, Utah 84112, USA*

^b*Tsung-Dao Lee Institute,
Shanghai Jiao Tong University, Shanghai 201210, China*

^c*Shanghai Key Laboratory for Particle Physics and Cosmology, Key Laboratory for Particle
Astrophysics & Cosmology (MOE), Shanghai Jiao Tong University, Shanghai 200240, China*

^d*Amherst Center for Fundamental Interactions, Department of Physics,
University of Massachusetts, Amherst, MA 01003, USA*

^e*Kellogg Radiation Laboratory, California Institute of Technology,
Pasadena, CA 91125, USA*

^f*Nordita, KTH Royal Institute of Technology and Stockholm University,
Hannes Alfvéns väg 12, SE-106 91 Stockholm, Sweden*

^g*Department of Physics and Helsinki Institute of Physics, PL 64, FI-00014 University of
Helsinki, Finland*

Abstract

Using thermal effective field theory, we present a self-consistent perturbative formulation of the Higgs phase sphaleron rate after a radiatively-induced first-order phase transition. This gauge-invariant formulation is based on dimensionally reduced effective field theory (3D EFT) at high temperatures and paves a way for including higher order corrections within the 3D EFT perturbation theory without double counting. Concretely, we compute the Higgs phase sphaleron rate in a semi-classical approximation within the two-loop resummed 3D EFT. We find compact results for the sphaleron rate and the baryon washout factor as well as criteria for the baryon number preservation by providing a clear connection to the results obtained using a similar 3D EFT description for the bubble nucleation. We demonstrate these calculations for the real triplet-extended Standard Model, and conclude that when all two-loop thermal effects for the matching are accounted, no sufficiently strong one-step electroweak phase transitions exist within the parameter space regime that can be mapped onto the 3D EFT we have considered.

Contents

1	Introduction	2
2	Electroweak Baryogenesis and Sphaleron	5
2.1	Qualitative Overview and Effective Descriptions	5
2.2	Effective Descriptions for Sphaleron Rate: A Brief Review	9
2.2.1	Early Computations of Sphaleron Rate	9
2.2.2	Effective Field Theory for Static Modes	10
2.2.3	Real Time Dynamics and Non-Perturbative Simulations	10
2.3	Towards a Self-Consistent Perturbative Formulation	11
3	Sphaleron Rate under Static 3D EFT Formulation	13
3.1	Higgs Phase Sphaleron Rate	13
3.2	Dimensional Reduction and 3D EFT	14
3.3	Power Counting within the EFT Perturbation Theory	19
3.4	Sphaleron Action and Scaling Properties	21
3.4.1	Second-Order Phase Transitions	24
3.4.2	First-Order phase transitions	25
3.5	Sphaleron Rate after Standard Model Crossover	27
3.6	Sphaleron Rate after First-Order Electroweak Phase Transition	30
4	Baryon Number in First-Order Electroweak Phase Transition	32
4.1	Sphaleron Decoupling Temperature	32
4.2	Baryon Number Preservation Criteria	35
5	Application to Real Triplet-Extended Standard Model	39
6	Conclusions and Perspectives	45
6.1	Summary	45
6.2	Discussion and Outlook	46
A	Properties of Sphaleron Ansatz, Action, and Equations of Motion	50
B	On Sphaleron Fluctuation Determinant	52
C	Temporal Gluon Effect to Sphaleron Rate via Dimensional Reduction	55

*mjrm@sjtu.edu.cn, mjrm@physics.umass.edu

†tuomas.tenkanen@helsinki.fi

‡xuxiang.li@utah.edu

§yanda.wu7@sjtu.edu.cn

1. Introduction

To this date, the origin of the observed matter-antimatter asymmetry of the universe still remains a mystery. The Standard Model (SM) of particle physics is unable to explain the small but non-vanishing ratio of net baryon over anti-baryon to photon number density¹

$$\eta \equiv \frac{n_B - n_{\bar{B}}}{n_\gamma} = (6.10 \pm 0.40) \times 10^{-10}, \quad (1.1)$$

observed from the Cosmic Microwave Background by the Planck satellite [1] and the Big Bang Nucleosynthesis measurements [2]. Among the most widely studied mechanisms to explain the observed value for η is the electroweak baryogenesis (EWBG) [3] in which the baryon asymmetry is generated dynamically during a first-order electroweak phase transition (EWPT). The EWBG is often considered attractive, as it links the baryon asymmetry to the Higgs mechanism and the origin of elementary particle masses, and is experimentally testable in particle colliders [4]. For reviews on the EWBG, see e.g. [5–8], and for its alternative competitors, such as leptogenesis e.g. [9] and references therein.

A successful mechanism to explain the observed value for η requires three general ingredients identified by Sakharov [10]: (i) a baryon number violating process, (ii) charge (C) and charge-parity (CP) violating processes and (iii) departure from thermal equilibrium. The condition (i) is obvious for generating a net baryon number from zero; the condition (ii) guarantees difference between the production rates of fermions and anti-fermions; the condition (iii) is necessary because the thermal average of the baryon number always vanishes in thermal equilibrium, enforced by the CPT symmetry.

The condition (i) can be realized in the Standard Model (SM) due to the chiral nature of weak interactions, via the electroweak *sphaleron* [11, 12]. In the semi-classical picture the electroweak sphaleron is an unstable topological field configuration of the SU(2) gauge-Higgs theory, which has half-integer Chern-Simons number separating topologically different vacua of the SU(2) Yang-Mills theory. A dynamic transition between vacua across a sphaleron, i.e. sphaleron transition, can induce an integer variation in the Chern-Simons number, leading to a variation of baryon (B) and lepton (L) numbers (while preserving $B-L$) through the Adler-Bell-Jackiw anomaly [13, 14]. The rate of these transitions is referred to as the sphaleron rate, or more generally in non-abelian gauge theories, as the Chern-Simons diffusion rate of topological charge density [15].

Conditions (ii) and (iii), on the otherhand, fall short: the SM does not have a first-order phase transition (in which the plasma surrounding expanding bubble walls would be driven out of equilibrium) but rather a smooth crossover [16, 17]. In addition, the CP-violating processes in the SM (observed in neutral kaon oscillations, and recently, in baryon decays

¹Or alternatively, the baryon-to-entropy ratio $Y_B \equiv n_B/s = (8.70 \pm 0.04) \times 10^{-11}$ [1, 2].

[18]), associated with the complex phases of the Cabibbo-Kobayashi-Maskawa matrix, are too heavily suppressed at high temperatures [19–24].

Therefore, realizing the EWBG mechanism requires ingredients of physics beyond the Standard Model (BSM) that can make the conditions (ii) and (iii) viable. In principle, additional scalar fields in the Higgs sector could accomplish both: catalyze a first-order electroweak phase transition and introduce enhanced C- and CP-violating processes,² see e.g. [29–31]. In the present article, we do not discuss new sources for C- and CP-violation, but focus on the conditions (i) and (iii), which provide *necessary*, yet not sufficient, conditions for the baryogenesis.

To accommodate a first-order electroweak phase transition, new BSM physics is required to be light enough and cannot interact with the SM Higgs boson too feebly [4]. These features make such models testable at the High-Luminosity run in the LHC [32] and in next-generation collider experiments, such as ILC [33], CLIC [34], FCC [35] and CEPC [36]. This relatively short-term testability of the EWBG makes it an appealing candidate for the baryogenesis, and is under active studies, see e.g. [37–52] and [53–64] for sphaleron-focusing studies. Furthermore, the existence of a first-order electroweak phase transition can also be probed by next-generation gravitational wave observatories, such as LISA [65, 66] and other similar experiments [67–69], also c.f. [70–77].

A modern approach to thermal first-order phase transitions and the bubble nucleation in perturbation theory in terms of thermal effective field theory (3D EFT) [78, 79] have been formulated in [80–85]. In this approach, a perturbative expansion is consistently organized based on strict power counting which accounts for relevant mass hierarchies. For perturbative analysis of a first-order electroweak phase transition, the key element for a consistent perturbative expansion is that the leading order effective potential includes a barrier in-between its minima, generated by the gauge fields [86]. In this article, we make a perturbative computation of the sphaleron rate in the Higgs phase compatible with this idea.

The key aspects of our present analysis and findings include:

- We investigate a minimal 3D EFT for the electroweak phase transition consisting of SU(2) gauge and Higgs fields, which serves as a universal 3D EFT for a broad class of Higgs-portal BSM theories where the new scalars are sufficiently heavy to be integrated out at high temperatures. It captures large two-loop thermal corrections (akin to [87]) and allows one to implement a non-perturbative criterion for first-order phase transitions [88]. Moreover, key features of bubble nucleation can be computed with comparable rigor [83].

²We emphasize that the electron electric-dipole moment (EDM) precision measurements [25] severely constrain the possibility of the generation of C- and CP-violations from BSM sectors [26]. Mechanisms for spontaneous violation occurring via dark sectors only at high temperatures, hence avoiding the EDM constraints, have been explored in [27, 28].

- Using the semi-classical approximation for the Higgs phase sphaleron rate, we demonstrate that the leading order effective action of the sphaleron can be obtained by retaining only the Yang-Mills term and the kinetic term of the Higgs field. The scalar potential enters solely the boundary condition, for which it is crucial to use the leading order effective potential where the potential barrier is generated by the gauge field [82]. We argue that since the energy scale of the sphaleron is higher than that of the critical bubble [80, 81, 83], perturbative expansion for the sphaleron rate converges relatively faster compared to the bubble nucleation rate.
- After rescaling the sphaleron effective action, we find compact and gauge invariant results for the sphaleron rate as well as the washout factor, ultimately solving all concerns raised in [89]. In addition, we argue that our setup provides conceptual clarity for a consistent perturbative expansion when compared to the approach in [87].
- Combining our results for the sphaleron rate and the washout factor with consistent perturbative calculation of the bubble nucleation rate, we provide a unified, consistent description (Fig. 7) for the baryon number preservation criteria (BNPC) [88–90] that incorporates EWPT thermodynamics, the bubble nucleation rate, and the sphaleron rate. In doing so, we provide a framework that allows one to track the sphaleron dynamics from the onset of nucleation to the completion of the transition. Self-consistency is ensured through adoption of the power counting in couplings given in Refs. [81, 82, 91] and renormalization group improvement as outlined in Ref. [92]. With this framework in hand, we obtain a range of requirements – “strong” to “weak” – for preservation of any baryon asymmetry produced at the onset of nucleation.

This analysis is encapsulated in Fig. 7 and related discussion, which considers two relevant dimensionless parameters x and y constructed from the Higgs thermal self-interaction coupling, λ_3 ; the effective gauge coupling, g_3^2 ; and thermal mass-squared parameter, μ_3^2 . In this context, a strong version of this condition is given by³

$$x(T_c) \lesssim 0.025 \quad (\text{BNPC}) \quad \text{with} \quad x(T) \equiv \frac{\lambda_3(T)}{g_3^2(T)}, \quad (1.2)$$

which guarantees to prevent the wash-out entirely. In addition, we obtain a weaker version of the BNPC as $0.025 \lesssim x(T_c) \lesssim 0.036$ for potential survival from exponential wash-out (for details, see Eq. (4.20)). These conditions are universal for all theories that can be mapped onto the 3D EFT considered. Hence, our result generalizes some discussions in [90] by combining the result of the sphaleron rate with modern treatment for the bubble nucleation (at leading order in 3D EFT perturbation theory).

³We stress, that this upper bound on $x(T_c)$ is obtained in the semi-classical approximation, and is subject to higher order corrections.

- We apply our analysis to one-step phase transitions in the real-triplet-extended Standard Model, focusing on a parameter regime where the triplet is heavy at high temperatures and can be integrated out. While one-loop calculation suggests the existence of strong first-order transitions sufficient to evade sphaleron washout, we find that sizable two-loop thermal corrections significantly alter the picture. In fact, all identified first-order transitions become very weak at two-loop order. This underscores the critical role of two-loop thermal effects in Higgs-portal models and aligns with [93].

In short, we are making sure that a first-order phase transition exists in accord with previous, universal non-perturbative lattice simulation results we can utilize – as well as provide comparison to non-perturbative determination of the sphaleron rate, when possible – and then determine the Higgs phase sphaleron rate perturbatively. Concretely, in our computations in this article at hand, we formulate a consistent perturbative expansion that resolves issues of the gauge dependence and the slow convergence, that have plagued the previous literature (see Sec. 6.2 for further discussion).

The remainder of this article is organized as follows. In Sec. 2 we provide a qualitative overview of the role of the sphaleron in the EWBG and a brief review of the developments in understanding the electroweak sphaleron rate. In Sec. 3 we compute the sphaleron rate in the Higgs phase, using $SU(2) + \text{Higgs}$ 3D EFT, and compare our perturbative computation with lattice results from the literature for temperatures below the SM crossover. In Sec. 4 we find a perturbative, gauge-invariant formulation for the washout factor and baryon number preservation. In Sec. 5 we present an application to the real-triplet extended Standard Model that admits first-order phase transitions that can be described using the 3D EFT of previous sections. In Sec. 6 we summarize, provide further discussions and outlook future directions, while several technical details of our computations are relegated to appendices.

2. Electroweak Baryogenesis and Sphaleron

We start with a qualitative tour to the EWBG and the sphaleron rate, before presenting our computations and quantitative discussions in sections that follow.

2.1. Qualitative Overview and Effective Descriptions

Should underlying BSM physics help to catalyze a first-order electroweak phase transition, generation of baryon asymmetry could be realized in the following processes [7] (illustrated in Fig. 1),⁴ for which we highlight the effective descriptions for the bubble nucleation and the sphaleron rates in terms of semi-classical pictures.

⁴See also [94] for an alternative mechanism.

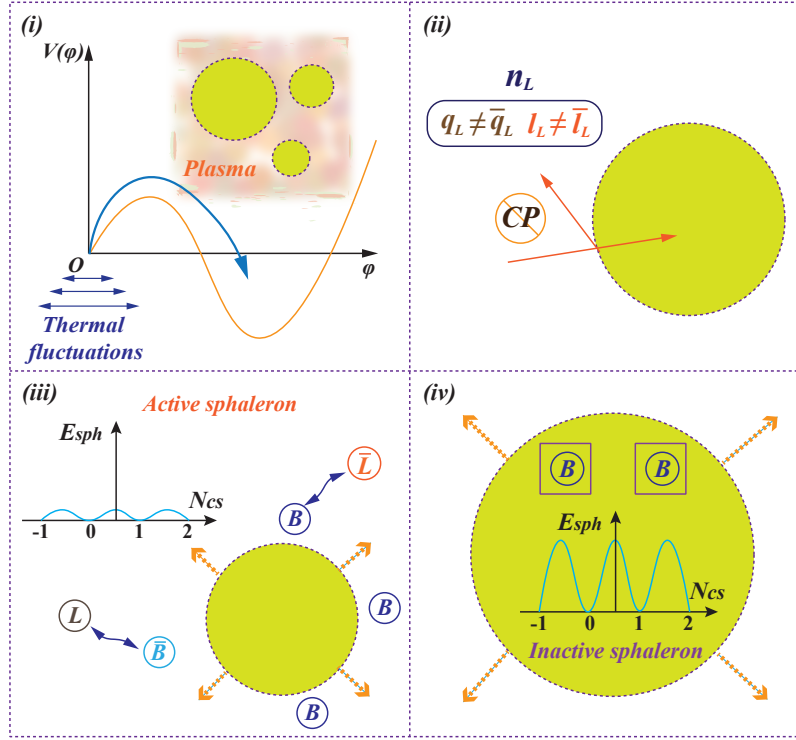


Figure 1: A schematic illustration of four stages of the electroweak baryogenesis: (i) In a first-order phase transition the thermal fluctuations drive the system from a false to a true vacuum and transitions occurs via the bubble nucleation; (ii) The generation of a non-zero left-handed fermion number density from the C- and CP-violating scattering between particles and the expanding bubble wall; (iii) In the confinement phase outside the bubbles, the non-zero left-handed fermion number density would bias the rapid sphaleron process to generate more baryons than anti-baryons; such baryon excess is then devoured by the expanding bubble. (iv) As the sphaleron energy increases inside the bubble, the baryon number violating process is suppressed. Nevertheless, the produced net baryon number may be preserved, partly washed out, or completely erased, depending on the value of the washout exponent factor (See Eq. (2.5)).

- (i) In a thermal phase transition in the expanding universe, at temperatures (T) below the critical temperature, thermal fluctuations drive the system over the potential energy barrier separating the high temperature “symmetric” phase and the low temperature “broken” electroweak Higgs phase.⁵ A phase transition occurs through nucleation of

⁵We note that these phases are analytically connected to each other [95], as it is not possible to spontaneously break local, gauge symmetry [96]. Instead of using the term “symmetric” phase, we stick to a more suitable terminology, e.g. the confinement phase. See also [97, 98].

bubbles, which eventually expand over macroscopic length scales and are subject to relativistic hydrodynamics. In microscopic scales, expanding bubbles disrupt the surrounding hot particle plasma out of equilibrium due to the released latent heat. The plasma can also be driven out of equilibrium by interactions of plasma particles with the bubble walls, turbulence and shock waves.

In an effective description for the bubble nucleation [80], short-distance thermal fluctuations screen long-distance, highly occupied bosonic modes, hence modifying their interactions in a thermal medium, i.e. the hot plasma. Due to the high occupation these modes are effectively classical, yet subject to quantum corrections: this brings in a semi-classical approximation, in which the scalar field configuration undergoing the transition, or the critical bubble, is described by a classical *bounce* solution φ_b .

In thermal equilibrium, the rate of the bubble nucleation is then described by a Boltzmann factor $e^{-S_{\text{eff}}(\varphi_b)}$ with effective action evaluated on the bounce, and quantum corrections are described through the fluctuation determinant. On the otherhand, the effective description for a dynamic, out-of-equilibrium contribution to the nucleation rate (related to damping and dissipation when the system crosses the energy barrier) is significantly more complicated. Once the bubble nucleation rate is rapid enough compared to the expansion rate of the universe, the entire system undergoes a phase transition.

- (ii) The C- and CP-violating scattering processes between the plasma particles and the expanding bubble wall lead to different diffusion rates among particles and their antiparticles and therefore a non-zero left-handed fermion number density in front of the bubble wall. An opposite asymmetry in the number density of right-handed particles n_R is also generated by the CP violation, but it is irrelevant to the baryogenesis since the sphaleron process happens only between $SU(2)_L$ vacua. The time scale for the process of n_L creation is typically much shorter than the electroweak sphaleron transitions, so the sphaleron bias process in step (iii) is decoupled from (ii). For studies of CP-violating transport properties of the plasma see e.g. [47, 99–110] and references therein.
- (iii) Outside the bubble, the rapid sphaleron process can induce a violation of baryon plus lepton number, $B + L$, while keeping $B - L$ unchanged. The non-zero number of left-handed fermions created in (ii) would bias sphaleron towards creating more baryons than anti-baryons in front of the bubble. Such baryon excess is then devoured by the expanding bubble.

For each fermion generation, the divergence of the left-handed baryonic and leptonic currents is proportional to the Yang-Mills field strength F (here and below we omit the

group indices for simplicity) and its dual [13, 14, 111]:

$$\partial_\mu j_B^\mu = \partial_\mu j_L^\mu \propto F \cdot \tilde{F}. \quad (2.1)$$

The temporal variation of the Chern-Simons number is then proportional to [112]

$$\Delta N_{\text{CS}}(t) = N_{\text{CS}}(t) - N_{\text{CS}}(t=0) \propto \int_{\Omega} F \cdot \tilde{F}, \quad (2.2)$$

where the integral is performed over both space and time. The integer variation of the Chern-Simons number will pass over the sphaleron field configuration which has a characteristic half-integer Chern-Simons number (c.f. [12, 58]). This implies that the Chern-Simons diffusion rate, $\Gamma_{\text{diff}} = \frac{\langle \Delta N_{\text{CS}}^2 \rangle_T}{Vt}$ (in the large volume and time limit) or twice the sphaleron rate, $\Gamma_{\text{diff}} = 2\Gamma_{\text{sph}}$ (c.f. [87, 113]) controls the rate of change for the baryon number density [89, 114, 115]

$$\frac{\partial}{\partial t} n_B \propto -\frac{\Gamma_{\text{sph}}}{T^3} n_B, \quad (2.3)$$

which we discuss in more detail in Sec. 4. We note that in the confinement phase, the sphaleron rate Γ_{sph} is unsuppressed, and a sophisticated combination of analytic effective descriptions and numerical simulations have found [112, 116]

$$\Gamma_{\text{sph}} \propto \alpha_w^5 T^4, \quad (2.4)$$

where $\alpha_w = g^2/4\pi$, in terms of the SU(2) gauge coupling g . We stress that the thermal Yang-Mills theory is strongly coupled and confining, and its dynamics – dictated by the so-called “magnetic” mass scale – are inherently non-perturbative [117–120].

- (iv) Inside the bubble, due to the activation of the Higgs mechanism, length scale of gauge boson fluctuations becomes smaller compared to the confinement phase (i.e. the Higgs mechanism introduces a new, larger mass scale compared to the magnetic mass), and this situation is reflected in the sphaleron dynamics. The energy of the sphaleron increases, and this suppresses the Chern-Simons number diffusion.

Three scenarios may occur:

- (I) Immediately after the bubble nucleation, the baryon number violation rate (see Eq. (4.3)) inside the bubble falls below the Hubble rate, and no washout takes place (strong BNPC).
- (II) The baryon number violation rate remains above the Hubble rate for a finite interval after the nucleation temperature, T_n , erasing part of the generated baryon asymmetry (weak BNPC):

$$n_B(T_*) = e^{-\mathcal{W}} n_B(T_n), \quad (2.5)$$

where $T_* < T_n$ is the decoupling temperature at which the baryon number violation rate and Hubble rate coincide, and \mathcal{W} is the washout exponent (see Eq. (4.11)). In this case, C- and CP-violating interactions must overproduce baryon asymmetry, to offset the washout.

- (III) The washout exponent \mathcal{W} is so large that essentially all of the generated baryon asymmetry is erased.

With respect to the thermal medium (with short-distance thermal fluctuations), the sphaleron length scale is still large, and this implies, that the sphaleron in the Higgs phase admits a semi-classical approximation akin to the critical bubble. Yet we stress, that the energy scale of the sphaleron in the Higgs phase is much larger than that of the critical bubble, and consequently these two effective descriptions turn out to have important differences.

In a semi-classical picture, the sphaleron is a classical, spatially varying scalar φ_{sph} and gauge field \mathbf{A}_{sph} configuration that can be found by extremizing the effective action. The sphaleron rate in thermal equilibrium can be computed from the Boltzmann factor

$$\Gamma_{\text{sph}} \propto e^{-S_{\text{eff}}(\varphi_{\text{sph}}, \mathbf{A}_{\text{sph}})}, \quad (2.6)$$

and quantum effects result in corrections through a fluctuation determinant. Again, out-of-equilibrium contributions to the rate are more complicated.

2.2. Effective Descriptions for Sphaleron Rate: A Brief Review

To set the stage for our own computations, we start with a brief review of the chronology of computations of the sphaleron rate focusing on the 3D EFT and the effective hard thermal loop (HTL) approaches.

2.2.1. Early Computations of Sphaleron Rate

The existence of the semi-classical sphaleron configuration within the Standard Model was first realized in [11, 12] and later extended by [121, 122]. The physics of the sphaleron in the EWBG was first studied in [3]. It was shown that the sphaleron transitions between different vacua can occur at high temperatures due to thermal fluctuations which leads to far less suppressed rate compared to mere zero temperature tunneling [111, 123]. In such thermal escape at temperature T , the sphaleron rate is classically described by a Boltzmann factor $\exp(-E_{\text{sph}}/T)$ where E_{sph} is the energy of a static sphaleron solution.

Higher order quantum corrections to this statistical (time-independent) exponential part are described by a prefactor – the fluctuation determinant – which were first discussed in [124, 125] and further approximated and fully computed in [126–130]. Notably, in these early-day computations high-temperature expansions were applied at leading order.

2.2.2. Effective Field Theory for Static Modes

To describe higher order thermal corrections to the EWPT thermodynamics one has account for the Debye screening that modifies interactions in a thermal medium. This can be achieved by resumming a class of low energy or large distance contributions that are enhanced at high temperatures [131, 132]. The most efficient way to incorporate effects of such thermal screening is by means of the effective field theory (EFT) approach [78, 79], which utilizes the technique of high-temperature dimensional reduction [133, 134] (see also [135, 136]).

The essence of dimensional reduction is the scale hierarchy at high temperatures: in the imaginary time formalism, which is used to compute static, equilibrium thermodynamics, all fields are composed as series of three-dimensional (3D), purely spatial Matsubara modes [137]. Characteristic mass scales for the non-static modes, i.e. the modes with non-zero Matsubara frequency, are dictated by high temperature and thereby heavier compared to modes with zero Matsubara frequency.

These light 3D zero Matsubara modes are responsible for large distance, *infrared* properties of the phase transition, including static properties of the critical bubble and the sphaleron (both of which in addition have real time dynamics). The ultraviolet (UV) scale of the heavy, non-zero Matsubara modes effectively screens the IR modes, and this can be captured by integrating out the UV scale [138]. This leads to a (resummed) 3D EFT. For previous perturbative studies of the sphaleron rate within 3D EFTs, see [87, 139].

Resulting 3D EFT can be studied at few first orders in perturbation theory [85, 140], but eventually perturbation theory breaks down for the modes deep at IR [117], since the electroweak theory is confining and strongly coupled at high temperatures [118, 141]. To comprehensively study the IR physics, one has to resort to non-perturbative techniques, for example the lattice Monte Carlo simulation of the 3D EFT [88, 142–144]. Ultimately, it was the use of 3D EFT lattice simulations that lead to a realization that there is no first-order electroweak phase transition but a smooth crossover in the Standard Model [16, 145] (see also [17]).

2.2.3. Real Time Dynamics and Non-Perturbative Simulations

In the high temperature confinement phase, the sphaleron rate is purely non-perturbative and one needs to resort to numerical methods. At early days, plenty attempts were made to determine dynamical sphaleron transitions by solving time evolution of fields using equations of motion, within the 3D EFT at classical level [146–154]. Indeed, at high temperatures bosonic excitations at IR (low momenta) are highly occupied, and can be described as classical fields, opposed to high momenta UV modes, which exhibit particle-like behaviour. These attempts were, however, troubled by the fact that in such analyses the gauge field dynamics are UV divergent due to Landau damping and results are cut-off dependent [155, 156], and

as such identifying the physical continuum limit of the classical theory requires care [15].

Some amelioration to such problems were provided by adding hard thermal loop effects [157–159]⁶ to otherwise classical theory, resulting in expensive simulations [116, 162]. Shortly after, however, it was realized that these HTL and damping effects can be captured in an effective approach based on Langevin dynamics for the real-time evolution [163]: bosonic modes with energy much less than the temperature $E \ll T$ are highly occupied, with Bose-Einstein distribution $n_b(E) \approx T/E \gg 1$, and their dynamics are, to first approximation, classical. Thermal loop corrections to the classical picture result from high energy modes with $E \sim T$, but when these are integrated out, one is left with effective parameters, damping and noise, described by the Langevin dynamics.⁷

In essence, the HTL effective theory [163] is the real-time analogue of the dimensionally reduced 3D EFT for static quantities. This formulation resulted in a lot of progress [165–169] and eventually non-perturbative simulations [90, 112, 113, 170] based on a combination of multicanonical and real time lattice techniques (similar non-perturbative simulations for the bubble nucleation rate were developed slightly after in [86, 171]).

In these lattice simulations, the sphaleron rate, or Chern-Simons number diffusion rate, is determined by defining a surface in-between topologically distinct vacua (a “separatrix” that sphaleron transitions will cross when changing the Chern-Simons number), and by computing a probability flux across this surface, multiplied by a dynamical prefactor describing what fraction of crossings lead to settling to a new vacuum (with HTL effects included in the dynamical prefactor). For details, see [90] and more recent lattice simulations [172–174].⁸

2.3. Towards a Self-Consistent Perturbative Formulation

In [90] it was concluded that the effect of the “dynamical prefactor” to the Higgs phase sphaleron rate, which depends on HTL effects, is not large. This suggests that one can compute the statistical, time-independent part of the sphaleron rate in the 3D EFT perturbation theory, and as the first approximation entirely neglect the most complicated, dynamical prefactor. Such computation was performed in [87], using a two-loop effective potential within the 3D EFT, and later compared against results of lattice simulations in [173, 174], showing remarkable agreement at temperatures below the SM crossover (c.f. Fig. 5). We emphasize here that both of these approaches rely on the exactly same 3D EFT construction by two-loop dimensional reduction [78].

This indicates that purely non-perturbative effects on the statistical part of the sphaleron rate are rather minor, and consequently prospects for purely perturbative calculations based on the use of 3D EFT are promising. However, despite its apparent success, the approach of

⁶See also [160, 161] and references therein, for recent developments on the higher order HTL corrections.

⁷For a compact, yet illuminating summary, see also Sec. 2 of [164].

⁸Other past numerical studies include [15, 175–177].

[87] includes approximations that could be improved. First, the setup of [87] is not based on a clear perturbative expansion, and as such is prone to double count loop corrections to the Boltzmann factor that are included via the effective potential as well as to the fluctuation determinant (statistical prefactor).⁹ To avoid this double counting, Ref. [87] sets the positive mode contributions of the determinant (factor κ therein) to unity by hand and argues that the use of the two-loop effective potential in the Boltzmann factor already (approximately) includes such contributions. We argue, that such manipulation by hand lacks a rigorous justification, and could be entirely avoided in a properly formulated perturbative expansion. Furthermore, use of the two-loop effective potential (which is computed around a spatially constant scalar background) cannot account for contributions of spatially varying scalar and gauge fields around the sphaleron background. Second, calculations (for the effective potential) in [87] are performed simply in Landau gauge, and the lack of well-defined perturbative expansion results in a gauge-dependent outcome.

Hence, in this work we implement a well-defined perturbative expansion for the statistical part of the sphaleron rate that maintains gauge-invariance. This was attempted previously in [89], for both the effective potential and equilibrium properties such as the critical temperature derived from it and the sphaleron energy (for the Boltzmann factor). Yet, a comprehensive framework for a consistent perturbative expansion incorporating the full set of higher-order thermal corrections remained to be addressed. See also similar discussions in [7, 180–182]. Nevertheless, multiple works [4, 183–189] that followed have focused on using the methodology of [89], and other works [28, 43, 190–198] have simply truncated their perturbative expansions to not include thermal resummations altogether.

Consistent perturbative expansions for the equilibrium properties of phase transitions, that reconcile the gauge-invariance and thermal resummations were found in [82, 85, 138, 179, 199] using the 3D EFT perturbation theory (see also [200] that does not include gauge fields, [201] that does not utilize the 3D EFT, and discussions in [84]). These approaches have shown great agreement with non-perturbative lattice simulations in the cases where comparisons have been possible [82, 83, 85, 140, 200, 202]. Similar consistent expansions for computing the thermal bubble nucleation rate – which is analogous to the calculation of the sphaleron rate – have been developed using the 3D EFT in [80, 81, 86, 171] building upon [203–207], with discussions on higher order corrections [208–212] (including dynamical part in [210, 213]) supported by fresh lattice simulations [83, 214, 215].

Thereby, resolutions to concerns raised in [89] have been found in 3D EFT perturbation theory, apart from a similar, consistent perturbative expansion for the sphaleron rate and for quantities derived from it, and that is what we will deliver in following sections.

⁹This is analogous to a danger of double counting similar contributions in the context of vacuum tunneling [178], as well as thermal bubble nucleation [80, 179].

3. Sphaleron Rate under Static 3D EFT Formulation

In this section, we get into technical details of our formulation. Our goal is to compute the Higgs phase sphaleron rate, i.e. the sphaleron rate inside the bubble, which is essential in determining the baryon-number-wash-out factor required for the baryon erasure bound.

3.1. Higgs Phase Sphaleron Rate

In analogy to the bubble nucleation rate in [210], we decompose the sphaleron rate as

$$\Gamma_{\text{sph}} = A_{\text{dyn}} \times A_{\text{static}} , \quad (3.1)$$

which is factorized into a non-equilibrium, dynamic part A_{dyn} and an equilibrium, time-independent statistical part A_{static} .

The calculation of the dynamical part A_{dyn} requires a real time – out of equilibrium – formalism [163, 168], where hard thermal loops are integrated out in order to obtain an effective description based on Langevin dynamics.¹⁰ The formalism captures non-equilibrium dynamics, such as Landau damping effects, which cannot be described solely within the 3D EFT for the equilibrium quantities. Incorporating such effects goes beyond the scope of our computation in this article. In the following calculations, we just estimate the dynamical part as $A_{\text{dyn}} \sim T$ by the dimensional analysis.

The statistical part, on the other hand, can be computed solely within the 3D EFT. In the semi-classical picture, the statistical part is calculated perturbatively in saddle point approximation as [126–130]

$$A_{\text{static}} \simeq [\text{det}]_{\text{sph}} e^{-S_{3\text{D}}(\phi_{3,\text{sph}}, \mathbf{A}_{3,\text{sph}})} , \quad (3.2)$$

where the leading-order contribution is described by the exponential Boltzmann factor, the prefactor – a one-loop fluctuation determinant $[\text{det}]_{\text{sph}}$ – denotes the next-to-leading order corrections within the 3D EFT perturbation theory and higher loop corrections are not written down explicitly. The 3D EFT action $S_{3\text{D}}$ in the Boltzmann factor is evaluated at the classical sphaleron solution of the equations of motion of the Higgs and gauge fields $\phi_{3,\text{sph}}$, $\mathbf{A}_{3,\text{sph}}$ within the 3D EFT. We emphasize that here higher order corrections (corresponding to long-distance fluctuations compared to short-distance fluctuations at length scales $\sim (\pi T)^{-1}$ related to the thermal scale) in the determinant (and beyond) refer to corrections computed in the 3D EFT perturbation theory [132], while the 3D EFT construction itself includes corrections up to next-to-leading order (two loops) from short distance fluctuations, captured in the effective parameters of the (resummed) 3D EFT [79]. This delineation will be detailed in the next section.

¹⁰ A_{dyn} is often misinterpreted as ω_- , i.e. a negative, unstable mode of the fluctuation determinant [122, 127], see discussion in [124, 210].

The fluctuation determinant $[\text{det}]_{\text{sph}}$, however, is an involved calculation. At the present stage, our aim is to compute the leading behaviour of the sphaleron rate within the 3D EFT, i.e. the Boltzmann factor in terms of the sphaleron energy. Hence, we do not compute the fluctuation determinant (or even higher-loop corrections beyond it) here but leave them to future work as well.¹¹

To organize our perturbative calculations, we employ a formal power counting parameter g , such that

$$-\ln \frac{\Gamma_{\text{sph}}}{T^4} \simeq \underbrace{S_{\text{3D}}}_{\sim g^{-1}} - \underbrace{\ln \frac{[\text{det}]_{\text{sph}}}{T^3}}_{\sim \pi^{-1}} - \ln \frac{A_{\text{dyn}}}{T}, \quad (3.3)$$

where the contribution of the fluctuation determinant is suppressed compared to the leading order by g/π , which corresponds to the magnitude of an expansion parameter within the 3D EFT. We demonstrate below in detail how to arrive to the power counting in Eq. (3.3). In the following we will compute the sphaleron 3D EFT action exactly meanwhile merely estimate the fluctuation determinant and simply omit the dynamical prefactor.

3.2. Dimensional Reduction and 3D EFT

Starting from a BSM theory with an extended scalar sector, defined by a Lagrangian

$$\mathcal{L}_{\text{BSM}}(A_\mu^a, B_\mu, C_\mu^\alpha, \Psi, \phi, S), \quad (3.4)$$

where A_μ^a , B_μ and C_μ^α are the SU(2), U(1) and SU(3) gauge fields, respectively, Ψ collectively denotes the all SM fermions, ϕ is the Higgs doublet and S describes a new scalar field, one can construct a dimensionally reduced effective field theory at high temperature [220], in terms of a corresponding bosonic 3D Lagrangian $\mathcal{L}_{\text{3D}}(A_{i,3}^a, \phi_3, S_3)$ that respects the same symmetries as its parent theory. Note that we neglect the U(1) sector within the 3D EFT (i.e. set 3D U(1) gauge-coupling $g'_3 = 0$ for simplicity), while the SU(3) sector essentially decouples (and only affects the dimensional reduction mapping, see Appendix C).

We denote parameters of the 3D EFT with subscript “3”. By further assuming that the scalar S_3 is much heavier than ϕ_3 (in the 3D EFT) around the temperature scale of the electroweak phase transition, by integrating out the new scalar one arrives to an EFT solely for the SU(2) gauge and Higgs fields, described by three parameters: the effective gauge coupling g_3^2 , the Higgs thermal mass μ_3^2 and the Higgs thermal self-coupling λ_3 that are functions of temperature, known SM parameters, and unknown new parameters related

¹¹Previously, fermionic contributions to the fluctuation determinant have been computed in [139] using higher-dimensional operators within the 3D EFT. Recently, similar studies [216–219] have surfaced that study such marginal operator effects within the 3D EFT, albeit not computing their effects to the sphaleron rate.

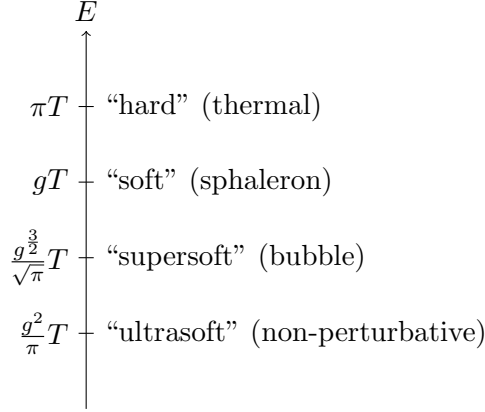


Figure 2: Hierarchy of energy scales E at high temperature T , in terms of formal weak expansion parameter g .

to the field S . As a concrete example, at leading order the EFT parameters have simple expressions

$$\mu_3^2 = \mu^2 + \frac{T^2}{16} \left(3g^2 + g'^2 + 4g_Y^2 + 8\lambda + Ca_2 \right), \quad (3.5)$$

which is the familiar scalar one-loop thermal mass, in terms of the SU(2) and U(1) gauge couplings g and g' , the top quark Yukawa coupling g_Y and the Higgs self-coupling λ . A possible BSM contribution in Higgs portal models is proportional to the portal coupling a_2 between the new scalar S and the Higgs field, given by contribution

$$V(\phi, S) = \frac{a_2}{2} \phi^\dagger \phi S^\dagger S, \quad (3.6)$$

to the scalar potential. The numerical coefficient C depends on the representation of S . At leading order couplings have only trivial temperature-scaling $g_3^2 = g^2 T$ and $\lambda_3 = T\lambda$, with possible BSM physics contributing at next-to-leading order (for details, see [78] and [220]). In order to make first-order phase transitions possible, contributions from BSM physics to λ_3 are crucial, and we discuss them in detail in Sec. 5.

To understand the construction of the dimensionally reduced effective theory, let us start with relevant energy scales of the problem, i.e. hierarchy of energy scales of using the imaginary-time formalism (or Matsubara formalism) of thermal field theory [221]. In terms of a formal power counting parameter¹² g these scales are (see Fig. 2)

¹²Conventionally g coincides with SU(2) gauge coupling in electroweak theories, but strictly speaking, in BSM theories it is the largest dimensionless coupling or ratio of dimensionful couplings, used to organize the perturbative expansion.

- (i) “Hard” scale πT : thermal scale of the non-static (non-zero) Matsubara modes. These “ultraviolet” (UV) modes are integrated out in dimensional reduction, including all fermionic modes.
- (ii) “Soft” scale gT : scale of the purely spatial zero Matsubara modes, described by the 3D EFT. This is the characteristic energy scale of Debye screened temporal gauge field components (and the BSM scalar S_3 in our setup), as well as the spatial gauge fields and sphaleron in the Higgs phase.
- (iii) “Supersoft” scale $\frac{g^{\frac{3}{2}}}{\sqrt{\pi}}T$: within the 3D EFT, characteristic scale for first-order phase transitions and the bubble nucleation is deeper in the IR compared to soft scale, see [80, 85].
- (iv) “Ultrasoft” scale $\frac{g^2}{\pi}T$: the most deep IR scale, which is strongly coupled due to spatial gauge fields developing a non-perturbative “magnetic mass” due to confining nature of SU(2) [117]. This is the characteristic energy scale of gauge fields and the sphaleron in the confinement phase [112].

Construction of the 3D EFT by matching the actions between hard and soft scales is done by means of the standard dimensional reduction.¹³ Formally in powers of g , the matching results in an accuracy [78, 138, 220]

$$S_{3D} \sim \int d^3x \left(\underbrace{\mathcal{O}(g^2)}_{\text{tree-level} + \text{hard 1-loop}} + \underbrace{\mathcal{O}(g^3)}_{\text{soft 1-loop}} + \underbrace{\mathcal{O}(g^4)}_{\text{hard/soft 2-loop}} + \mathcal{O}(g^5) \right) T^3, \quad (3.7)$$

for the 3D EFT action. The leading order (LO) $\mathcal{O}(g^2)$ terms are those of tree-level and one-loop thermal masses, the next-to-leading order (NLO) $\mathcal{O}(g^3)$ terms originate from the one-loop soft scale contributions and the next-to-next-to-leading order (NNLO) $\mathcal{O}(g^4)$ terms result from two-loop thermal masses and one-(two)-loop corrections to couplings from hard (soft) scale.

As explained in [78, 92, 131, 132], the renormalization group improvement effect enters first at $\mathcal{O}(g^4)$: running of the LO terms is cancelled by explicit logarithms of the renormalization scale that appear at NNLO in high- T expansion, i.e. running of the couplings inside one-loop thermal mass are cancelled by the logarithms in the two-loop thermal mass. We truncate the matching relations at $\mathcal{O}(g^4)$ when deriving the effective action, and concretely demonstrate

¹³We comment a following subtlety in the standard literature, related to temporal gauge field components: these soft fields are often integrated out in a “2nd step” of dimensional reduction [78], to construct a final EFT below the soft scale. In our computation, however, the sphaleron lives at the soft scale, so it might not seem immediately clear whether temporal components such as A_0^a triplet field can be integrated out. However, in the Higgs phase they are much heavier than other mass scales, including the sphaleron, and can hence be safely integrated out [112]. For a related discussion, see [132, 222, 223].

in Sec. 3.5 that it is crucial to perform the computation at this order. Furthermore, the matching relations at $\mathcal{O}(g^4)$ are gauge-invariant [81, 179, 199].

Higher order corrections at $\mathcal{O}(g^5)$ originate from three-loop soft contributions of temporal gauge field components. However, hard scale contributions to higher dimensional or marginal operators appear at $\mathcal{O}(g^6)$, and in the SM these are dominant compared to neglected soft contributions, which formally appear at lower orders [78].

Concretely, the 3D EFT action at the soft scale of the SU(2)-Higgs theory in the Euclidean space reads as

$$S_{\text{3D}} = \int d^3x \left[\frac{1}{4} F_{ij,3}^a F_{ij,3}^a + (D_i \phi)_3^\dagger (D_i \phi)_3 + \mu_3^2 \phi_3^\dagger \phi_3 + \lambda_3 (\phi_3^\dagger \phi_3)^2 \right], \quad (3.8)$$

where a and i denotes the adjoint isospin index and the spatial Lorentz index respectively, and we have truncated the order at $\mathcal{O}(g^4 T^3)$.¹⁴ The subscript “3” is used to highlight quantities living in the 3D space: in the 3D EFT, the SU(2) doublet Higgs ϕ_3 and the gauge field $A_{i,3}^a$ have mass dimension $T^{\frac{1}{2}}$ and couplings λ_3 and g_3^2 have mass dimension T . The field strength tensor is defined as

$$F_{ij,3}^a = \partial_i A_{j,3}^a - \partial_j A_{i,3}^a + g_3 f^{abc} A_{i,3}^b A_{j,3}^c, \quad (3.9)$$

where f^{abc} is the SU(2) structure constant and the scalar covariant derivative reads as

$$(D_i \phi)_3 = \partial_i \phi_3 - ig_3 A_{i,3}^a T^a \phi_3, \quad (3.10)$$

with SU(2) generators $T^a = \sigma_a/2$ in terms of Pauli matrices σ_a . For simplicity, we neglect (minor) effects of the U(1) subgroup within the 3D EFT [225]. This choice of the specific 3D EFT allows us to formulate a perturbative framework for the Higgs phase sphaleron rate after the SM crossover (for which 3D EFT effects of the U(1) subgroup can be ignored up to good accuracy [174]). It is also the same EFT we can apply when new BSM fields are heavy enough to be integrated out from the EFT at high temperatures. A specific application is provided in Sec. 5.

Thermodynamic properties of the 3D EFT in Eq. (3.8) are governed by two dimensionless ratios

$$y \equiv \frac{\mu_3^2}{g_3^4}, \quad x \equiv \frac{\lambda_3}{g_3^2}. \quad (3.11)$$

¹⁴We note, that beyond $\mathcal{O}(g^4)$ accuracy that we work on, Eq. (3.8) will include higher dimensional operators, including marginal operators. These are schematically build from kinetic pieces F^2 , $(D\phi)^2$ as well as pure scalar terms. The effects of such operators within the 3D EFT framework have been discussed in [179, 209, 211, 216, 218, 219, 224] and in [139] in the context of the sphaleron rate, but for simplicity we do not include marginal operators, but assume that their effects are negligible. For example, a sextic operator of form $(\phi_3^\dagger \phi_3)^3$ appears at $\mathcal{O}(g^6)$ in terms of contributions from the hard modes. When soft scale BSM physics is integrated out, such an operator can have significantly larger Wilson coefficient, since the soft scale contributions are enhanced. This is also the case for the effect of temporal gauge field component, which contributes formally at $\mathcal{O}(g^3)$ to $(\phi_3^\dagger \phi_3)^3$, but this effect is still subleading compared to $\mathcal{O}(g_Y^6)$ effect from the top quark loop [78].

The critical temperature T_c occurs when relation $y(T_c) = y_c(x)$ holds, where the curve $y_c(x)$ has been found non-perturbatively in [83, 88] (and perturbatively in [82, 140]). The character (as well as the strength) of the phase transition is controlled by $x_c \equiv x(T_c)$, and for $x_c \lesssim 0.098$ the character is of first order, second-order exactly at $x_c \approx 0.098$ (with $y_c \approx -0.0175$). For $x_c \gtrsim 0.098$ there is no phase transition, but merely a smooth crossover between confinement phase and the Higgs phase [83, 88].¹⁵ In the minimal Standard Model, $x_c \approx 0.29$ corresponding to a crossover [16]. For BSM physics to alter this story (within validity of the 3D EFT of Eq. (3.8)) it has to reduce x_c , and we discuss a concrete example of this in Sec. 5.

We stress that it is the (gauge-invariant) ratio of the thermal Higgs self-interaction coupling to the effective gauge coupling that sets the strength of the phase transition (which is proportional to x^{-2}). This can be intuitively understood in a clear perturbative picture of [82]: a strong phase transition is a result of a mass hierarchy between a light transitioning-field (the Higgs scalar) and a heavy transition-inducing field (the gauge field), see also [86, 226, 227]. This relation between a first-order phase transition and mass hierarchy is general to all (perturbative) first-order phase transitions [85].¹⁶

Indeed, already in seminal Ref. [90] the baryon number preservation condition is given in terms of x by $x_c < 0.037$, which is gauge-invariant, includes all non-perturbative physics of the sphaleron rate including the dynamical part, and can account two-loop thermal resummations via dimensional reduction. Unfortunately, major of the past studies have failed to recognize these features and the physics behind it.

However, the condition $x_c < 0.037$ for sufficiently strong transition to prevent the sphaleron washout can be improved. Not by improving the determination of the sphaleron rate (which, we stress, was determined on the lattice in [90]), but by providing a more accurate connection to the bubble nucleation, compared to what was done in [90].

In analogy to $y_c(x)$ curve, Ref. [83] has determined a condition $y(T_p) = y_p(x)$ (both in perturbation theory and non-perturbatively) for percolation temperature T_p , defined by a condition that a phase transition completes by percolation, i.e. that eventually the expanding bubbles of the Higgs phase fill the universe.¹⁷ This condition is obtained by connecting the bubble nucleation rate with cosmological expansion in terms of the Hubble parameter (for details, see [83]).

In this work at hand, one of our goals is to find a similar curve $y_f(x)$ that describes the

¹⁵In smooth crossover, the free-energy, or the pressure, does not have a discontinuity, and hence strictly speaking there is only a single continuously connected phase.

¹⁶As another example, see [228]: in the scalar-Yukawa model, a Dirac fermion plays the role of a transition-inducing heavy field, and consequently the transition strength is controlled by the ratio of scalar self-coupling to Yukawa coupling, smaller ratio corresponding to stronger transitions.

¹⁷In this work at hand, we refer the same curve, obtained in leading order perturbation theory within the 3D EFT, as $y(T_n) = y_n(x)$ at the onset of nucleation at temperature T_n , since in practice $T_n \approx T_p$ in this class of models.

sphaleron freeze-out inside the bubbles, that we can obtain by computing the sphaleron rate at leading order in perturbation theory within the 3D EFT. Yet, we stress that since we work in the 3D EFT that accounts for large two-loop thermal corrections from the hard scale, in that regard our following discussion is greatly improved upon in contrast to e.g. [124–130] that work at leading order in the high-temperature expansion.

In this work at hand, for the first time we combine information from both the nucleation and sphaleron freeze-out in terms of the curves $y_n(x)$ and $y_f(x)$ (c.f. Fig. 7), and hence we can generalize the discussion of [90]. We note that our leading order results in perturbation theory can then be upgraded in the future, by determining $y_f(x)$ non-perturbatively [229] to match the level of rigor in [90].

To achieve this goal, we start by discussing power counting for a suitable perturbative expansion.

3.3. Power Counting within the EFT Perturbation Theory

In pure 3D Yang-Mills theory, the only appearing mass scale is the non-perturbative, magnetic mass of the gauge boson (i.e. the ultrasoft “glueball” mass) and this sets the length scale for the sphaleron, i.e. $(g^2T)^{-1}$. In the gauge-Higgs theory, in the confinement phase (“symmetric” phase) there is an another mass scale coming from the Higgs thermal mass, and the effect of the Higgs field has been studied in [112]. We note that the semi-classical approximation for the sphaleron cannot be used in the confinement phase, as the Higgs field does not acquire its non-zero vacuum expectation value, so a semi-classical sphaleron solution does not exist.

In the Higgs phase, on the other hand, the gauge boson acquires a major contribution to its mass through the Higgs mechanism. This contribution, lying at the soft scale (Fig. 2), is larger compared to the magnetic mass. Intuitively, the length scale of the sphaleron is controlled by the gauge boson mass, and therefore parametrically smaller in the Higgs phase compared to the confinement phase. Since the soft scale can be treated perturbatively, we should be able to compute a relatively reliable sphaleron rate in the Higgs phase.

Concretely, let us go forth and count powers of terms in the soft scale action in eq. (3.8), again using g for counting. All the terms in the action should be of equal size, for them to contribute at the leading order. Omitting Lorentz indices, we formally count $F_3^2 \sim (\partial A_3)^2 \sim m_{W,3}^2 A_3^2$ by balancing the Yang-Mills term with the 3D W-boson mass term from the scalar kinetic term. Using $\phi_3 \sim T^{\frac{1}{2}}$, the characteristic momentum scale k for the sphaleron schematically obeys $k \sim \partial \sim m_{W,3} \sim g_3 \phi_3 \sim gT$. Thus k is at the soft scale, and the sphaleron size $R_{\text{sph}} \sim (gT)^{-1}$, set by the gauge field mass scale. Balancing the other terms in the Yang-Mills term results in $g_3 A_3^2 \partial A_3 \sim g_3^2 A_3^4$ and, therefore, $A_3 \sim \phi_3 \sim T^{\frac{1}{2}}$.

By this formal exercise, we find that the kinetic terms in Eq. (3.8) scale as $\sim g^2 T^3$. The scaling of the scalar potential, on the otherhand, is slightly more complex. In a wide

temperature range, generally the scalar thermal mass and the thermal self-coupling have scaling

$$\mu_3^2 \sim (gT)^2, \quad \lambda_3 \sim g^2 T, \quad (3.12)$$

inherited from the full parent theory with $\mu^2 \sim g^2 T^2$ which follows from the high-temperature expansion and $\lambda \sim g^2$ which simply assigns a same size for scalar and gauge loops at zero temperature (this latter assumption, however, is not necessary, as we shall discuss shortly). Scaling of Eq. (3.12) implies that the scalar potential scales as $g^2 T^3$, and this leads to our power counting in Eq. (3.3) by noting that the characteristic length scale for the soft scale is gT , i.e. $d^3x \sim (gT)^{-3}$ in the action. The scaling of the fluctuation determinant is discussed in further detail in appendix B. In particular, we apply the scalings in Eq. (3.12) to compute the sphaleron rate below the SM crossover.

However, it has been long known, that the general scalings of Eq. (3.12) do *not* apply around and below the critical temperature of a first-order phase transition [86, 131, 164, 226, 227, 230, 231]. Instead, an appropriate scaling is

$$\mu_3^2 \sim (g^{\frac{3}{2}} T)^2, \quad \lambda_3 \sim g^3 T, \quad (3.13)$$

which follow from assumptions that around the critical temperature partial cancellations in the thermal mass make it smaller compared to Eq. (3.12), and furthermore to accomodate a first-order phase transition, scalar loops have to be relatively suppressed compared to gauge field loops, and hence $\lambda \sim g^3$ in the parent theory.¹⁸

In perturbation theory, scaling of Eq. (3.13) has striking implications for computations of both equilibrium thermodynamics and bubble nucleation: the leading order potential is not described by the mere tree-level scalar potential, but in addition includes the one-loop contribution from the gauge bosons [86, 226]. The appearance of the gauge boson contributions at leading order potential (that we discuss in more technical detail in Sec. 3.6) has been made rigorous in [82, 83, 138] in terms of a new EFT specific to the Higgs phase, at the scale $g^{\frac{3}{2}} T$ (c.f. Fig. 2), where the gauge fields have been integrated out. This scale has been referred as the “nucleation scale” in the context of the bubble nucleation [80, 81, 91] and as the “supersoft scale” in [85] which demonstrates that this scale below the soft scale (gT) is widely applicable to first-order phase transitions in more general context. In particular, scaling of Eq. (3.13) is necessary for a perturbative description of nucleation to be possible, and furthermore ensures a consistent perturbative expansion, including gauge-invariance.

Returning back to the sphaleron, we emphasize that the mass scale of the sphaleron (in the Higgs phase) is at the soft scale, and this is independent of the scalar potential, i.e. whether the scaling of scalar parameters follows Eq. (3.12) or (3.13). This implies, that

¹⁸We note, that any convention for the parent theory scaling relating λ and g is not of thermal nature (unlike the scaling for the thermal mass), but merely a convention how to set up a perturbative expansion that can accommodate first-order phase transitions, in perturbation theory [131].

while a perturbative computation of the sphaleron rate in the semi-classical approximation is similar to the computation of the bubble nucleation rate, it is not based on a construction of any further EFT below the soft scale. In the following sections, we describe in detail how the scalar potential is accounted when computing the sphaleron rate.

Finally, we point out that power countings of Eqs. (3.12) and (3.13) are only a necessary tool to organize perturbation theory. On the lattice, the 3D EFT of Eq. (3.8) is directly discretized and thermodynamics as well as bubble- and sphaleron-dynamics are calculated by non-perturbative Monte-Carlo evaluation of the underlying path integral.

3.4. Sphaleron Action and Scaling Properties

Now that we have established our perturbative setup based on the 3D EFT at the soft scale, we compute the sphaleron rate. To solve the sphaleron equations of motion and calculate the sphaleron energy, it is advantageous to scale the fields and parameters in the 3D action (Eq. (3.8)) into dimensionless form.

In the literature, Ref. [127] scales the fields with the (temperature-dependent) Higgs vacuum expectation value v (directly in the full theory, with high-temperature expansion). After such scaling, the resulting sphaleron energy is proportional to v . As such, v corresponds to the minimum of the scalar potential with a second-order phase transition. Instead of using v , one might be tempted to use the 3D mass parameter, $\bar{\mu} \equiv \sqrt{-\mu_3^2}$ to scale the fields (see also discussion related to gauge-invariance in [89]). However, the scaling with $\bar{\mu}$ can only be used in a situation in which $\mu_3^2 < 0$. Hence it is not suitable for describing a first-order phase transition, since in the Higgs phase at temperatures below the critical temperature μ_3^2 can vary from positive to negative values (and hence also vanish at some temperature).

We shall use the dimensional quantity g_3^2 for scaling, which is positive definite at all temperatures (as well as gauge-invariant [179]). Therefore, we use following scaling of fields and coordinates

$$A_3 = g_3 \hat{A}_3, \quad \phi_3 = g_3 \hat{\phi}_3, \quad x_i = \frac{\xi_i}{g_3^2}, \quad (3.14)$$

and consequently the action in Eq. (3.8) is scaled into

$$S_{3D} \rightarrow \hat{S}_{3D} = \int d^3\xi \left[\frac{1}{4} \hat{F}_{ij,3}^a \hat{F}_{ij,3}^a + (\hat{D}_i \hat{\phi})_3^\dagger (\hat{D}_i \hat{\phi})_3 + V_3(\hat{\phi}_3, x, y) \right], \quad (3.15)$$

where the $\hat{F}_{ij,3}^a$ and $(\hat{D}_i \hat{\phi})_3$ do not include the gauge coupling anymore.

While the 3D scalar potential at tree-level is given by the one in Eq. (3.8) and contains only quadratic and quartic terms in the field, for our purposes it is useful to consider a more general form, which also includes a cubic term

$$V_3(\hat{\phi}_3, x, y) = y \hat{\phi}_3^\dagger \hat{\phi}_3 - q (\hat{\phi}_3^\dagger \hat{\phi}_3)^{3/2} + x (\hat{\phi}_3^\dagger \hat{\phi}_3)^2, \quad (3.16)$$

where y and x are defined in Eq. (3.11).

At this stage, for generality we keep the value of the numerical coefficient q undetermined in equations that follow, yet we strongly emphasize that it is not arbitrary variable, but will be directly fixed by requirement that Eq. (3.16) consistently describes the leading order effective potential of a given situation. Concretely, below we will directly focus on two cases: $q = 0$ for a second-order transition (that we apply to study the sphaleron rate for the SM crossover scenario); while for a first-order phase transition $q = \frac{1}{4\sqrt{2}\pi}$. This particular value arises from the consistent treatment of gauge field modes in case of first-order phase transitions, and in particular provides gauge-invariant treatment, as we shall discuss in Sec. 3.6. Furthermore, for now we work with the cubic potential of Eq. (3.16) as our *starting* point, and return later to discuss in detail which contributions should be accounted in the sphaleron energy to contribute to the Boltzmann factor of the sphaleron rate, see Sec. 3.6.

Within the 3D EFT, the classical sphaleron ansatz for scalar and gauge fields reads as¹⁹

$$\hat{\phi}_3 = h(\xi) \begin{pmatrix} 0 \\ v_3(x, y) \end{pmatrix}, \quad (3.17)$$

$$\hat{A}_{i,3}^a T^a dx^i = [1 - f(\xi)] \sum_{i=1}^3 F_i T^i, \quad (3.18)$$

where $v_3(x, y)$ is the classical background field at the minimum of the 3D effective potential $V_3(\phi_3, x, y)$, and $h(\xi)$ is the radial profile function. Hereafter hatted fields are used to denote the sphaleron ansatz. For the gauge field ansatz, $f(\xi)$ denotes the radial profile function and the 1-form F_i are functions of the spherical coordinates θ and φ as well as a topological loop parameter μ [11, 121]. We demonstrate that our 3D gauge ansatz is consistent with the original ansatz of [232] in Appendix A, and relegate there additional technical details about the sphaleron action, while focusing on the key features in the main body.

Using Eq. (3.16), the scalar field minimum $v_3(x, y)$ then reads²⁰

$$v_3(x, y) = \frac{3q + \sqrt{-32xy + 9q^2}}{8x}. \quad (3.19)$$

Although the action in Eq. (3.15) has already been scaled into a dimensionless form, it is further advantageous to rescale the fields and the radial coordinate with the dimensionless $v_3(x, y)$, that is

$$\hat{\phi}_3 = v_3(x, y) \hat{\phi}_3', \quad \hat{A}_3 = v_3(x, y) \hat{A}_3', \quad \xi = \frac{1}{v_3(x, y)} \xi'. \quad (3.20)$$

¹⁹The gauge field configuration used here is not unique, and the $U(1)$ field has been neglected. For a discussion of sphaleron ansatz under alternative conventions and the inclusion of the $U(1)$ field, see Ref. [58] and references therein.

²⁰Note that we choose $v_3(x, y)$ to be the vacuum expectation value of the complex scalar field $\hat{\phi}_3$.

The benefit of this rescaling will be demonstrated in the context of our numerical computations below. We stress that our rescaling with $v_3(x, y)$ here is intrinsically different with the v -scaling in Ref. [127]. First, v_3 is dimensionless, while v in Ref. [127] is dimensional, and second, v_3 is manifestly gauge-invariant (it is the minimum of the leading order effective potential, which is independent of gauge fixing), and while v used in Ref. [127] is the minimum of the tree-level potential (with the thermal mass), and hence also gauge-invariant, multiple later works (see discussion in Sec. 6.2) have used results of [127] and have included loop corrections to v in a manner which is gauge-dependent. The motivation of our rescaling here is simply to facilitate numerical determination of the action, as we shall observe that the sphaleron action in case of a first-order phase transition is approximately equal to $v_3(x, y) \times \text{constant}$, which will greatly simplify the computation of the washout factor in Sec. 4.

Consequently, the sphaleron action transforms into

$$\hat{S}_{3D} = v_3(x, y) \mathcal{C}_{\text{sph}}(x, y) , \quad (3.21)$$

where

$$\mathcal{C}_{\text{sph}}(x, y) = \int d^3\xi \left[\frac{1}{4} \hat{F}_{ij,3}^a \hat{F}_{ij,3}^a + (\hat{D}_i \hat{\phi})_3^\dagger (\hat{D}^i \hat{\phi})_3 + \bar{V}_3(\hat{\phi}_3, x, y) \right] , \quad (3.22)$$

and the transformed potential is

$$\bar{V}_3(\hat{\phi}_3, x, y) = \frac{y}{v_3^2(x, y)} \hat{\phi}_3^\dagger \hat{\phi}_3 - \frac{q}{v_3(x, y)} (\hat{\phi}_3^\dagger \hat{\phi}_3)^{3/2} + x (\hat{\phi}_3^\dagger \hat{\phi}_3)^2 , \quad (3.23)$$

where we have omitted the prime on the fields and the coordinates to reduce notational clutter. Henceforth, \hat{A}_3 and $\hat{\phi}_3$ will denote fields scaled by v_3 , and \bar{V}_3 will denote the scalar potential scaled by v_3 . It is important to note, that the Yang-Mill term and the second term in the effective action, which we refer as the covariant derivative term, do not explicitly depend on x, y , while $\bar{V}_3(\hat{\phi}_3, x, y)$ does. After the rescaling, the sphaleron ansatz for the gauge fields remain unchanged, while the ansatz for the scalar field becomes

$$\hat{\phi}_3 = h(\xi) \begin{pmatrix} 0 \\ 1 \end{pmatrix} , \quad (3.24)$$

which only depends on the radial profile function. The equations of motion (EOMs) for the sphaleron can be obtained by applying the action principle to the scaled action \mathcal{C}_{sph} , which leads into

$$f'' - \frac{2f(-1+f)(-1+2f)}{\xi^2} - \frac{2}{3} J(1+J)h^2 = 0 , \quad (3.25)$$

$$h'' + \frac{2h'}{\xi} - \frac{8}{3\xi^2} J(1+J)(-1+f)^2 h - \frac{1}{2} \frac{\partial \bar{V}_3}{\partial h} = 0 , \quad (3.26)$$

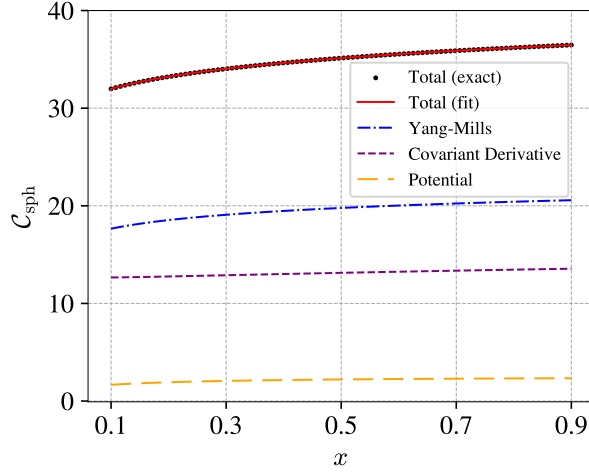


Figure 3: Scale-transformed sphaleron action \mathcal{C}_{sph} as function of x . The black dots present the exact numerical computation of \mathcal{C}_{sph} , and the red line is the fitting curve, the Eq. (3.29). These two results align on top of each other, and are almost indiscernible. Dashed curves illustrate different contributions to \mathcal{C}_{sph} : blue, purple, and orange curves depict contributions from the Yang-Mills, covariant derivative and potential terms in Eq. (3.22), respectively.

where prime denotes derivative with respect to the radial parameter. We observe that the EOM of f does not directly depend on x, y , while the EOM of h depends on x, y through V_3 . We conclude that x, y enter into the sphaleron action and the EOMs only through $\bar{V}_3(\hat{\phi}_3, x, y)$. In the following, we will discuss applications for the sphaleron rate at temperatures below SM crossover and first-order phase transitions, separately.

3.4.1. Second-Order Phase Transitions

The tree-level scalar potential, which corresponds to setting $q = 0$, describes a second order phase transition, in which the second derivative of the pressure is discontinuous at the critical temperature, which occurs when the effective mass changes its sign, i.e. at $y = 0$. For $y < 0$, we can compute the sphaleron rate in the Higgs phase. In such case, the $v_3(x, y)$ reads

$$v_3(x, y) = \sqrt{\frac{-y}{2x}}, \quad (3.27)$$

and the scaled (tree-level) potential \bar{V}_3 depends only on x :

$$\bar{V}_3(\hat{\phi}_3, x) = -2x\hat{\phi}_3^\dagger\hat{\phi}_3 + x(\hat{\phi}_3^\dagger\hat{\phi}_3)^2. \quad (3.28)$$

Note that here both terms depend linearly on x : for the first term, this form arises due to the scale transformation. We can then solve sphaleron EOMs numerically, and consequently compute the sphaleron action in Eq. (3.22) numerically. The result for $\mathcal{C}_{\text{sph}}(x)$ can be expressed

as a fit

$$\mathcal{C}_{\text{sph}}(x) = A + Bx^C \log(Dx), \quad (3.29)$$

with coefficients

$$A = 26.12, \quad B = -2.145, \quad C = 0.4237, \quad D = 0.00717. \quad (3.30)$$

In Fig. 3, we present a comparison between the fitting formula and the exact numerical result of the rescaled sphaleron action \mathcal{C}_{sph} , as well as contributions from different terms in Eq. (3.22).

From Fig. 3, we can make an important observation: after the scaling transformation, the direct contribution from the scalar potential to \mathcal{C}_{sph} is completely subleading compared to kinetic terms. In our formal power counting, all terms in the action contribute as $\int d^3x (g^2 T)^{-3} \sim 1/g$, but after the scale transformation and numerical determination of the action, we see that the potential has only a minor effect, except that it dictates the form of the scalar background field at the minimum, i.e. v_3 in Eq. (3.27), while to a great approximation \mathcal{C}_{sph} is governed by the kinetic terms only. Below we will take full advantage of this observation, when we consider first-order phase transitions.

The fitting expression in Eq. (3.29) is really powerful: it precisely provides the sphaleron action of any given theory as long as the theory can be mapped onto the SU(2) Higgs 3D EFT for which leading order minimum at the Higgs phase is described by Eq. (3.27) at leading order, for any $y < 0$. The temperature dependence is solely captured by the dimensional reduction matching relations through x and y , which can be calculated e.g. by automated package DRalgo [220, 233].

3.4.2. First-Order phase transitions

For a first-order transition, in perturbation theory the leading-order potential has to contain a barrier between the two phases, and such a potential then sets the expression for the Higgs phase minimum. For now, we concretely fix $q = \frac{1}{4\sqrt{2}\pi}$, hence both x and y appear in the \bar{V}_3 . This value of q corresponds to the leading order scalar potential of the SU(2) gauge-Higgs theory [82], and we explain in more detail in Sec. 3.6 how this term arises. In this case, a general, closed form fitting expression for the dependence of $\mathcal{C}_{\text{sph}}(x, y)$ over two, instead of one, variables x and y turns out to be hard to obtain. However, it turns out that the contribution from the potential term is very small (in analogy to previous case of a second-order transition), and \mathcal{C}_{sph} is, to a good approximation, a constant. In Fig. 4 (top row), we demonstrate results for the scaled sphaleron action in fixed benchmarks with x or y fixed respectively. We see that the contribution from the potential term is negligible, and it is indeed a good approximation to regard the v_3 -scaled sphaleron action as a constant, and we furthermore observe this trend to be general.

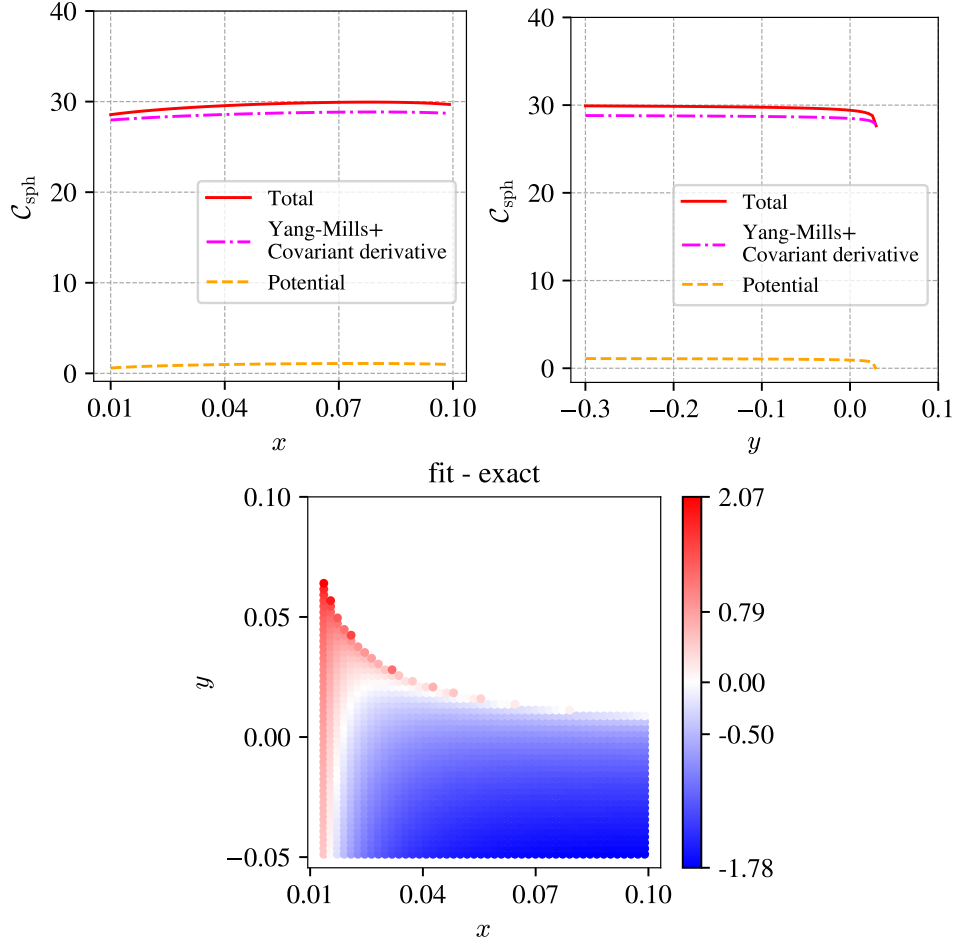


Figure 4: Top row: v_3 -scaled sphaleron action in the case of cubic potential. Left: \mathcal{C}_{sph} as function of x with fixed for $y = 0.008$. The red curve depicts the total action, magenta curve shows contributions from the Yang-Mills and covariant derivative terms, and orange curve contributions of the the scalar potential term. Right: similarly \mathcal{C}_{sph} as function of y with fixed $x = 0.03$. Bottom row: Difference of the approximate sphaleron action (Eq. (3.31)) and the full numerical action in the (x, y) -plane. This plot demonstrates that our approximate sphaleron action is in good agreement with the numerically obtained exact sphaleron action across a broad range of x and y .

To that end, we propose an approximation in which the sphaleron action is approximately equal to $v_3(x, y)$ multiplied with a constant $\mathcal{C}_{\text{sph}}(x, y) \approx 29$, i.e.

$$\hat{S}_{3\text{D}} = v_3(x, y) \times 29, \quad (3.31)$$

where $v_3(x, y)$ is defined in Eq. (3.19) with $q = \frac{1}{4\sqrt{2}\pi}$. We further justify Eq. (3.31), by comparing with the result of exact numerical computation in the (x, y) -plane, which is shown

in Fig. 4 (bottom row). The consistency between the approximation and the full numerical result indicates that the effect of x and y to the equations of motion and \mathcal{C}_{sph} is almost negligible, especially in the most interesting region where $y > 0$, as we will discuss in Sec. 3.6.

3.5. Sphaleron Rate after Standard Model Crossover

As a direct application of previous section, we next compute the Higgs phase sphaleron rate for temperatures below the Standard Model crossover. In the case of a crossover, there are no two separate phases, but only a one phase, and consequently all temperature derivatives of the pressure of the system are continuous. Perturbation theory cannot describe the crossover properly, as it predicts a second-order phase transition exactly at $y = 0$. This does not, however, affect our computation in the Higgs phase, with $y < 0$. Hence, we assume a semi-classical picture in which the scalar potential is governed by the tree-level potential, i.e. our description for the second-order phase transition case, and consider region $y < 0$.

We depict our result in Fig. 5. The SM crossover occurs at pseudo-critical temperature around ~ 160 GeV [173, 174, 231]. Here one should keep in mind, that as there is no phase transition, there is no order parameter to distinguish any physical phases.²¹ In a temperature window $120 < T/\text{GeV} < 160$ the value of $x(T) \approx 0.29$ is approximately a constant.

At leading order, our result, which is shown as the blue dashed curve in Fig. 5, is

$$\Gamma_{\text{sph,LO}} = T^4 \times e^{-v_3(x,y)\mathcal{C}_{\text{sph}}(x)}, \quad (3.32)$$

i.e. we estimate the prefactor solely based on dimensional grounds with $A_{\text{dyn}} \times \det_{\text{sph}} \sim T^4$; the expressions for $v_3(x,y)$ and $\mathcal{C}_{\text{sph}}(x)$ are given by Eq. (3.27) and Eq. (3.29), respectively. This naive estimate for the prefactor can be improved upon by evaluating the fluctuation determinant more rigorously (see Appendix B), which leads to the NLO result

$$\Gamma_{\text{sph,NLO}} = T \times \kappa(x) \times \mathcal{N}_{\text{tr}}(\mathcal{NV})_{\text{rot}} v_3^9(x,y) g_3^6 e^{-v_3(x,y)\mathcal{C}_{\text{sph}}(x)}. \quad (3.33)$$

Note that in this expression g_3^6 has the mass dimension T^3 . In general, $\mathcal{N}_{\text{tr}}(\mathcal{NV})_{\text{rot}}$ is a function of x , and we can approximate it as $\mathcal{N}_{\text{tr}}(\mathcal{NV})_{\text{rot}} \approx \exp(8.813)$ using a result reported in Ref. [126], for $x \approx 0.29$ in our case. Contributions of positive modes are encoded by the function $\kappa(x)$. For simplicity, we do not compute it but merely set it to be unity, as a first approximation (in order to compare against the result of [87]). The T factor in $\Gamma_{\text{sph,NLO}}$ again comes from our rough estimation $A_{\text{dyn}} \sim T$.²² Under all these approximations, $\Gamma_{\text{sph,NLO}}$ is shown as the red dashed curve in Fig. 5.

²¹Instead, physical properties, such as the Higgs field susceptibility or the sphaleron rate, change smoothly from their high- T to low- T behaviour around the pseudo-critical temperature.

²²As an exploration, one could also approximate the dynamic prefactor as $A_{\text{dyn}} \sim \frac{\omega_-}{2\pi}$ in terms of a negative eigenmode ω_- , for which result of [126] gives $\omega_- \approx 2\pi \exp(-2.05)$. However, as already discussed in Sec. 2.2.3, this is not a consistent treatment for the non-equilibrium dynamic prefactor in terms of the effective HTL description in accord of [156, 163] (see also recent [210]).

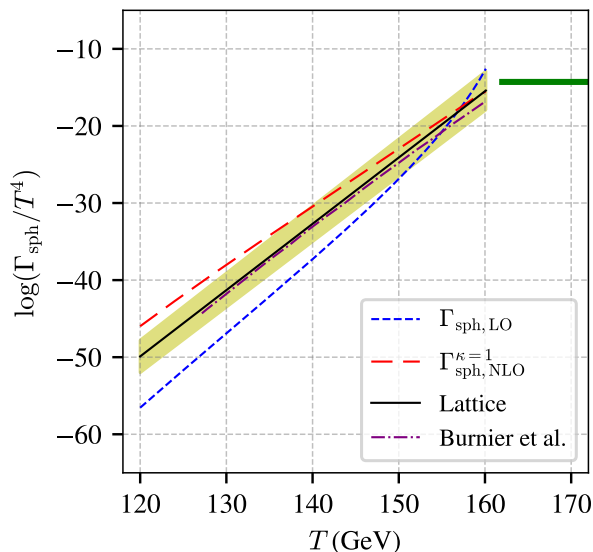


Figure 5: Sphaleron rate as function of temperature for the Standard Model crossover. Results of our perturbative computations in the Higgs phase based on two-loop dimensional reduction ($\Gamma_{\text{sph,LO}}$, $\Gamma_{\text{sph,NLO}}^{\kappa=1}$ defined in the main text), contrasted with the previous perturbative results of Burnier et. al. [87] and non-perturbative lattice simulation of [174] (black solid line with statistical error band in yellow). Green band depicts the confinement phase sphaleron rate, determined from the lattice.

In addition, in Fig. 5, we contrast our computations to the previous perturbative result by Burnier et al. [87] (marked in purple dot-dashed curve), as well as non-perturbative lattice simulations of [173, 174] (marked in solid black curve, with statistical error estimates in yellow). Additionally we show the results in the confinement phase by lattice simulations of [112, 174] (in green) above the pseudo-critical temperature.

We observe that our LO/NLO results have the same qualitative behaviour with results from more rigorous evaluations. We emphasize, that this reasonable agreement of our purely perturbative computations (at LO and NLO) with the lattice, follows from a virtue that our treatment for the large thermal corrections from the hard scale, i.e. the dimensional reduction mapping, is the same as that has been used for the lattice analysis [174] (as well as that in perturbative result of [87]).²³

To further highlight the importance of performing the dimensional reduction at two-loop order to accurately capture these thermal effects, in the right panel of Fig. 6, we replot our perturbative results using different orders for the dimensional reduction matching results.²⁴

²³For the Standard Model dimensional reduction, see [78]. However, this pioneering computation does not include an effect from the temporal gluon sector, that we discuss in Appendix C.

²⁴We note that while Fig. 5 uses the exactly same dimensional reduction mapping as used in [174], in Fig. 6

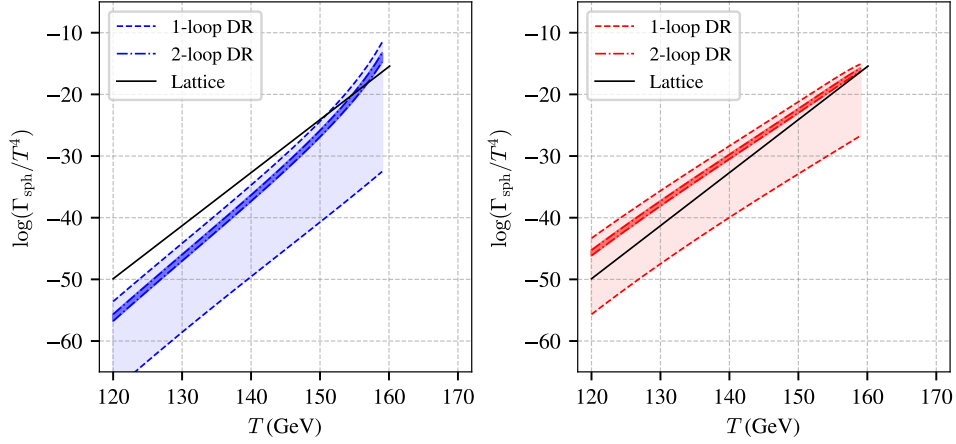


Figure 6: Similar to fig. 5, but varying the effect of the renormalization scale μ at different dimensional reduction matching orders for our perturbative results $\Gamma_{\text{sph,LO}}$ (left plot) and $\Gamma_{\text{sph,NLO}}^{\kappa=1}$ (right plot).

For both the LO and NLO sphaleron rates, the results from mere one-loop dimensional reduction are shown as bands with dashed lines, while the two-loop results are shown as bands with solid lines. The band is a consequence of the variation in the renormalization scale Λ used in the dimensional reduction between $\Lambda = 0.5\pi T$ and $\Lambda = 4\pi e^\gamma T$,²⁵ (where γ is the Euler–Mascheroni constant) and it is clear that while the two-loop mapping depends only mildly on the renormalization scale (c.f. narrow bands in-between solid lines), by contrast the result at one-loop comes with a significant theoretical uncertainty (bands in-between dashed lines) [92].

These comparisons of different results in the case of the SM crossover demonstrate that our perturbative computation, based on the use of 3D EFT, manages to capture large thermal effects (from the hard scale) in the Higgs phase sphaleron rate. Hence, higher order *soft* effects – beyond the Boltzmann factor and the prefactor – are not as large, let alone purely non-perturbative effects: as we have already discussed, the characteristic scale of the sphaleron in the Higgs phase is set by the gauge boson mass, and is hence the soft scale. As result, we have demonstrated that the sphaleron rate in the Higgs phase can be computed fairly accurately in perturbation theory. That being said, the fact that the soft scale effects captured by the statistical prefactor lead to quantitatively important corrections, motivates to extend our computation to fully compute the fluctuation determinant, i.e. the full effect of $\kappa(x)$. We leave such computation as well as studying the non-equilibrium effects captured by the

we use the SM part of such mapping from [234]. The slight difference between the two is caused by different implementation of the zero temperature vacuum renormalization for the input parameters, c.f. [78, 234].

²⁵Renormalization scale of the 3D EFT is kept fixed at $\Lambda_3 = T$, and varying it leads to negligible change.

dynamical prefactor to future works.

3.6. Sphaleron Rate after First-Order Electroweak Phase Transition

To accomodate a first-order phase transition at leading order in perturbation theory, the dimensionless scalar potential at leading order includes a cubic term from integrating out the soft gauge bosons in the Higgs phase as [81, 82]

$$\bar{V}_{\text{LO}}(\hat{\phi}_3) = y\hat{\phi}_3^\dagger\hat{\phi}_3 + x(\hat{\phi}_3^\dagger\hat{\phi}_3)^2 - \frac{1}{2\pi}\left(\frac{\hat{\phi}_3^\dagger\hat{\phi}_3}{2}\right)^{\frac{3}{2}}. \quad (3.34)$$

In terms of the scale hierarchies of Fig. 2, this potential corresponds to the leading order potential of the EFT at the supersoft scale [80, 85, 140]. Furthermore, Eq. (3.34) is gauge-invariant [80, 179], and thereby resolves the problems discussed in [89]. The cubic potential of Eq. (3.34) obeys the power counting of Eq. (3.13): in the vicinity of the critical temperature, power counting for the mass of the scalar field yields $\mu_3^2 \sim \frac{g^3}{\pi}T^2$, while the mass of the gauge boson is soft $m_{W,3} = g_3\sqrt{\phi_3^\dagger\phi_3} \sim gT$, and hence the one-loop contribution $-\frac{1}{6\pi}m_{W,3}^3 \sim \frac{g^3}{\pi}T^3$ from the gauge bosons – which is gauge-invariant – contributes at the LO, while all other one-loop diagrams contribute at higher orders (and could introduce spurious gauge-dependency, if not treated properly).

Due to the cubic term, the potential of Eq. (3.34) has a barrier between the origin and the Higgs phase minimum, and at the critical temperature (c.f. Fig. 7)

$$y(T_c) = y_c(x) = \frac{1}{128\pi^2 x}, \quad (3.35)$$

the two minima have degenerate free energies. We note that Eq. (3.35) describes the leading order result in the 3D EFT perturbation theory, but for Eq. (3.34) to accurately describe the leading order effective potential, x has to be sufficiently small, as otherwise gauge bosons are not heavy enough to be integrated out reliably in the Higgs phase.

At non-perturbative level, $y_c(x)$ has been determined in [88, 214], and in stark contrast to perturbation theory – which always describes a first-order transitions (when leading order potential has the cubic term and hence a barrier) – a first-order transition exists only for $0 < x \lesssim 0.1$, i.e. at large x there is no transition but a crossover. In perturbation theory, $y_c(x)$ has been computed perturbatively at first five orders²⁶ as an expansion in \sqrt{x} , i.e. up to next-to-next-to-next-to-next-leading order (N⁴LO) [140], and the result matches that from the lattice remarkably well until $x \sim 0.055$.²⁷

²⁶Any order beyond that receives contributions from non-perturbative magnetic mass of the gauge boson, and is hence beyond the reach of perturbation theory, c.f. Linde’s IR problem [117].

²⁷However, nothing in perturbation theory alone indicates any kind of breakdown at $x \gtrsim 0.05$, so it remains elusive why the second-order end point occurs at $x \sim 0.1$ and not at some other, smaller or larger value. To

To compute the sphaleron action, we can now directly follow the prescription of Sec. 3.4. There is, however, a subtlety that we need to address: the leading-order scalar potential in Eq. (3.34) with the cubic term, is formally the potential of the EFT within the supersoft scale, because this is the scale where the transition takes place [85]. Sphaleron, on the otherhand, lives in the soft scale, and it is clear in technical level that in order to describe the sphaleron in the semi-classical approximation, we cannot integrate out the soft gauge boson. Hence, one might ask, is it consistent to use the cubic potential in Eq. (3.34) to compute the sphaleron action?

An attempt to resolve this by limiting to the mere (soft-scale) tree-level potential to describe the sphaleron fails immediately: the Higgs phase minimum of the tree-level potential does not exist for $y > 0$, yet this is the region where the $y_c(x)$ curve lies, as well as the region where the bubble nucleation takes place (c.f. Fig.7). Hence, we desire to be able to compute the sphaleron rate for $y > 0$.

A resolution to this is already provided in Sec. 3.4: after the v_3 -scaling transformation, it is clear that the major role of the scalar potential to the sphaleron action comes only from the boundary condition to the sphaleron scalar profile function (as is apparent before the scale transformation), while the direct effect of the potential to the sphaleron action is negligible, as it is dominated by the kinetic terms. While the sphaleron lives in the soft scale, this boundary condition for the scalar field minimum is set by the supersoft scale physics that dictates how the Higgs minimum v_3 – or to be precise beyond the leading-order semi-classical picture – the Higgs condensate, behaves in (x, y) -plane [140]. The scalar potential that corresponds to v_3 (or the Higgs condensate) in leading order perturbation theory, is the one in Eq. (3.34).

Furthermore, we note that the scalar potential in Eq. (3.34) scales as $\sim g^3 T^3 / \pi$ according to our power counting in Eq. (3.13). Hence, it is parametrically of same order as the fluctuation determinant for spatially varying gauge and scalar modes, and hence its direct effect to the sphaleron energy contributes at NLO, rather than at LO, in the “soft scale expansion” in g/π . A numerical consistency check of the above power counting can clearly be observed in Fig. 4, and a comparison to Fig. 3 shows that in the small x regime the contribution of the potential to the sphaleron energy is even more negligible than at large x .

In summary, once the boundary condition to the scalar field radial profile function is correctly identified from the supersoft scale scalar potential for first-order transitions, that describes how the scalar field behaves at large distance scales $(g^{\frac{3}{2}} T)^{-1}$ (and hence at spatial infinity in sphaleron EOMs), the potential itself contributes only at NLO to the sphaleron rate, and its effect can be omitted in the semi-classical approximation.²⁸ In practical terms,

shed light into this, lattice simulations could be used to reveal the details of the magnetic scale confinement phenomena, that presumably cause the termination of first-order transitions (see also [235, 236]). We also note, that the value of x_c where the end-point occurs depends on the representation of the scalar field under the gauge symmetry, e.g. $x_c \sim 0.3$ in the case of an adjoint scalar c.f. [227, 237, 238] or more recent [239–241].

²⁸In order to concretely scrutinize the consistency of our perturbative expansion for the sphaleron rate, one

we can compute the sphaleron rate using Eq. (3.31), as the difference between the exact solution (with the direct contribution of the entire potential relegated to NLO and hence omitted at LO) and the fit is numerically of the same order as difference of exact solutions with and without the potential term.

Before moving on, we point out that since first-order phase transitions take place for smaller values of x (compared to the SM crossover), we can expect that in such cases our leading perturbative computation for the Higgs phase sphaleron rate is even more accurate than our results in the case of the SM crossover in Fig. 5, since x is the soft scale expansion parameter. This expectation could be put to test by fresh lattice simulations for the Higgs phase sphaleron rate, in the small x regime that governs first-order phase transitions, and treating y as an input parameter, rather than fixing it by any dimensional reduction mapping.

4. Baryon Number in First-Order Electroweak Phase Transition

Perturbative description of first-order phase transitions in $SU(2) + \text{Higgs}$ 3D EFT was originally presented in [131, 132], and recently reformulated in [82, 140] in order to consistently add higher order corrections in perturbative expansion in $x \equiv \lambda_3/g_3^2$. In [209, 211] the bubble nucleation rate [83, 86] was computed in similar formulation. In this section we build upon these works, by including computation of the sphaleron rate and finding conditions in (x, y) -plane for the sphaleron decoupling (or freeze-out) and washout.

4.1. Sphaleron Decoupling Temperature

Now that we have computed the sphaleron rate in the Higgs phase (for any x and y using Eq. (3.31)), let us use cosmology to impose a condition for the sphaleron decoupling (or freeze-out). We define the sphaleron decoupling by a condition that the baryon number violation rate Γ_B equals the Hubble parameter H , or equivalently the mean free path for baryon preservation is equal to the horizon size H^{-1} . Hence, the decoupling temperature T_* is defined as

$$\Gamma_B(T_*) = H(T_*), \quad (4.1)$$

should make sure that a treatment of all NLO contributions – both the spatially varying fields contributing to the determinant and the role of the scalar potential, and furthermore the role of the potential in computing the determinant – avoids any double counting. We leave such study for future work, yet speculate, that such computation might include a resummation by adding and subtracting the cubic term to the tree-level potential in analogy to [242]. In this reference the bubble nucleation rate was computed at higher orders in terms of the bubble fluctuation determinant without resorting to the derivative expansion, and such resummation was used to eliminate the double counting related to the cubic term, which is essential for the bounce to exist at the leading order, yet is also contained in the determinant.

and for $T < T_*$ the baryon number is conserved. In the radiation dominated period, the relation of Hubble parameter with temperature reads

$$H(T) = \sqrt{\frac{4g_*\pi^3}{45}} \frac{T^2}{m_{\text{Pl}}}, \quad (4.2)$$

with $m_{\text{Pl}} = 1.22 \times 10^{19} \text{ GeV}$ the Planck mass, $g_* = 106.75 + N$ the number of relativistic degrees of freedom with N encoding the BSM physics. The relation between Γ_B and the sphaleron rate Γ_{sph} reads as [87, 114, 124]²⁹

$$\Gamma_B(T) = 2N_\rho \frac{\Gamma_{\text{sph}}}{T^3}, \quad (4.3)$$

where $N_\rho = n_G^2 \rho$; ρ is a coefficient relating the baryon number to the free energy [243], $n_G = 3$ is the number of generations of the fermions and we are taking the limit that $\frac{\Gamma_{\text{sph}}}{T^4}$ is rapidly and monotonically decreasing with temperature. We will use the approximation $N_\rho \approx \frac{13}{4} \times 3$ in this work [87].

In order to translate our cosmological condition into a condition on 3D parameters, we first write the sphaleron rate (see the beginning of Sec. 3) as

$$\Gamma_{\text{sph}} = A_{\text{dyn}} \times [\text{det}]_{\text{sph}} e^{-\hat{S}_{3\text{D}}(x,y)}, \quad (4.4)$$

then, we convert the decoupling condition (Eq. (4.1)) into

$$\hat{S}_{3\text{D}}(x, y) = \ln \left(\frac{A_{\text{dyn}} \times [\text{det}]_{\text{sph}}}{T^3} \frac{2N_\rho}{H(T)} \right) \approx \mathcal{S}_0 \equiv 39, \quad (4.5)$$

at $T = T_*$. That is, by simply estimating $A_{\text{dyn}} \times [\text{det}]_{\text{sph}} \sim T^4$ using dimensional analysis, we find that the logarithm of Eq. (4.5) is approximately a constant, \mathcal{S}_0 . We can thus approximate the $\hat{S}_{3\text{D}}(x, y)$ as a T -independent constant $\mathcal{S}_0 \approx 39$. Subsequently, we can invert the equation $\hat{S}_{3\text{D}}(x, y(T_*)) = \mathcal{S}_0$ numerically to find a curve $y_f(x)$, i.e. the value of $y(T_*)$ for each x that satisfies eq. (4.5).³⁰ This is in complete analogy to treatment for nucleation condition $y_n(x)$ in [140], and we show y_f in Fig. 7, together with y of x curves at the critical temperature $y_c \equiv y(T_c)$ and the nucleation temperature $y_n \equiv y(T_n)$.

In Fig. 7, regions above (below) the $y_f(x)$ curve correspond to baryon number violation rate that exceed (fall below) the Hubble constant. The area between the y_n and y_f curves represents the baryon washout region inside the bubble. Depending on the value of x , three scenarios arise: (i) no baryon washout occurs ($x < \bar{x}$); (ii) the generated baryon asymmetry

²⁹We note that the diffusion rate used in [87] is twice the sphaleron rate. The sphaleron rate is a response rate to the chemical potential [124], while the diffusion rate is the Chern-Simons diffusion rate, $\Gamma_{\text{diff}(T)} \equiv \lim_{V, t \rightarrow \infty} \frac{\langle Q^2(t) \rangle_T}{Vt}$, where $Q(t) \equiv N_{\text{CS}}(t) - N_{\text{CS}}(0)$ [87, 90].

³⁰For y_f , we choose subscript to stand for sphaleron *freeze-out* at T_* .

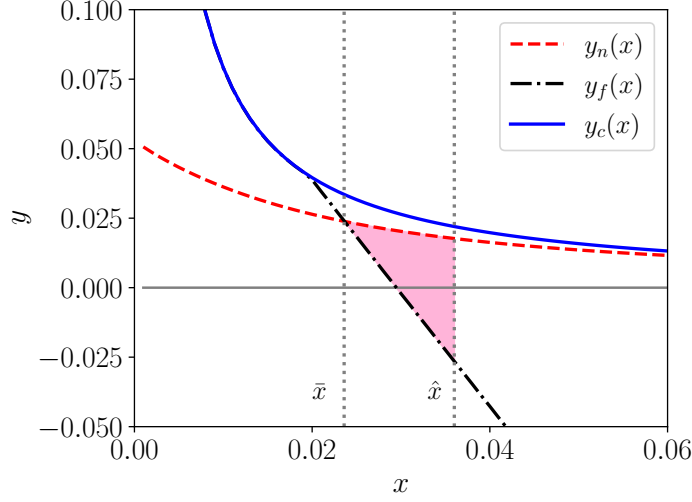


Figure 7: Universal curves $y(T_c) = y_c(x)$ for the critical, $y(T_n) = y_n(x)$ for the nucleation and $y(T_*) = y_f(x)$ for sphaleron freeze-out temperatures in the (x, y) -plane, at leading order in the perturbation theory. Vertical lines are drawn to $\bar{x} \approx 0.025$ at intersection of y_n and y_f , as well as at $\hat{x} \simeq 0.036$. For $x < \bar{x}$ sphalerons are decoupled immediately upon nucleation, while survival from baryon number wash-out is possible in the region $\bar{x} < x < \hat{x}$ (depicted in pink). For $x > \hat{x}$ washing out all possible baryon asymmetry cannot be realistically prevented. BSM theories are mapped into this plane by dimensional reduction mapping $\{x(T), y(T)\}$, and crossing with y_c , y_n and y_* determines T_c , T_n and T_* , respectively.

is partly washed out ($\bar{x} < x < \hat{x}$); and (iii) practically all of the generated baryon asymmetry is erased ($x > \hat{x}$). The calculations supporting cases (ii) and (iii) are presented in the next subsection. Here we comment further on scenario (i), where the curves for the nucleation and sphaleron decoupling intersect at $\bar{x} \approx 0.025$. This implies, that for the very strong transitions with $x < \bar{x} \approx 0.025$ sphalerons are immediately decoupled when the transition starts, since $T_* > T_n$. Since x depends on temperature only weakly [78], this means that for strong transitions with $x_c \sim x_n < \bar{x} \approx 0.025$, wash-out is not possible at all, and all baryon excess generated in front of the bubble wall is immediately preserved in the Higgs phase.

4.2. Baryon Number Preservation Criteria

Baryon number density n_B satisfies a rate equation [89, 124]³¹

$$\frac{\partial}{\partial t} n_B = -\Gamma_B(T) n_B, \quad (4.6)$$

where $\Gamma_B(T)$ is given by Eq. (4.3). Upon integrating over time, we have

$$\mathcal{R}_B(t) \equiv \frac{n_B(t)}{n_B(0)} = \exp \left(-2N_\rho \int_{t=0}^t \frac{\Gamma_{\text{sph}}(T(t))}{T^3(t)} dt \right) \equiv e^{-\mathcal{W}}, \quad (4.7)$$

where $t = 0$ corresponds to $T = T_n$ and $t > 0$ corresponds to lower temperature epoch. The quantity $\mathcal{R}_B(t)$, the ratio of remaining baryon number at time t to the initial baryon number at $T = T_n$, measures a washout factor of the created baryon asymmetry and decreases as time goes. The upper limit of t , t_* is given by the temperature where the sphaleron decouples $T(t_*) = T_*$, which has been discussed in the previous section.

Assuming radiation-dominated universe (with the Friedmann-Robertson-Walker metric), we can switch from the time t to the temperature T using

$$\frac{d}{dt} = -\frac{\sqrt{24\pi}}{m_{\text{Pl}}} \frac{\sqrt{e(T)}}{d \log s(T)/dT} \frac{d}{dT}, \quad (4.8)$$

where $s(T)$ is the entropy density and $e(T)$ is the energy density of the universe. For a discussion on non-standard cosmologies, see [244]. Using the ideal gas approximation³² $p(T) = g_* \pi^2 T^4/90$ and thermodynamic relations $s(T) = p'(T)$ and $e(T) = Ts(T) - p(T)$, we can write

$$dt = -\frac{1}{H(T)} \frac{dT}{T}. \quad (4.9)$$

We can then convert the time integral in Eq.(4.7) into an integration of T as

$$\mathcal{R}_B(T_*) = \frac{n_B(T_*)}{n_B(T_n)} = \exp \left(-2N_\rho \int_{T_*}^{T_n} \frac{\Gamma_{\text{sph}}}{T^3} \frac{1}{H(T)} \frac{dT}{T} \right). \quad (4.10)$$

Thereby, we get the baryon number washout exponent factor

$$\mathcal{W} = 2N_\rho \int_{T_*}^{T_n} \frac{\Gamma_{\text{sph}}}{T^3} \frac{1}{H(T)} \frac{dT}{T}, \quad (4.11)$$

³¹On the left-hand-side of Eq. (4.6), we have dropped the expansion term, $3Hn_B$, under the assumption $\Gamma_B(T) \gg H$. This approximation can fail in the narrow neighborhood of \bar{x} , where the y_n curve is very close to y_f curve (y_f is defined by $\Gamma_B(T) = H$). However, this potentially problematic region is very narrow and for $x > \bar{x}$ beyond this neighborhood, the condition $\Gamma_B(T) \gg H$ holds and our approximation is therefore justified.

³²In principle, one can add higher order corrections to the pressure, see e.g. [245], but such corrections are model dependent.

and consequently

$$n_B(T_*) = e^{-\mathcal{W}} n_B(T_n). \quad (4.12)$$

In this prescription, should some C- and CP-violating processes have generated a baryon excess $n_B(T_n)$ at vicinity of the bubble wall at the onset of the phase transition, in the Higgs phase sphalerons will dilute the baryon density by a factor of $e^{-\mathcal{W}}$ until sphaleron processes decouple at $T = T_*$ and a final baryon density $n_B(T_*)$ remains, which can be used to compare with the observed value in the Eq. (1.1). Furthermore, the washout starts at the time when the first generation of baryons moves into the bubble. This time is identified as the formation time of the bubble, which in our approximation corresponds to T_n . In principle, as the bubble expands, new net baryons that have been created continuously outside the bubble wall, are being swept inside the bubble. However, in our setup the initial baryon number is the one created at $T = T_n$, i.e. $n_B(T_n)$, and we have assumed that the bubble expansion is very rapid. In other words, the difference between temperature where bubbles form and the percolation temperature when the transition completes is very small compared to the difference between T_n and the sphaleron decoupling temperature T_* .³³

Dividing both sides of eq. (4.12) by the photon number density n_γ we can solve the initial baryon to photon density ratio

$$\frac{n_B(T_n)}{n_\gamma(T_n)} = e^{\mathcal{W}} \eta, \quad (4.13)$$

where η is the observed value in the Eq. (1.1). Eq. (4.13) can be used to put a constraint on C- and CP-violating processes that generate an over-abundance of initial asymmetry, which is then washed out to produce the experimentally observed value.

Next, our task is to compute the wash-out exponent \mathcal{W} . For this, we use the leading order sphaleron rate

$$\Gamma_{\text{sph}} \approx T^4 e^{-\hat{S}_{3D}(x,y)}. \quad (4.14)$$

Futher, we define

$$\eta_y \equiv T \frac{dy}{dT}, \quad \eta_x \equiv T \frac{dx}{dT}, \quad (4.15)$$

and assume $\eta_y \gg \eta_x$ (see [246]), i.e. the T -dependence of x is subleading, and hence can be neglected. Upon change of variables from T to y , the wash-out exponent \mathcal{W} can be estimated as

$$\mathcal{W} \approx 2N_\rho \frac{\bar{T}}{H(\bar{T})} \eta_y^{-1}(\bar{T}) \int_{y_f}^{y_n} e^{-\hat{S}_{3D}(x,y)} dy \quad (4.16)$$

³³Again, this assumption may break down in the region near \bar{x} , as we discussed in a similar situation in the footnote of Eq. (4.6). Here, we assume that the region where the approximation fails is very narrow. A more comprehensive analysis of this approximation is deferred to future work.

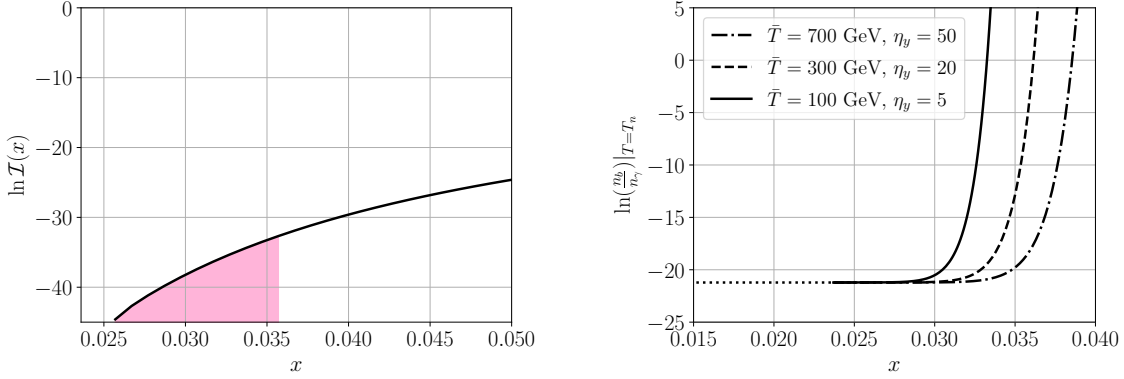


Figure 8: Left: logarithm of the 3D washout integral $\mathcal{I}(x)$. Since the function increases exponentially rapidly, survival of any baryon asymmetry is limited to a small range of $\bar{x} < x < \hat{x} \lesssim 0.036$ (pink). Right: the required initial baryon asymmetry at the nucleation temperature, that leads to the observed value of η , as function of x (i.e. the y -axis is given by Eq. (4.20)). The horizontal dotted line represents the logarithm of the observed baryon asymmetry, the Eq. (1.1). For $x > \bar{x} = 0.025$, the washout exponent \mathcal{W} grows exponentially with x , resulting in an exponential rise along the y -axis.

where $\bar{T} \equiv \frac{1}{2}(T_* + T_n)$. Here we have taken the factor $\bar{T}/H(\bar{T})$ ³⁴ outside of the integral, given that the integration is dominated by the exponential, and hence this factor can be approximated as a constant, as well as the factor η_y^{-1} .

The usefulness of the expression Eq. (4.16) lies in a fact that we have factorized UV and IR contributions, i.e. thermal contributions of a parent theory and contributions of the 3D EFT, respectively. For the pure 3D part of the wash-out integral we obtain a closed form expression

$$\mathcal{I}(x) \equiv \int_{y_*}^{y_n} e^{-\hat{S}_{3D}(x,y)} dy = \left[e^{-\hat{S}_{3D}(x,y)} \left(\frac{4x}{841} + \frac{\sqrt{\frac{9}{2} - 512\pi^2 xy}}{232\pi} \right) \right]_{y_f}^{y_n}, \quad (4.17)$$

This result for $\mathcal{I}(x)$ is depicted in Fig. 8 (left).

In summary, the washout exponent can be computed using

$$\mathcal{W} \approx 2N_\rho \frac{\bar{T}}{H(\bar{T})\eta_y(\bar{T})} \times \mathcal{I}(x), \quad (4.18)$$

where terms are factorized into UV and IR parts, respectively, that are evaluated using the

³⁴This quantity is numerically large and slowly varying with temperature; for example, $\bar{T}/H(\bar{T}) \approx e^{36.5}$ when $\bar{T} \simeq 100$ GeV.

dimensional reduction mapping into the (x, y) -plane. For any 3D EFT mapping $(x(T), y(T))$, crossing with y_c , y_n and y_* determines T_c , T_n and T_* , respectively, c.f. Fig. 7.

As we have already seen, for very strong transitions with $x < \bar{x} \approx 0.025$ sphalerons are immediately shut off when the transition starts, since $T_* > T_n$. This allows us to define a strong version of the baryon number preservation condition (BNPC)

$$\text{“Strong BNPC”}: \quad x(T_n) < \bar{x} \approx 0.025, \quad (4.19)$$

at the leading order of the perturbation theory. We note, that typically in dimensional reduction mapping x depends on temperature weakly, and hence $x(T_n) \approx x(T_c)$.³⁵ For parameter points which satisfy the strong BNPC, C- and CP-violating processes are constrained to produce the experimentally observed amount of baryon asymmetry, without any washout.

For slightly larger values of x , the baryon number density gets washed out by a factor of $e^{-\mathcal{W}}$. Since the exponent \mathcal{W} increases exponentially with x , the baryon number density before the bubble nucleation needs to be incredibly huge to survive the washout. Instead of investigating which mechanism could produce such a large baryon number density, we put an upper bound on \mathcal{W} by hand as $\mathcal{W} \lesssim 100$ which results in an upper bound on $x < \hat{x}$ and we get a weaker form of BNPC:

$$\text{“Weak BNPC”}: \quad \ln\left(\frac{n_b}{n_\gamma}\right)|_{T=T_n} = \mathcal{W} + \ln \eta \implies \bar{x} < x(T_n) < \hat{x} \approx 0.036. \quad (4.20)$$

This ties together the required initial baryon asymmetry at T_n , and x , as well as η_y and \bar{T} , both of which are determined through temperature evolution of $y(T)$. This relationship is illustrated in the Fig. 8 (right). We note, that since $\mathcal{I}(x)$ is exponentially rapidly increasing, regardless of T -dependence of $y(T)$, the weak BNPC requires $x_n < \hat{x} \approx 0.036$. According to the weaker form of BNPC, if C- and CP-violating processes generate over-abundance of baryon asymmetry, it is still possible to wash it out to produce experimentally observed asymmetry. For larger values $\hat{x} < x \lesssim 0.1$ that still govern first-order transitions, exponential washout can be expected to dilute any potential initial asymmetry.

In summary, for any BSM theory that maps onto the SU(2) + Higgs 3D EFT at high temperatures and has a first-order phase transition, indicated by $x_c \lesssim 0.1$, preserving any generated baryon number necessarily requires $x_c \lesssim 0.036$ (assuming $x_n \approx x_c$). If $x_c < \bar{x} \approx 0.025$ then all generated baryon number is automatically preserved (strong BNPC), while for $\bar{x} < x_c < \hat{x} \approx 0.036$ the Eq. (4.20) has to be satisfied (weak BNPC). We note, that despite us working merely at leading order in the semi-classical approximation, we have obtained bounds on x that agree fairly well with seminal studies in [88, 90, 113].

³⁵Translating this bound to the Higgs expectation value gives $\frac{v_c}{T_c} = \sqrt{2} \frac{g_3 v_3(y_c)}{\sqrt{T_c}} = \frac{g}{8\pi x_c} > 1.03$, for $x_c < \bar{x}$ and $g^2 = 0.42$, which agrees fairly well with [90], yet we point out that here $\frac{v_c}{T_c}$ is the leading order result for the Higgs condensate, which is gauge-independent.

5. Application to Real Triplet-Extended Standard Model

Finally, we turn to a concrete BSM application where a real triplet scalar is used to catalyze a first-order phase transition.³⁶ We choose to work with this particular BSM extension, as its dimensional reduction has been well-documented [247], and its phase structure has been previously studied in terms of non-perturbative lattice simulations [202]. In particular, we can integrate out the triplet in wide regions of the model parameter space (c.f. [247]), and hence use tools developed in the previous sections, to study sphaleron freeze-out and washout in the Higgs phase. We stress, that any other Higgs portal model can be studied along these lines, at least in a part of its full parameter space.

In this model, the Standard Model Lagrangian is augmented with

$$\mathcal{L}_{\text{triplet}}(\phi, \Sigma) = \frac{1}{2}(D_\mu \Sigma^a)^2 + \frac{1}{2}\mu_\Sigma^2 \Sigma^a \Sigma^a + \frac{b_4}{4}(\Sigma^a \Sigma^a)^2 + \frac{a_2}{2}\phi^\dagger \phi \Sigma^a \Sigma^a, \quad (5.1)$$

where the triplet Σ^a transforms, as the name suggests, as an adjoint under SU(2), with isospin index $a = 1, 2, 3$, and trivially under SU(3) and U(1) groups. Our definition of the covariant derivative aligns with [247], and convention for the sign of the mass term that of [85]. Electroweak phase transition in this model has been previously studied perturbatively in [85, 183, 247–249] and using non-perturbative lattice simulations in [202].

At high temperatures, we work in a setup where the triplet field is sufficiently heavy at the soft scale 3D EFT, so it can be further integrated along with temporal modes of the gauge fields. Details of this 3D EFT and its dimensional reduction mapping can be found in [247, 250] (and can be reproduced in automated fashion using `DRalgo` package [220, 233]). In short, thermal masses (couplings) are determined at two-loop (one-loop), as is customary for dimensional reduction [78]. This setup in which we integrate out the soft triplet allows us to study triplet-induced one-step phase transitions. When soft modes are integrated, at one-loop order

$$\lambda_3 = \lambda_{3,\text{hard}} - \frac{1}{8\pi} \frac{h_3^2}{m_D} - \frac{1}{8\pi} \frac{3}{4} \frac{a_{2,3}^2}{\mu_{\Sigma,3}}, \quad (5.2)$$

where we $\lambda_{3,\text{hard}}$ is the 3D self-coupling before integrating out the soft modes,³⁷ and results for the SU(2) Debye mass m_D and the Higgs-temporal portal coupling h_3 can be found in [247]. We did not write contributions from U(1) temporal modes (see [247]), for simplicity, as it is not essential to our following discussion. The main mechanism for the triplet to reduce the effective Higgs self-coupling λ_3 (and hence x)³⁸ is the soft triplet contribution

³⁶This model does not introduce new sources for CP-violation, and as such can only be used as a probe or theoretical template for studying sphaleron-related aspects of the EWBG.

³⁷Note, that our $\lambda_{3,\text{hard}}$ is denoted as λ_3 , and our λ_3 as $\bar{\lambda}_3$ in [247], and we have chosen our notation here to be consistent with the earlier sections.

³⁸Triplet also contributes to the effective gauge coupling g_3^2 , but these effects are completely subdominant in x , compared to the triplet effects in λ_3 , see [247].

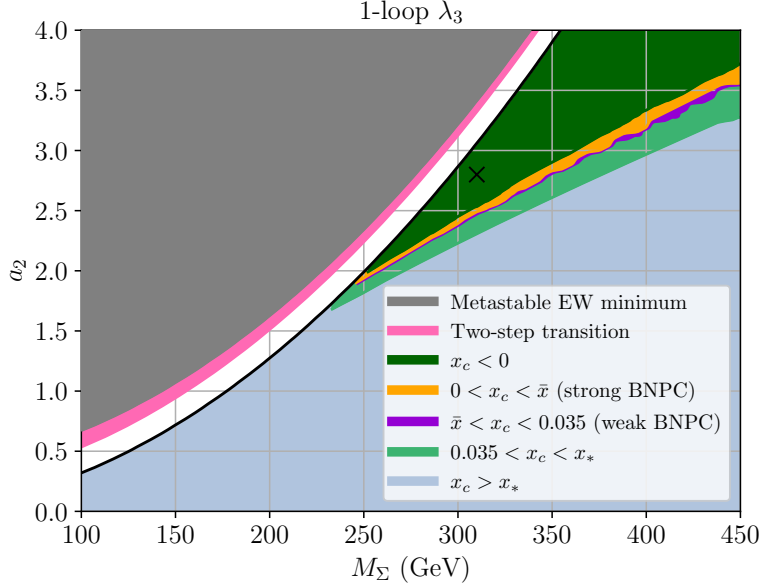


Figure 9: Phase structure of the triplet-extended SM in (M_Σ, a_2) -plane with $b_4 = 0.25$ based on one-loop result for λ_3 , depicting different regions where BNPC can be satisfied in the one-step transition region. In white region, triplet mass parameter $\mu_\Sigma^2 < 0$ and the triplet cannot (necessarily) be integrated out. In region with $x_c < 0$ (dark green) 3D EFT construction fails, which signals that some higher order contributions are missing.

in Eq. (5.2), while triplet contributions in $\lambda_{3,\text{hard}}$ have subdominant effects: triplet affects $\lambda_{3,\text{hard}}$ by corrections from hard modes, as well as modifying the $\overline{\text{MS}}$ value of λ at initial M_Z -scale through one-loop zero temperature corrections [247].

To proceed with numerics, we fix $b_4 = 0.25$ and compute the critical value $x_c = x(T_c)$, where the critical temperature T_c is determined through leading order perturbative result $y(T_c) = y_c(x_c)$, in a uniform scan in the (M_Σ, a_2) -plane, where M_Σ is the physical triplet pole mass. Our result is shown in Fig. 9. In the gray region, the electroweak Higgs phase is not global minimum at zero temperature, and is hence excluded. Solid black line denotes a contour of $\mu_\Sigma^2 = 0$, and above this line – in white region – μ_Σ^2 is negative, indicating that the triplet can undergo a phase transition of its own at some temperature range, so in this region we do not integrate out the triplet. In principle, there can also be first-order one-step electroweak phase transitions in this region, but our approximation does not allow us to describe them accurately.³⁹ In the pink region, the electroweak phase transition proceeds

³⁹In region with $\mu_\Sigma^2 < 0$, one can integrate out the triplet in a different manner, following [85, 140]: in a temperature window where the triplet mass eigenvalue $m_\Sigma^2 \equiv \mu_\Sigma^2 + \frac{1}{2}a_{2,3}v_3^2$ is dominated by the Higgs

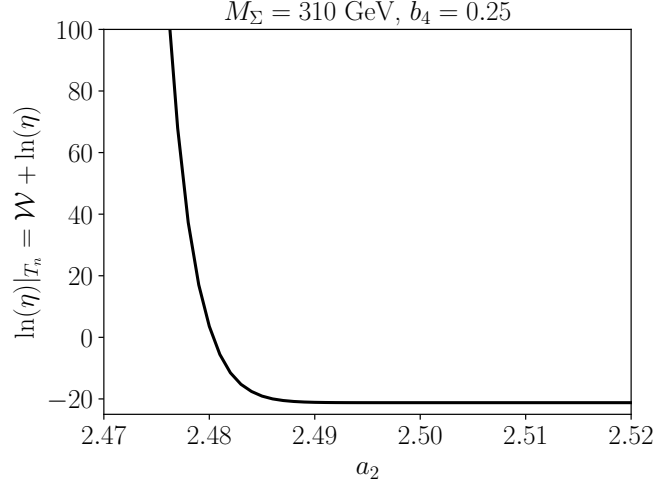


Figure 10: Initial baryon asymmetry $\ln \eta$ at T_n , that produces the observed value, as dictated by the washout exponent as function of a_2 .

in two steps, according to leading order perturbation theory, c.f. [202]. In light blue region, $x_c > x_* \approx 0.1$, and there is no phase transition but a crossover.

For our analysis, the most interesting regions are those with $x_c < x_*$ that display a first-order one-step transition, albeit in the dark green region $x_c < 0$ and our final 3D EFT is not valid, as its scalar potential is not bounded from below due to the negative effective Higgs self-coupling. This is a clear signal that some higher order corrections are missing, either higher-order loop corrections to $\bar{\lambda}_3$, or higher-dimensional, marginal operators. We return to this issue below, but point out, that non-perturbative simulations of [202] confirm that there indeed is a first-order phase transition in the point $M_\Sigma = 310$ GeV and $a_2 = 2.8$ (x marks the spot in Figs. 9 and 11). In light green region, we find a first-order phase transitions that are too weak to prevent the sphaleron washout, while regions shown in purple and orange satisfy weak and strong BNPC, respectively. We observe, that these regions are relatively narrow, especially the regime of the weak BNPC. This region (purple) is also prone to artificial numerical issues (wobbles) related to interpolation, which however could be eliminated by an extremely dense (and hence much slower) scan.

We illustrate the sphaleron washout further in Fig. 10, by fixing $M_\Sigma = 310$ GeV and plotting the initial asymmetry $\ln(\eta)$ at T_n at the onset of the transition, that is required to produce the observed asymmetry, as function of a_2 (we compute the sphaleron washout exponent \mathcal{W} in accord to Eq. (4.18)). In this example case, when we vary $a_2 \in [2.47, 2.52]$

background field v_3 , one can study the phase transition in terms of a supersoft EFT expansion. Here, we do not perform such analysis.

we have $x_c \in [0.036, 0.011]$ and $\eta_y \approx 5.75$ for all a_2 . Interpretation of this result is clear: for $a_2 \gtrsim 2.497$ strong BNPC holds and there is no washout, which would enforce a constraint to produce the exact observed asymmetry at the bubble wall (should this be a realistic model for the EWBG with extra sources for CP-violation, as explained earlier). For slightly smaller values of a_2 the washout sets a tight constraint to produce much larger asymmetry at the bubble wall. This example illustrates, that if there would be an additional constraint from the CP-violation side of the computation for an upper bound for asymmetry that could be generated, it would put a tight constraint on the lower bound for the portal coupling. This is, of course, a simplified interpretation as in reality values of M_Σ and b_4 also effect the situation, yet illustrates the fact that we have now a tool for such analyses.

Our discussion so far exemplifies how the minimal SU(2) gauge-Higgs 3D EFT can be used to study the sphaleron rate and to impose the BNPC in a part of parameter space of a BSM theory. Until now, we have used the exactly same dimensional reduction mapping as in [247] and in particular, determined λ_3 (Eq. (5.2)) at one-loop (this is the same accuracy used in e.g. [251, 252] in the context of the Two-Higgs Doublet Model).

However, using the mere one-loop result of Eq. (5.2) has a following crucial caveat, in a context general to all Higgs portal models as pointed out in [93, 140]. When the soft triplet is integrated out, its dominant contributions to the Higgs effective self-coupling come as a perturbative expansion in $a_{2,3}/(4\pi\mu_{\Sigma,3})$. The triplet 3D mass can indeed be large enough to justify to integrate the triplet out, e.g. $\mu_{\Sigma,3} > m_D$ compared to the Debye mass of the temporal scalar, but the 3D portal coupling $a_{2,3}$ is also required to be large enough to make it possible to reduce x_c enough compared to its SM value $x_c \approx 0.29$. For this reason, the perturbative expansion for the soft triplet modes converges much slower compared to the expansion for temporal gauge field modes, which is expansion in $h_3/(4\pi m_D)$. For example, for the parameter space point $M_\Sigma = 310$ GeV and $a_2 = 2.8$ (marked by x in Fig. 9) around the critical temperature we find $h_3/(4\pi m_D) \approx 0.01$ but for the triplet $a_{2,3}/(4\pi\mu_{\Sigma,3}) \approx 0.25$. This implies, that while further corrections from the temporal gauge field mode are miniscule, triplet corrections at two-loop and beyond can have a significant effect.

To scrutinize this, we compute such two-loop corrections from the soft triplet for the first time and find overall

$$\begin{aligned} \lambda_3 = \lambda_{3,\text{hard}} - \frac{1}{8\pi} \frac{h_3^2}{m_D} - \frac{1}{8\pi} \frac{3}{4} \frac{a_{2,3}^2}{\mu_{\Sigma,3}} \\ + \frac{1}{(4\pi)^2 \mu_{\Sigma,3}^2} \left(\frac{3}{4} a_{2,3}^3 - \frac{3}{2} a_{2,3}^2 g_3^2 + \frac{3}{8} a_{2,3} g_3^4 - \frac{1}{128} (3g_3^6 + g_3^4 g_3'^2) \right). \end{aligned} \quad (5.3)$$

Within the two-loop corrections on the second line, the term proportional to $a_{2,3}^3$ indeed dominates over the other terms.

In Fig. 11 (top left) we depict our results similar to Fig. 9 but with two-loop corrections in accord with Eq. (5.3). Strikingly, these two-loop corrections have a rather dramatic effect:

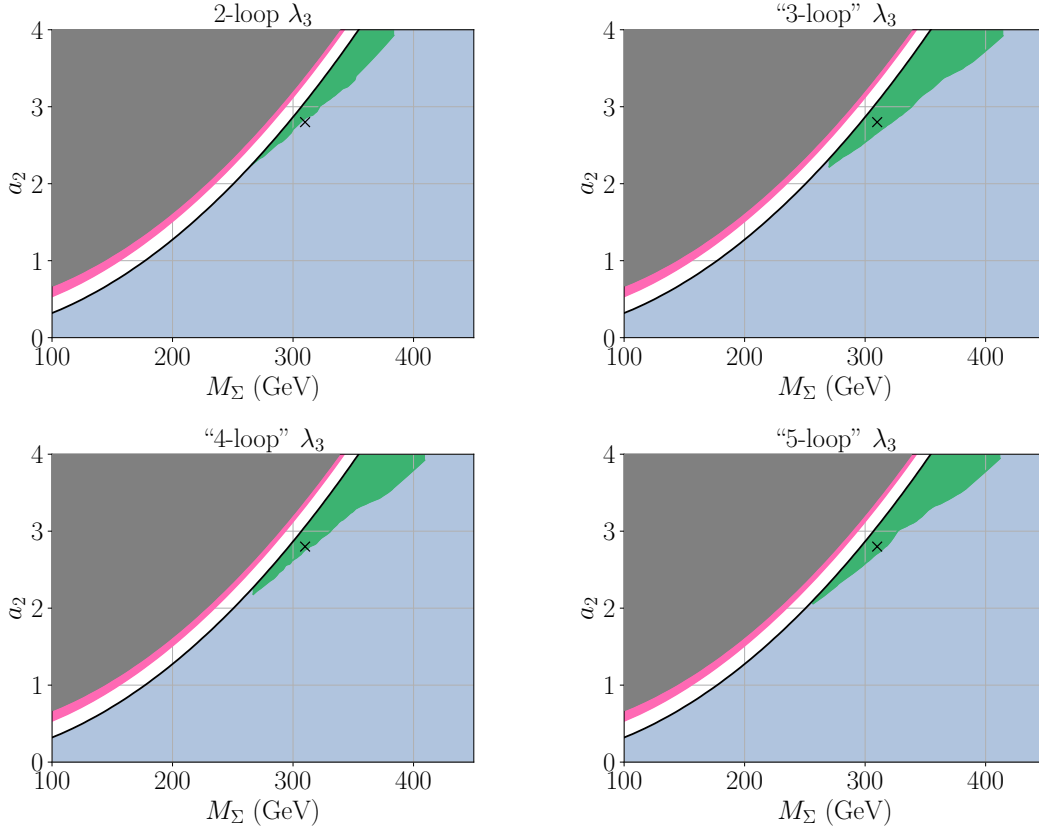


Figure 11: Similar to Fig. 9, but with full two-loop corrections to λ_3 from Eq. (5.3) (top left) and estimated higher loop effects of Eq. (5.4). Crucially, contrary to Fig. 9 there are no regions where the BNPC can be satisfied (as $x_c > 0.06$ for all the points), when full two-loop effects are accounted.

the small x_c region indicating first-order phase transitions in Fig. 9 shrinks significantly. This vividly highlights the fact that even predicting the character of a phase transition correctly, i.e. to ensure the existence of a first-order phase transition, is far more non-trivial than most often realized in the literature of phase transitions and their cosmological ramifications. In other words, predictions for all parameter space points in Fig. 9 that indicate first-order phase transitions, are not just quantitatively inaccurate, but qualitatively incorrect as there is no phase transitions but a crossover. Furthermore all points displaying first-order transitions have $x_c \gtrsim 0.06$, i.e. the most strongest transitions (as well as the region with $x_c < 0$) are completely absent. This indicates, that all one-step transitions in the region that can be studied by integrating out the soft triplet are rather weak, and hence can not prevent sphaleron washout (and hence would exclude the EWBG even if one would devise additional C- and CP-violations to produce the initial asymmetry).

In order to further inspect the convergence, we envision a following form for further higher order corrections

$$-c_3 \frac{1}{(4\pi)^3} \frac{a_{2,3}^4}{\mu_{\Sigma,3}^3} + c_4 \frac{1}{(4\pi)^4} \frac{a_{2,3}^5}{\mu_{\Sigma,3}^4} - c_5 \frac{1}{(4\pi)^5} \frac{a_{2,3}^6}{\mu_{\Sigma,3}^5}, \quad (5.4)$$

at three-, four- and five-loops based on the expansion parameter, where c_3 , c_4 and c_5 are numerical coefficients that would need to be determined by direct computation. We do not perform such computations here, but merely use the above form as a heuristic, semi-quantitative probe for convergence, and for this we fix each numerical coefficient to unity: a choice which is arbitrary, but it turns out that our conclusions are not terribly sensitive to this particular choice.

We show the result of these heuristic estimates in other panels of Fig. 11, and observe that while the boundary of first-order transition and crossover regions slightly shift, our conclusion from adding two-loop corrections remains intact: none of the transitions are strong enough to prevent the sphaleron washout. Furthermore, by inspecting heuristically the higher order corrections, we gain confidence that the full two-loop result we have used could be fairly accurate. This confidence is boosted by the non-perturbative confirmation of the first-order one-step transition in a single test point, marked by x in Fig. 11.

This brings us to our final conclusion for (radiatively-generated) first-order, one-step phase transitions in Higgs portal models, which we summarize as

- Reliable analyses of phase transition thermodynamics — including ensuring the existence of the transition – and sphaleron properties, require to consistently include *all two-loop* thermal corrections related to the hard thermal scale (thermal resummations in dimensional reduction) and corrections from the soft scale perturbation theory (within the 3D EFT), if soft-scale extra scalar fields are used to trigger the phase transition.

This conclusion aligns with those previously obtained in e.g. [93, 179, 253] (see also [254]). In this context, ubiquitous one-loop studies of the EWBG in the literature, let alone studies that do not consider thermal resummations at all but resort to mere leading order high-temperature expansions (perhaps with a motive to avoid spurious gauge-dependence, which would be an outcome of incorrect formulation of the perturbative expansion) could be not merely quantitatively inaccurate, but qualitatively flawed. This would be the case, if there is no phase transition but a crossover, or if a first-order phase transition exists but is far too weak to prevent the washout.

We remark, that based on our study in this work at hand alone, above conclusion can not be drawn for multi-step phase transitions that are not necessarily induced radiatively by the soft-scale loops. However, even for such multi-step phase transitions similar soft scale two-loop corrections have found to be crucially important for quantitatively reliable perturbative analyses, c.f. [85].

6. Conclusions and Perspectives

We conclude by summarizing our present work and by providing further discussion and outlook.

6.1. Summary

In this article, working with high temperature effective field theory (3D EFT), we have reformulated the perturbative computation of (the statistical part of) the Higgs phase sphaleron rate. This reformulation was designed to ensure that (i) large thermal resummations are incorporated, (ii) results are gauge-invariant, and (iii) calculations are based on a consistent perturbative expansion that avoids double counting at higher orders (for the sphaleron determinant).

We concretely demonstrated features (i) and (ii) (bringing clarity to issues raised in [89]), but relegated the aspect (iii) to future work, postponing the computation of the sphaleron determinant. We remark, that at present the dynamical, real-time part of the sphaleron rate is entirely out-of-reach of our formulation.

Besides solely theoretical motives to seek a sound perturbative formulation for the Higgs phase sphaleron rate, there is also a clear practical motive: for more complicated BSM theories that include several light scalar fields within the 3D EFT, at present there are no lattice simulations for the sphaleron rate. Furthermore, due to the expense of such lattice simulations, scanning of wide free parameter spaces are not feasible without a perturbative approach. In this work at hand, we have worked towards such a general perturbative formulation, yet limited our investigations for the minimal 3D EFT used previously for the SM at high temperatures.

Concretely, within the 3D EFT that captures large thermal corrections (thermal resummations), we resorted to a semi-classical approximation for the sphaleron rate. We found that the sphaleron action is dominated by the Yang-Mills and scalar covariant kinetic terms, while the scalar potential itself results directly in a sub-leading effect. By rescaling the sphaleron action, we found a powerful formulation of the action in terms of the expectation value of the scalar condensate (c.f. [255]), and we could further approximate the rate by simple analytic fitting formulae.

To put our semi-classical computation to test, we compared it directly to previous non-perturbative lattice simulations of the sphaleron rate for temperatures below the Standard Model crossover and found a reasonable agreement. In the same SU(2) gauge-Higgs 3D EFT a first-order phase transition requires the ratio of the effective thermal Higgs self-coupling and the effective gauge coupling to be small enough, i.e. $x \equiv \lambda_3/g_3^2 \lesssim 0.1$ at the critical temperature. While this condition is not met in the SM, in many BSM extensions with extra fields this criterion could be realized (when extra scalars are sufficiently heavy at high

temperatures, and can hence be integrated out from the 3D EFT).

For such first-order phase transitions, we combined our computation of the sphaleron rate in the Higgs phase with perturbative treatment of the bubble nucleation rate, and formulated conditions for avoiding the sphaleron washout that would erase any baryon asymmetry generated in front of expanding bubble walls. Concretely, we found that the washout is not possible at all for $x \lesssim 0.025$ as sphalerons decouple in the Higgs phase immediately when bubbles can nucleate, while for $0.025 \lesssim x \lesssim 0.036$ sphalerons can (exponentially) washout more or less any amount of asymmetry while still providing the observed asymmetry, yet such balancing sets a tight constraint on the initial asymmetry and x .⁴⁰

As a direct application, we demonstrated these calculations for the real triplet-extended Standard Model in parts of the parameter space that can be mapped into the 3D EFT we have considered. Crucially, we found out that taking into account two-loop order corrections for x by integrating out the heavy triplet, none of one-step the transitions (that can be found in this particular 3D EFT framework and have been reported in the past) were strong enough to prevent total washout. Such result demonstrates that this part of the parameter space would be ruled out as a possible explanation for the baryogenesis, even if it would be incorporated with a mechanism to add new sources of C- and CP-violation to generate the initial asymmetry across the bubble wall.

Furthermore, we emphasized that to reach this conclusion, aforementioned two-loop corrections to x (or λ_3) – that were not considered in earlier studies – studies, were crucial. This conclusion does not come as a surprise, as by now there are ample examples in the literature that have highlighted the importance of thermal two-loop effects. This further raises serious doubts on reliability of low-order computations for the sphaleron rate and phase transition thermodynamics in general, in myriad studies of the past and present literature.

6.2. Discussion and Outlook

Next, let us provide some perspectives by reflecting our present work to the past literature, and envisioning future directions.

v_c/T_c : gauge-dependence and convergence We stress that ensuring the existence of a first-order phase transition is more non-trivial than often appreciated in the vast literature. Indeed, myriads of EWBG studies in BSM theories (c.f. e.g. [53–55, 115, 256–275]) resort to a condition $v_c/T_c \gtrsim 1$ for the existence of a strong enough first-order phase transition (strong enough to prevent sphalerons washing out the baryon asymmetry in the Higgs phase), where

⁴⁰Note, that here one assumes that x is a constant within a range of temperatures from T_c to T_n and T_f , i.e. critical, nucleation and sphaleron decoupling temperatures. This assumption could be relaxed, which leads to more specific, model-dependent conditions between x_c , x_n and x_* , dictated by $x = x(T)$ dimensional reduction mapping.

v_c is the Higgs field expectation value at the critical temperature T_c . Such approaches are plagued by two problems: gauge dependence and (at first sight) bad convergence.

As discussed in detail in [89, 276], the quantity v_c/T_c is gauge-dependent and hence unphysical: according to the Nielsen-Fuguda-Kugo identities [277, 278], only the values of the effective potential at its extrema are gauge invariant, but the field values of extrema can be shifted around in terms of a gauge fixing parameter. More often than not, this fact has been ignored, and otherwise serious calculations have been performed simply in Landau gauge as a leap of faith. Landau gauge greatly simplifies computations of the thermal effective potential, and v_c/T_c (in Landau gauge) has been observed to positively correlate with the phase transition strength in terms of the latent heat, a physical observable obtainable by gauge-invariant means (see e.g. [199, 234, 257, 279]), and hence v_c/T_c has been used as a heuristic measure of existence of a first-order phase transition, which is characterized by a discontinuity in its free-energy.

However, such discontinuity exists in perturbation theory whenever two minima of the thermal effective potential are separated by a barrier, and hence in such cases perturbation theory always predicts a first-order transition. This is in stark contrast with non-perturbative simulations, that can reveal that there is no phase transition at all, but a crossover (see e.g. [83, 88] and recent [254] for a BSM application). On the otherhand, such simulations have also indicated, that transitions that are strong according to the perturbation theory, are also of first order non-perturbatively.

On the surface, this might be taken as absolution for using v_c/T_c in Landau gauge as a (heuristic) measure of the phase transition strength and limiting to large enough values, but this strategy is short-lived, upon closer examination: lots of studies have resorted to using ring-resummed thermal effective potential at one-loop order, but it has been known for a long time that large two-loop thermal corrections can jeopardize such analyses [131, 132, 280]. In a recent work [93] it has been shown that such two-loop corrections can not only strengthen transitions compared to one-loop, but also significantly weaken them so much that there is no indication for a first-order transition. In general, two-loop corrections were found to lead to narrower regions of strong first-order transitions in a large-scale parameter space scan of a BSM theory (see also [179, 253]).

On the otherhand, one might then wonder why a two-loop result would be any more reliable than a one-loop result, if the overall convergence is bad? It has turned out, that convergence at high temperatures is often not bad at all, but rather *slow*: thermally enhanced bosonic contributions hamper the perturbative expansion (and require resummations), and reaching the same accuracy as zero temperature analogues requires significantly more work with two-loop (and even three-loop [140, 200, 228, 281]) calculations [92, 131, 132]. These higher order calculations beyond the realm of one-loop resummations have been shown to provide remarkable agreements with lattice simulations, for strong phase transitions [82, 85, 140,

Previous (gauge-invariant) results for BNPC Contrasting our results for baryon number preservation condition in terms of bounds on x to previous results in [90, 113], we found a fair agreement, yet point out that our bound $x \lesssim 0.025$ to prevent the washout entirely is slightly stronger. This indicates that the electroweak phase transition has to be even stronger than previously believed, in order to prevent the washout completely. We note, that while the results for the sphaleron rate in [90, 113] are non-perturbative and hence superior to our leading, semi-classical approximation, the treatment of the bubble nucleation in these references was not accounted up to same standard, with the modern 3D EFT picture for the bubble nucleation [83, 86].

It is illuminating to further reflect our perturbative formulation to a discussion in [113]. Therein, it is argued that it is in fact easier to perform non-perturbative simulation of the sphaleron rate, rather than to perform it at “two loops” in perturbation theory, meaning two-loop corrections beyond the one-loop determinant. Arguably, such computation indeed resembles a nightmare: one has to compute such corrections around spatially varying sphaleron background, which requires using propagators based on Green’s functions that have to be determined (and eventually integrated) numerically inside two-loop diagrams (this can be compared with an analogous situation with the bubble nucleation [210] or vacuum tunneling [284]).

Ref. [113] expects such two-loop corrections to be of sizable importance, as two-loop corrections were known to be large for the expectation value of the Higgs condensate $\sqrt{\langle \phi_3^\dagger \phi_3 \rangle}$ (in the 3D EFT), that contributes to the height of the sphaleron barrier. Ref. [113] correctly addresses that the perturbative expansion for the condensate is at best an expansion in λ_3/g_3^2 , and concludes that there is no known reason why the expansion for the sphaleron rate should be any better, i.e. why two-loop effects for it would be less important. But now such reason is indeed known, as it has been worked out that the expansion for the Higgs condensate is an expansion in $\sqrt{\lambda_3/g_3^2}$ [82, 140] and, crucially, it does not align with a loop expansion: the result for the condensate at leading order includes contribution from gauge bosons at one-loop, and their two-loop contribution gives first correction suppressed by λ_3/g_3^2 (with all further corrections suppressed by $\sqrt{\lambda_3/g_3^2}$). Intuitively, such expansion appears since the scale of the phase transition is not the soft, but rather the supersoft scale deeper in the IR.

For the sphaleron rate on the otherhand, already the one-loop determinant is suppressed by factor λ_3/g_3^2 , and based on a physical picture of [85], the expansion parameter for the

⁴¹We stress, that both the lattice and perturbative calculations are based on high-temperature expansions, which might fail in presence of large BSM couplings, and large background field values in case of strong transitions, that lead to large masses in the Higgs phase. Hence, it is crucial to scrutinize the validity of the high- T expansion, see [282, 283].

sphaleron rate is λ_3/g_3^2 because sphalerons live at the soft scale, i.e. aforementioned complicated two-loop corrections around the sphaleron background are further suppressed as $(\lambda_3/g_3^2)^2$, and have parametrically same suppression as three-loop corrections to the Higgs condensate [140]. Therefore, we can expect that already a one-loop computation within the 3D EFT for the sphaleron rate is fairly accurate, assuming one still accounts for two-loop level hard scale corrections in dimensional reduction mapping into the 3D EFT. Consequently, for the sphaleron rate we expect better convergence than for the bubble nucleation rate [211], as characteristic scale for the sphaleron is higher in UV than the scale of the critical bubble, and hence perturbation theory convergences faster.

This discussion is supported by the results of [87] that included the computation of the sphaleron determinant (in 3D EFT), and its great agreement with non-perturbative simulations in [172–174]. This certainly motivates to push our present formulation one order further, and compute the sphaleron determinant in future works.

Outlook As for other future prospects, our findings motivate to perform a set of fresh lattice simulations for the sphaleron rate akin to [172–174] without using any concrete dimensional reduction mapping, but for all (input) y and x within the 3D EFT, with x in range relevant for first-order phase transitions (in analogue for simulations of the bubble nucleation rate in [83]). This would ultimately test reliability of our perturbative computation⁴² (and future computations of the sphaleron determinant), and our results for the baryon number preservation condition. We note, that since such comparison for the sphaleron rate has already provided a fair agreement in the case of $x = 0.29$ relevant for temperatures below the Standard Model crossover, we can expect similar (or better) agreement for smaller x as well, since the perturbative expansion of the sphaleron rate is in positive integer powers of x .

Furthermore, our perturbative formulation of the sphaleron rate can be generalized to other 3D EFTs, where BSM fields that catalyze first-order phase transitions are light and are not integrated out. In such case, new fields contribute in the sphaleron equations of motion and sphaleron action, and their effect for the bubble nucleation has to be accounted as well. This is especially relevant for strong two-step phase transitions, prominent to produce strong primordial gravitational wave signatures. To study both the EWBG and gravitational wave production in such scenarios using 3D EFTs, computational tools such as `DRalgo` [220, 233] for the EFT construction can be utilized, and computations of gravitational wave thermal parameters follow those presented in [92, 248, 286, 287], and for computing previously elusive terminal velocity of the bubble wall, a new code `WallGo` [288] could be used.

Finally, we envision that our perturbative formulation for the Higgs phase sphaleron rate

⁴²In principle, one – with enough valor – could also strive for studying the real-time, HTL-resummed effects to the dynamical part of the sphaleron rate in BSM theories, c.f. [160, 161, 164, 210, 213, 285].

can be used in the future in an end-to-end computation of the electroweak baryogenesis, under a concrete BSM theory that contains all necessary ingredients including new sources for C- and CP-violation and consistent predictions for generated initial asymmetry across the bubble wall. Combined with BSM collider phenomenology for such a model, this would allow to probe concrete and testable scenarios of what lies beyond the Standard Model – reliably with refined theoretical tools for thermal bubble and sphaleron dynamics – with aim to explain the observed baryon asymmetry of our universe.

Acknowledgments

We thank Jaakko Annala, Andreas Ekstedt, Leon Friedrich, Oliver Gould, Joonas Hirvonen, Jaakko Hällfors, Xiyuan Jin, Benoît Laurent, Johan Löfgren, Tobias Rindlisbacher, Lauri Niemi, Kari Rummukainen, Riikka Seppä, Ville Vaskonen, Jorinde van de Vis, Guotao Xia and Jiang Zhu for illuminating discussions. This work was supported in part by National Natural Science Foundation of China grant 12375094 (MJRM and YW) and partly funded by the European Union (ERC, CoCoS, 101142449). TT thanks Nils Hermansson-Truedsson and University of Edinburgh, Djuna Croon and Durham University, as well as Oliver Gould and University of Nottingham, for hospitality during completion part of this work.

A. Properties of Sphaleron Ansatz, Action, and Equations of Motion

In this appendix, we present more details about the sphaleron ansatz, action and equations of motion.

Sphaleron 3D ansatz We propose the sphaleron ansatz in 3D that reads

$$\hat{A}_{i,3}^a T^a dx^i = [1 - f(\xi)] \sum_{i=1}^3 F_i T^i, \quad (\text{A.1})$$

where F_i are functions of the spherical coordinates θ and φ as well as a loop parameter μ [121]

$$\begin{aligned} F_1 &= - (2 \sin^2 \mu \cos(\mu - \varphi) - \sin 2\mu \cos \theta \sin(\mu - \varphi)) d\theta \\ &\quad - (\sin 2\mu \cos(\mu - \varphi) \sin \theta + \sin^2 \mu \sin 2\theta \sin(\mu - \varphi)) d\varphi, \\ F_2 &= - (2 \sin^2 \mu \sin(\mu - \varphi) + \sin 2\mu \cos \theta \cos(\mu - \varphi)) d\theta \\ &\quad + (-\sin 2\mu \sin(\mu - \varphi) \sin \theta + \sin^2 \mu \sin 2\theta \cos(\mu - \varphi)) d\varphi, \\ F_3 &= - \sin 2\mu \sin \theta d\theta + 2 \sin^2 \theta \sin^2 \mu d\varphi. \end{aligned} \quad (\text{A.2})$$

Technically, μ is the non-contractible loop parameter that connects topologically different vacua [11].

Now, we demonstrate that this 3D ansatz is consistent with the previous one in the full four-dimensional (4D) theory [232]. Relations (at leading order in dimensional reduction) between 3D and 4D fields is following: in 3D $A_{i,3}^a = g_3 \hat{A}_{i,3}^a$; and the 4D gauge field $A_i^a = \sqrt{T} A_{i,3}^a = g_3 \sqrt{T} \hat{A}_{i,3}^a = g T \hat{A}_{i,3}^a$, where $g_3 = g \sqrt{T}$ at leading order. Then, the gauge field ansatz in Eq.(3.18) implies the 4D gauge ansatz

$$A_i^a T^a dx^i = g T [1 - f(\xi)] \sum_{i=1}^3 F_i T^i, \quad (\text{A.3})$$

Since

$$\sum_{i=1}^3 F_i T^i = i(U^{\infty-1}) \partial_i U^{\infty}, \quad (\text{A.4})$$

where U^{∞} is the sphaleron matrix.⁴³ The ∂_i in dimensionless 3D theory differs a factor of $1/g_3^2$ with 4D, so we need to multiply by this factor for the 4D convention. Hence, the 4D gauge field sphaleron ansatz reads

$$A_i^a T^a dx^i = \frac{1}{g} [1 - f(\xi)] \sum_{i=1}^3 F_i T^i. \quad (\text{A.5})$$

which is the sphaleron ansatz in conventional 4D approach [58, 232]. Note that an additional scaling by v_3 (Eq. 3.20) does not alter the above conclusion, since the factor of v_3 cancels out when rescaling $\hat{A}_{i,3}$ and ∂_i .

Sphaleron action In the main text, the sphaleron action transforms into

$$\hat{S}_{3\text{D}} = v_3(x, y) \mathcal{C}_{\text{sph}}(x, y), \quad (\text{A.6})$$

where

$$\mathcal{C}_{\text{sph}}(x, y) = \int d^3\xi \left[\frac{1}{4} \hat{F}_{ij,3}^a \hat{F}_{ij,3}^a + (\hat{D}_i \hat{\phi})_3^\dagger (\hat{D}_i \hat{\phi})_3 + \bar{V}_3(\hat{\phi}_3, x, y) \right]. \quad (\text{A.7})$$

where we have omitted the prime on the transformed coordinates and fields. The transformed Yang-Mills and covariant derivative terms are given by

$$\frac{1}{4} \hat{F}_{ij,3}^a \hat{F}_{ij,3}^a = \frac{8(-1+f)^2 f^2 \sin^4 \mu}{\xi^4} + \frac{4f'^2 \sin^2 \mu}{\xi^2}, \quad (\text{A.8})$$

$$(\hat{D}_i \hat{\phi})_3^\dagger (\hat{D}_i \hat{\phi})_3 = \frac{[3J(1+J) - J_3^2 + (J+J^2 - 3J_3^2) \cos 2\theta] (-1+f)^2 h^2 \sin^2 \mu}{\xi^2} + h'^2, \quad (\text{A.9})$$

⁴³The construction of U^{∞} for a general $\text{SU}(2)$ scalar multiplet is given in Ref. [58]

where μ and θ are aforementioned sphaleron parameters, the prime on the radial profile functions denotes the derivative with respect to ξ , J refers to the representation dimension for scalar field under SU(2). The covariant derivative expression is given in a form of a general dimensional SU(2) multiplet, where for the SM complex doublet, $J = 1/2$ and $J_3 = 1/2$. The spherical angles φ, θ in the action can be integrated over, and remaining integration is over the radial parameter, such that

$$\mathcal{C}_{\text{sph}}(x, y) = \int_0^\infty d\xi [E_{\text{YM}}(\xi) + E_{\text{COD}}(\xi) + E_{\bar{V}}(\xi)] , \quad (\text{A.10})$$

where different terms refer to Yang-Mills, covariant derivative (“COD”) and potential terms, for which

$$E_{\text{YM}}(\xi) = 16\pi \sin^2 \mu \left[\frac{2(-1+f)^2 f^2 \sin^2 \mu}{\xi^2} + f'^2 \right] , \quad (\text{A.11})$$

$$E_{\text{COD}}(\xi) = \frac{4\pi}{3} [8J(1+J)(-1+f)^2 h^2 \sin^2 \mu + 3\xi^2 h'^2] , \quad (\text{A.12})$$

$$E_{\bar{V}}(\xi) = 4\pi \xi^2 \bar{V}_3(h) , \quad (\text{A.13})$$

where $\mu = \pi/2$ is taken for sphaleron energy, and the $\bar{V}_3(h)$ is defined through

$$\bar{V}_3(h) = \bar{V}_3\left(h, \mu = \frac{\pi}{2}\right) - \bar{V}_3\left(h, \mu = -\frac{\pi}{2}\right) . \quad (\text{A.14})$$

where $\mu = -\frac{\pi}{2}$ corresponds to the vacuum configuration. For more details, see Ref. [58].

Equations of motion The equations of motion for the radial profile functions can be obtained from the variation principle

$$f'' - \frac{2f(-1+f)(-1+2f)}{\xi^2} - \frac{2}{3}J(1+J)h^2 = 0 , \quad (\text{A.15})$$

$$h'' + \frac{2h'}{\xi} - \frac{8}{3\xi^2}J(1+J)(-1+f)^2 h - \frac{1}{2} \frac{\partial \bar{V}_3}{\partial h} = 0 . \quad (\text{A.16})$$

B. On Sphaleron Fluctuation Determinant

First, let us review the derivation of the sphaleron rate prefactor given in Ref. [124]. We start from the sphaleron rate expression, formulated as

$$\Gamma \simeq \frac{\omega_-}{2\pi} \text{Im} \left(\frac{\det g_3^{-2} \Omega_0^2}{\det g_3^{-2} \Omega_{\text{sph}}^2} \right)^{1/2} e^{-\beta E_{\text{sph}}} \quad (\text{B.1})$$

where $\beta \equiv 1/T$, and Ω_0^2 is the quadratic operator at the vacuum, and Ω_{sph}^2 is the quadratic operator at the sphaleron configuration. Translational invariance implies that Γ must be

proportional to the volume $V(\xi)$, which is $V_\xi = (gv)^3 V_r$ ($\xi = gvr$ in Ref. [124]). The V_ξ is dimensionless, and V_r is of dimension $[m]^{-3}$.

The zero modes must be integrated separately using the method of collective coordinates. When we integrate them out, we will obtain products of form $\mathcal{N}\mathcal{V}$ where \mathcal{N} is a normalization factor and \mathcal{V} is the volume of the symmetry group responsible for zero modes. There are four symmetries in the system: translations, rotations, the $SU(2)_L$ of the weak gauge group and the global, custodial $SU(2)_R$ of the Higgs sector. We get

- Translation: $\mathcal{N}_{\text{tr}} V_\xi = \mathcal{N}_{\text{tr}} (gv)^3 V_r$,
- Rotation: $(\mathcal{N}\mathcal{V})_{\text{rot}}$,
- $SU(2)_L$: the gauge freedoms are fixed, either local or global,
- $SU(2)_R$: turns out to be linear combination of others,

so that

$$\Gamma \simeq \frac{\omega_-}{2\pi} \mathcal{N}_{\text{tr}} V_r (\mathcal{N}\mathcal{V})_{\text{rot}} (gv)^3 g_3^{-N_0} \text{Im} \left(\frac{\det g_3^{-2} \Omega_0^2}{\det' g_3^{-2} \Omega_{\text{sph}}^2} \right)^{1/2} e^{-\beta E_{\text{sph}}} \quad (\text{B.2})$$

where the $g_3^{-N_0}$ is from the N_0 more eigenvalues in the numerator compared to denominator. We can transform this expression into a more familiar form

$$\Gamma_{\text{sph}} \equiv \frac{\Gamma}{V_r} \simeq \frac{\omega_-}{2\pi} \mathcal{N}_{\text{tr}} (\mathcal{N}\mathcal{V})_{\text{rot}} (gv)^3 g_3^{-6} \text{Im} \left(\frac{\det g_3^{-2} \Omega_0^2}{\det' g_3^{-2} \Omega_{\text{sph}}^2} \right)^{1/2} e^{-\beta E_{\text{sph}}} \quad (\text{B.3})$$

where we take $N_0 = 6$ for three translation and three rotations. The $(gv)^3 g_3^{-6}$ can be further written as

$$(gv)^3 g_3^{-6} = (4\pi\alpha_3)^{-3} (gv)^3 = \alpha_3^{-6} \left(\frac{gv}{4\pi} \right)^3 \left(\frac{gT}{4\pi v} \right)^3 = \alpha_3^{-6} \left(\frac{\alpha_W T}{4\pi} \right)^3, \quad (\text{B.4})$$

where we have used the relations

$$\alpha_3 = \frac{g_3^2}{4\pi} = \alpha_W \frac{T}{gv}, \quad \alpha_W = \frac{g^2}{4\pi}. \quad (\text{B.5})$$

By further denoting

$$\kappa \equiv \text{Im} \left(\frac{\det g_3^{-2} \Omega_0^2}{\det' g_3^{-2} \Omega_{\text{sph}}^2} \right)^{1/2}, \quad (\text{B.6})$$

the sphaleron rate expression of Eq. (B.3) can be expressed as

$$\Gamma_{\text{sph}} \simeq \frac{\omega_-}{2\pi} \mathcal{N}_{\text{tr}} (\mathcal{N}\mathcal{V})_{\text{rot}} \alpha_3^{-6} \left(\frac{\alpha_W T}{4\pi} \right)^3 \kappa e^{-\beta E_{\text{sph}}}. \quad (\text{B.7})$$

Next, we want to reformulate this expression using the language of the 3D EFT. Such derivation follows the same lines as above. We start from the $v_3(x, y)$ -scaled action

$$\hat{S}_{3D} = v_3(x, y) \mathcal{C}_{\text{sph}}(x, y). \quad (\text{B.8})$$

First, we need to notice that $\mathcal{N}_{\text{tr}} V_\xi = \mathcal{N}_{\text{tr}} v_3^3(x, y) g_3^6 V_r$. Second, we expect an additional $v_3^6(x, y)$ factor come from the six zero modes. Hence, the sphaleron rate can be written as

$$\Gamma_{\text{sph}} = \frac{\omega_-}{2\pi} \mathcal{N}_{\text{tr}}(\mathcal{N}\mathcal{V})_{\text{rot}} v_3^9(x, y) g_3^6 \kappa e^{-v_3(x, y) \mathcal{C}_{\text{sph}}} \quad (\text{B.9})$$

where the definition of κ is same with Eq.(B.6). The ω_- has mass dimension one, g_3^6 is of dimension three, Γ_{sph} is of dimension four and other quantities are dimensionless. The ω_- and $\mathcal{N}_{\text{tr}}(\mathcal{N}\mathcal{V})_{\text{rot}}$ are functions of x and y .

If we only keep the leading order result, the sphaleron rate is expressed as

$$\Gamma_{\text{sph}} = T^4 \times e^{-v_3(x, y) \mathcal{C}_{\text{sph}}}. \quad (\text{B.10})$$

If we keep the leading order and the zero mode contributions to the determinant, the result for the sphaleron rate is

$$\Gamma_{\text{sph}} = T \times \mathcal{N}_{\text{tr}}(\mathcal{N}\mathcal{V})_{\text{rot}} v_3^9(x, y) g_3^6 e^{-v_3(x, y) \mathcal{C}_{\text{sph}}}. \quad (\text{B.11})$$

These are the approximations we have used in Sec. 3.5.

Finally, let us address the power counting for the determinant in Eq. (3.3). Formally,

$$\ln \frac{[\det]_{\text{sph}}}{T^3} \sim \text{Tr} \ln \mathcal{Q}(\hat{\phi}_3, \hat{A}_3), \quad (\text{B.12})$$

where $\mathcal{Q}(\hat{\phi}_3, \hat{A}_3)$, depending on the sphaleron background $(\hat{\phi}_3, \hat{A}_3)$, is the second functional derivative of the 3D action S_{3D} in Eq. (3.8) or Eq. (3.15) with the potential replaced by the tree-level one. To obtain $\mathcal{Q}(\hat{\phi}_3, \hat{A}_3)$, one simply shifts the fields by $\hat{\phi}_3 \rightarrow \hat{\phi}_3 + \hat{\eta}_3$ and $\hat{A}_3^a \rightarrow \hat{A}_3^a + \hat{a}_{3,i}^a$ and collects the terms quadratic in $(\hat{\phi}_3, \hat{A}_3)$, where new $\hat{\phi}_3, \hat{A}_3$ are the sphaleron background fields and $\hat{\eta}_3, \hat{a}_{3,i}$ are the dimensionless fluctuating fields. The explicit form of \mathcal{Q} can be found in Eq. (40) in [126] or Eq. (12) in [127] and we present it here as well for completeness:

$$\begin{aligned} \delta^2 S_{3D} &= \int d^3\xi \left\{ \frac{1}{2} (\hat{D}_i \hat{a}_j)_3^a (\hat{D}_i \hat{a}_j)_3^a + \epsilon^{abc} \hat{F}_{3,ij}^a \hat{a}_{3,i}^b \hat{a}_{3,j}^c + \frac{1}{4} \hat{\phi}_3^\dagger \hat{\phi}_3 \hat{a}_{3,i}^a \hat{a}_{3,i}^a \right. \\ &\quad + 2i \left[\hat{\eta}_3^\dagger \hat{a}_{3,i}^a \tau^a (\hat{D}_i \hat{\phi})_3 - (\hat{D}_i \hat{\phi})_3^\dagger \hat{a}_{3,i}^a \tau^a \hat{\eta}_3 \right] + (\hat{D}_i \hat{\eta})_3^\dagger (\hat{D}_i \hat{\eta})_3 \\ &\quad \left. + y \hat{\eta}_3^\dagger \hat{\eta}_3 + \left(2x + \frac{1}{2} \right) \hat{\phi}_3^\dagger \hat{\phi}_3 \hat{\eta}_3^\dagger \hat{\eta}_3 + \left(x - \frac{1}{8} \right) (\hat{\phi}_3^\dagger \hat{\eta}_3 + \hat{\eta}_3^\dagger \hat{\phi}_3)^2 \right\} \\ &= \int d^3\xi \begin{pmatrix} \hat{a}_{3,i}^a & \hat{\eta}_3^\dagger & \hat{\eta}_3^T \end{pmatrix} \left[-\hat{D}^2 - M^2(\hat{\phi}_3, \hat{A}_3) \right] \begin{pmatrix} \hat{a}_{3,i}^a \\ \hat{\eta} \\ \hat{\eta}^* \end{pmatrix}, \quad (\text{B.13}) \end{aligned}$$

where we have reformulated various terms into $\mathcal{Q}(\hat{\phi}_3, \hat{A}_3) = \hat{D}^2 + M^2(\hat{\phi}_3, \hat{A}_3)$ in the last line. The derivative independent part, $M^2(\hat{\phi}_3, \hat{A}_3)$, hence scales like $M^2(\hat{\phi}_3, \hat{A}_3) \sim \hat{F}_3 \sim \hat{\phi}_3^\dagger \hat{\phi}_3 \sim (\hat{D}_i \hat{\phi})_3 \sim g^{-2}$, using $\phi_3 = g_3 \hat{\phi}_3$, $F_3 = g_3^2 \hat{F}_3$ and $D_i = g_3^2 \hat{D}_i$ as well as the scaling of terms in Sec. 3.3. In the dimensionless coordinates, the characteristic length scale of the sphaleron is $d^3\xi = g_3^6 d^3x \sim g^3$.

In analogy to the calculation of the Coleman-Weinberg effective potential, the size of the fluctuation determinant can be estimated by

$$\begin{aligned} \ln \frac{[\det]_{\text{sph}}}{T^3} &\sim \text{Tr} \ln \left[\hat{D}^2 + M^2(\hat{\phi}_3, \hat{A}_3) \right] \\ &\sim \int d^3\xi \int \frac{d^3k}{(2\pi)^3} \ln \left[k^2 + M^2(\hat{\phi}_3, \hat{A}_3) \right] \\ &= \int d^3\xi \frac{1}{6\pi} M^3(\hat{\phi}_3, \hat{A}_3). \end{aligned} \quad (\text{B.14})$$

Together with our estimation of the scaling of $M^2(\hat{\phi}_3, \hat{A}_3)$ and $d^3\xi$, we then have

$$\ln \frac{[\det]_{\text{sph}}}{T^3} \sim \pi^{-1}. \quad (\text{B.15})$$

Hence the contribution of the determinant is suppressed by $\frac{g}{\pi}$ compared to the leading order contribution, as stated in Eq. (3.3).

C. Temporal Gluon Effect to Sphaleron Rate via Dimensional Reduction

For the Standard Model crossover, lattice simulations (see Fig. 5) of [173, 174] are based on the dimensional reduction mapping of [78], and do not include the effect from the temporal gluon sector, as pointed out in [289] (and later included in [179, 234, 247, 251, 252, 290] as well as in automated `DRalgo` package [220, 233]). In the 3D EFT, this sector originates from the hot SU(3) sector of the Standard Model, and couples to the Higgs field via the portal operator

$$\omega_3(\phi^\dagger \phi) C_0^\alpha C_0^\alpha, \quad (\text{C.1})$$

with the portal coupling

$$\omega_3 = -\frac{2}{(4\pi)^2} g_s^2 g_Y^2, \quad (\text{C.2})$$

which is generated through a top quark loop, where g_Y is the top quark Yukawa coupling and g_s is SU(3) gauge coupling. Temporal gluon fields C_0^α , with SU(3) adjoint index $\alpha = 1, \dots, 8$ have the Debye screening mass

$$m_D'^2 = T^2 g_s^2 \left(1 + \frac{N_f}{3} \right), \quad (\text{C.3})$$

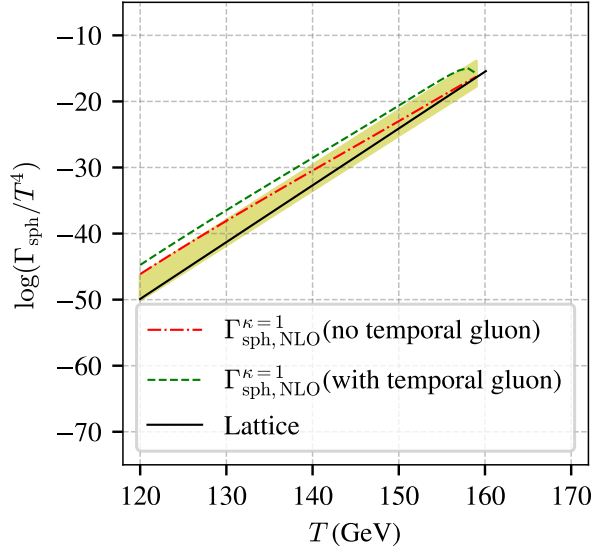


Figure 12: Similar to Fig. 5, but including the effect of temporal gluons to the dimensional reduction mapping, when computing $\Gamma_{\text{sph,NLO}}^{\kappa=1}$ (in green), compared to not including it (in red). In both results renormalization scale is fixed to $\mu = 4\pi e^{-\gamma}T$. This effect increases the sphaleron rate, and accordingly the lattice result (in black) can be expected to increase, when this effect would be considered.

with $N_f = 3$ fermion families. When (soft scale) temporal gluons are integrated out, they modify the Higgs thermal mass $\bar{\mu}_{h,3}^2$ via contribution

$$-\frac{8}{4\pi}\omega_3 m_D'' . \quad (\text{C.4})$$

Parametrically this contribution scales as $\sim g_s^3 g_y^2 \sim \mathcal{O}(g^5)$, and was hence omitted in [78] which truncates to $\mathcal{O}(g^4)$. However, this contribution can nevertheless lead to a non-negligible effect due to large numerical values of $g_Y \sim g_s \sim 1$.

In Fig. 12 we replot the Higgs phase sphaleron rate after SM crossover, depicting the effect of including the temporal gluon contribution, which modifies the $y(T)$ dimensional reduction mapping. We observe, that this contribution slightly increases the Higgs phase sphaleron rate, and emphasize, that since it is the dimensional reduction mapping that has changed, comparison to the lattice result is not fair. Indeed, we anticipate that the lattice result would increase accordingly, when the temporal gluon contribution is added. Similarly, this contribution would also result in a slight shift to the value of the SM pseudo-critical temperature.

References

- [1] N. Aghanim et al. In: *Astron. Astrophys.* 641 (2020). [Erratum: *Astron.Astrophys.* 652, C4 (2021)], A6. DOI: 10.1051/0004-6361/201833910. arXiv: 1807.06209 [astro-ph.CO].
- [2] B. D. Fields et al. In: *JCAP* 03 (2020). [Erratum: *JCAP* 11, E02 (2020)], p. 010. DOI: 10.1088/1475-7516/2020/03/010. arXiv: 1912.01132 [astro-ph.CO].
- [3] V. A. Kuzmin, V. A. Rubakov, and M. E. Shaposhnikov. In: *Phys. Lett.* 155B (1985), p. 36. DOI: 10.1016/0370-2693(85)91028-7.
- [4] M. J. Ramsey-Musolf. In: *JHEP* 09 (2020), p. 179. DOI: 10.1007/JHEP09(2020)179. arXiv: 1912.07189 [hep-ph].
- [5] V. A. Rubakov and M. E. Shaposhnikov. In: *Usp. Fiz. Nauk* 166 (1996), pp. 493–537. DOI: 10.1070/PU1996v039n05ABEH000145. arXiv: hep-ph/9603208.
- [6] W. Bernreuther. In: *Lect. Notes Phys.* 591 (2002), pp. 237–293. arXiv: hep-ph/0205279.
- [7] D. E. Morrissey and M. J. Ramsey-Musolf. In: *New J. Phys.* 14 (2012), p. 125003. DOI: 10.1088/1367-2630/14/12/125003. arXiv: 1206.2942 [hep-ph].
- [8] D. Bodeker and W. Buchmuller. In: *Rev. Mod. Phys.* 93.3 (2021), p. 035004. DOI: 10.1103/RevModPhys.93.035004. arXiv: 2009.07294 [hep-ph].
- [9] S. Biondini et al. In: *Int. J. Mod. Phys. A* 33.05n06 (2018), p. 1842004. DOI: 10.1142/S0217751X18420046. arXiv: 1711.02864 [hep-ph].
- [10] A. D. Sakharov. In: *Pisma Zh. Eksp. Teor. Fiz.* 5 (1967), pp. 32–35. DOI: 10.1070/PU1991v034n05ABEH002497.
- [11] N. S. Manton. In: *Phys. Rev. D* 28 (1983), p. 2019. DOI: 10.1103/PhysRevD.28.2019.
- [12] F. R. Klinkhamer and N. S. Manton. In: *Phys. Rev. D* 30 (1984), p. 2212. DOI: 10.1103/PhysRevD.30.2212.
- [13] S. L. Adler. In: *Phys. Rev.* 177 (1969), pp. 2426–2438. DOI: 10.1103/PhysRev.177.2426.
- [14] J. S. Bell and R. Jackiw. In: *Nuovo Cim. A* 60 (1969), pp. 47–61. DOI: 10.1007/BF02823296.
- [15] M. Laine et al. In: *JHEP* 11 (2022), p. 126. DOI: 10.1007/JHEP11(2022)126. arXiv: 2209.13804 [hep-ph].
- [16] K. Kajantie et al. In: *Phys. Rev. Lett.* 77 (1996), pp. 2887–2890. DOI: 10.1103/PhysRevLett.77.2887. arXiv: hep-ph/9605288 [hep-ph].

- [17] F. Csikor, Z. Fodor, and J. Heitger. In: *Phys. Rev. Lett.* 82 (1999), pp. 21–24. DOI: 10.1103/PhysRevLett.82.21. arXiv: hep-ph/9809291 [hep-ph].
- [18] R. Aaij et al. In: *Phys. Rev. Lett.* 134.10 (2025), p. 101801. DOI: 10.1103/PhysRevLett.134.101801. arXiv: 2411.12178 [hep-ex].
- [19] M. E. Shaposhnikov. In: *Nucl. Phys. B* 299 (1988), pp. 797–817. DOI: 10.1016/0550-3213(88)90373-2.
- [20] G. R. Farrar and M. E. Shaposhnikov. In: *Phys. Rev. D* 50 (1994), p. 774. DOI: 10.1103/PhysRevD.50.774. arXiv: hep-ph/9305275.
- [21] G. R. Farrar and M. E. Shaposhnikov. In: *Phys. Rev. Lett.* 70 (1993). [Erratum: *Phys.Rev.Lett.* 71, 210 (1993)], pp. 2833–2836. DOI: 10.1103/PhysRevLett.70.2833. arXiv: hep-ph/9305274.
- [22] M. B. Gavela et al. In: *Nucl. Phys. B* 430 (1994), pp. 382–426. DOI: 10.1016/0550-3213(94)00410-2. arXiv: hep-ph/9406289.
- [23] T. Brauner et al. In: *Phys. Rev. Lett.* 108 (2012), p. 041601. DOI: 10.1103/PhysRevLett.108.041601. arXiv: 1110.6818 [hep-ph].
- [24] T. Brauner et al. In: *JHEP* 11 (2012), p. 076. DOI: 10.1007/JHEP11(2012)076. arXiv: 1208.5609 [hep-ph].
- [25] V. Andreev et al. In: *Nature* 562.7727 (2018), pp. 355–360. DOI: 10.1038/s41586-018-0599-8.
- [26] V. Keus, N. Koivunen, and K. Tuominen. In: *JHEP* 09 (2018), p. 059. DOI: 10.1007/JHEP09(2018)059. arXiv: 1712.09613 [hep-ph].
- [27] V. Keus. In: *Phys. Rev. D* 101.7 (2020), p. 073007. DOI: 10.1103/PhysRevD.101.073007. arXiv: 1909.09234 [hep-ph].
- [28] S. J. Huber, K. Mimasu, and J. M. No. In: *Phys. Rev. D* 107.7 (2023), p. 075042. DOI: 10.1103/PhysRevD.107.075042. arXiv: 2208.10512 [hep-ph].
- [29] M. Laine and K. Rummukainen. In: *Nucl. Phys. B* 545 (1999), pp. 141–182. DOI: 10.1016/S0550-3213(99)00077-2. arXiv: hep-ph/9811369.
- [30] T. Alanne et al. In: *JCAP* 08 (2016), p. 057. DOI: 10.1088/1475-7516/2016/08/057. arXiv: 1607.03303 [hep-ph].
- [31] J. M. Cline. In: (2017). Ed. by E. Auge, J. Dumarchez, and J. Tran Thanh Van, pp. 339–348. DOI: 10.1098/rsta.2017.0116. arXiv: 1704.08911 [hep-ph].
- [32] In: 4/2017 (2017). Ed. by G. Apollinari et al. DOI: 10.23731/CYRM-2017-004.
- [33] In: (June 2013). Ed. by H. Baer et al. arXiv: 1306.6352 [hep-ph].

- [34] J. de Blas et al. In: 3/2018 (Dec. 2018). DOI: 10.23731/CYRM-2018-003. arXiv: 1812.02093 [hep-ph].
- [35] A. Abada et al. In: *Eur. Phys. J. C* 79.6 (2019), p. 474. DOI: 10.1140/epjc/s10052-019-6904-3.
- [36] M. Dong et al. In: (Nov. 2018). Ed. by J. B. Guimarães da Costa et al. arXiv: 1811.10545 [hep-ex].
- [37] T. Liu, M. J. Ramsey-Musolf, and J. Shu. In: *Phys. Rev. Lett.* 108 (2012), p. 221301. DOI: 10.1103/PhysRevLett.108.221301. arXiv: 1109.4145 [hep-ph].
- [38] J. Shu and Y. Zhang. In: *Phys. Rev. Lett.* 111.9 (2013), p. 091801. DOI: 10.1103/PhysRevLett.111.091801. arXiv: 1304.0773 [hep-ph].
- [39] S. Inoue, G. Ovanessian, and M. J. Ramsey-Musolf. In: *Phys. Rev. D* 93 (2016), p. 015013. DOI: 10.1103/PhysRevD.93.015013. arXiv: 1508.05404 [hep-ph].
- [40] C.-W. Chiang, K. Fuyuto, and E. Senaha. In: *Phys. Lett. B* 762 (2016), pp. 315–320. DOI: 10.1016/j.physletb.2016.09.052. arXiv: 1607.07316 [hep-ph].
- [41] J. de Vries et al. In: *JHEP* 01 (2018), p. 089. DOI: 10.1007/JHEP01(2018)089. arXiv: 1710.04061 [hep-ph].
- [42] M. J. Ramsey-Musolf, P. Winslow, and G. White. In: *Phys. Rev. D* 97.12 (2018), p. 123509. DOI: 10.1103/PhysRevD.97.123509. arXiv: 1708.07511 [hep-ph].
- [43] N. F. Bell et al. In: *JHEP* 09 (2019), p. 012. DOI: 10.1007/JHEP09(2019)012. arXiv: 1903.11255 [hep-ph].
- [44] J. M. Cline and K. Kainulainen. In: *Phys. Rev. D* 101.6 (2020), p. 063525. DOI: 10.1103/PhysRevD.101.063525. arXiv: 2001.00568 [hep-ph].
- [45] R. Zhou and L. Bian. In: *Phys. Lett. B* 829 (2022), p. 137105. DOI: 10.1016/j.physletb.2022.137105. arXiv: 2001.01237 [hep-ph].
- [46] K. Enomoto, S. Kanemura, and Y. Mura. In: *JHEP* 01 (2022), p. 104. DOI: 10.1007/JHEP01(2022)104. arXiv: 2111.13079 [hep-ph].
- [47] K. Kainulainen. In: *JCAP* 11.11 (2021), p. 042. DOI: 10.1088/1475-7516/2021/11/042. arXiv: 2108.08336 [hep-ph].
- [48] J. M. Cline and B. Laurent. In: *Phys. Rev. D* 104.8 (2021), p. 083507. DOI: 10.1103/PhysRevD.104.083507. arXiv: 2108.04249 [hep-ph].
- [49] T. Modak and E. Senaha. In: *Phys. Lett. B* 822 (2021), p. 136695. DOI: 10.1016/j.physletb.2021.136695. arXiv: 2107.12789 [hep-ph].
- [50] K. Enomoto, S. Kanemura, and Y. Mura. In: *JHEP* 09 (2022), p. 121. DOI: 10.1007/JHEP09(2022)121. arXiv: 2207.00060 [hep-ph].

- [51] S. Liu and L. Wang. In: *Phys. Rev. D* 107.11 (2023), p. 115008. DOI: 10.1103/PhysRevD.107.115008. arXiv: 2302.04639 [hep-ph].
- [52] M. Aoki and H. Shibuya. In: *Phys. Lett. B* 843 (2023), p. 138041. DOI: 10.1016/j.physletb.2023.138041. arXiv: 2302.11551 [hep-ph].
- [53] A. Ahriche, T. A. Chowdhury, and S. Nasri. In: *JHEP* 11 (2014), p. 096. DOI: 10.1007/JHEP11(2014)096. arXiv: 1409.4086 [hep-ph].
- [54] K. Fuyuto and E. Senaha. In: *Phys. Rev. D* 90.1 (2014), p. 015015. DOI: 10.1103/PhysRevD.90.015015. arXiv: 1406.0433 [hep-ph].
- [55] K. Fuyuto and E. Senaha. In: *Phys. Lett. B* 747 (2015), pp. 152–157. DOI: 10.1016/j.physletb.2015.05.061. arXiv: 1504.04291 [hep-ph].
- [56] X. Gan, A. J. Long, and L.-T. Wang. In: *Phys. Rev. D* 96.11 (2017), p. 115018. DOI: 10.1103/PhysRevD.96.115018. arXiv: 1708.03061 [hep-ph].
- [57] D. Kharzeev, E. Shuryak, and I. Zahed. In: *Phys. Rev. D* 102.7 (2020), p. 073003. DOI: 10.1103/PhysRevD.102.073003. arXiv: 1906.04080 [hep-ph].
- [58] Y. Wu, W. Zhang, and M. J. Ramsey-Musolf. In: (July 2023). arXiv: 2307.02187 [hep-ph].
- [59] M. Hong, K. Kamada, and J. Yokoyama. In: *Phys. Rev. D* 108.6 (2023), p. 063502. DOI: 10.1103/PhysRevD.108.063502. arXiv: 2304.13999 [hep-ph].
- [60] J. Hu, B. Yu, and S. Zhou. In: *JHEP* 10 (2023), p. 004. DOI: 10.1007/JHEP10(2023)004. arXiv: 2307.04713 [hep-ph].
- [61] R. Qin and L. Bian. In: *JHEP* 08 (2024), p. 157. DOI: 10.1007/JHEP08(2024)157. arXiv: 2407.01981 [hep-ph].
- [62] K. T. Matchev and S. Verner. In: (May 2025). arXiv: 2505.05607 [hep-ph].
- [63] K. T. Matchev and S. Verner. In: (May 2025). arXiv: 2505.05608 [hep-ph].
- [64] M. Tanaka. In: (May 2025). arXiv: 2505.09984 [hep-ph].
- [65] P. Amaro-Seoane et al. In: (Feb. 2017). arXiv: 1702.00786 [astro-ph.IM].
- [66] P. Auclair et al. In: *Living Rev. Rel.* 26.1 (2023), p. 5. DOI: 10.1007/s41114-023-00045-2. arXiv: 2204.05434 [astro-ph.CO].
- [67] S. Kawamura et al. In: *Class. Quant. Grav.* 28 (2011). Ed. by S. Buchman and K.-X. Sun, p. 094011. DOI: 10.1088/0264-9381/28/9/094011.
- [68] W.-H. Ruan et al. In: *Int. J. Mod. Phys. A* 35.17 (2020), p. 2050075. DOI: 10.1142/S0217751X2050075X. arXiv: 1807.09495 [gr-qc].
- [69] J. Luo et al. In: *Class. Quant. Grav.* 33.3 (2016), p. 035010. DOI: 10.1088/0264-9381/33/3/035010. arXiv: 1512.02076 [astro-ph.IM].

- [70] H. Kudo et al. In: *Phys. Rev. D* 73 (2006), p. 064006. DOI: 10.1103/PhysRevD.73.064006. arXiv: gr-qc/0511145.
- [71] J. Crowder and N. J. Cornish. In: *Phys. Rev. D* 72 (2005), p. 083005. DOI: 10.1103/PhysRevD.72.083005. arXiv: gr-qc/0506015.
- [72] K. Yagi and N. Seto. In: *Phys. Rev. D* 83 (2011). [Erratum: Phys.Rev.D 95, 109901 (2017)], p. 044011. DOI: 10.1103/PhysRevD.83.044011. arXiv: 1101.3940 [astro-ph.CO].
- [73] X. Gong et al. In: *J. Phys. Conf. Ser.* 610.1 (2015). Ed. by G. Ciani, J. W. Conklin, and G. Mueller, p. 012011. DOI: 10.1088/1742-6596/610/1/012011. arXiv: 1410.7296 [gr-qc].
- [74] M. Musha. In: *Proc. SPIE Int. Soc. Opt. Eng.* 10562 (2017). Ed. by B. Cugny, N. Karafolas, and Z. Sodnik, 105623T. DOI: 10.1117/12.2296050.
- [75] W.-R. Hu and Y.-L. Wu. In: *Natl. Sci. Rev.* 4.5 (2017), pp. 685–686. DOI: 10.1093/nsr/nwx116.
- [76] Y.-M. Hu, J. Mei, and J. Luo. In: *Natl. Sci. Rev.* 4.5 (2017), pp. 683–684. DOI: 10.1093/nsr/nwx115.
- [77] Z.-C. Liang et al. In: *Phys. Rev. D* 105.2 (2022), p. 022001. DOI: 10.1103/PhysRevD.105.022001. arXiv: 2107.08643 [astro-ph.CO].
- [78] K. Kajantie et al. In: *Nucl. Phys. B* 458 (1996), pp. 90–136. DOI: 10.1016/0550-3213(95)00549-8. arXiv: hep-ph/9508379.
- [79] E. Braaten and A. Nieto. In: *Phys. Rev. D* 51 (1995), pp. 6990–7006. DOI: 10.1103/PhysRevD.51.6990. arXiv: hep-ph/9501375 [hep-ph].
- [80] O. Gould and J. Hirvonen. In: *Phys. Rev. D* 104.9 (2021), p. 096015. DOI: 10.1103/PhysRevD.104.096015. arXiv: 2108.04377 [hep-ph].
- [81] J. Hirvonen et al. In: *JHEP* 07 (2022), p. 135. DOI: 10.1007/JHEP07(2022)135. arXiv: 2112.08912 [hep-ph].
- [82] A. Ekstedt, O. Gould, and J. Löfgren. In: *Phys. Rev. D* 106.3 (2022). [Erratum: Phys.Rev.D 110, 019901 (2024)], p. 036012. DOI: 10.1103/PhysRevD.106.036012. arXiv: 2205.07241 [hep-ph].
- [83] O. Gould, S. Güyer, and K. Rummukainen. In: *Phys. Rev. D* 106.11 (2022), p. 114507. DOI: 10.1103/PhysRevD.106.114507. arXiv: 2205.07238 [hep-lat].
- [84] J. Löfgren. In: *J. Phys. G* 50.12 (2023), p. 125008. DOI: 10.1088/1361-6471/ad074b. arXiv: 2301.05197 [hep-ph].
- [85] O. Gould and T. V. I. Tenkanen. In: *JHEP* 01 (2024), p. 048. DOI: 10.1007/JHEP01(2024)048. arXiv: 2309.01672 [hep-ph].

- [86] G. D. Moore and K. Rummukainen. In: *Phys. Rev. D* 63 (2001), p. 045002. DOI: 10.1103/PhysRevD.63.045002. arXiv: hep-ph/0009132.
- [87] Y. Burnier, M. Laine, and M. Shaposhnikov. In: *JCAP* 02 (2006), p. 007. DOI: 10.1088/1475-7516/2006/02/007. arXiv: hep-ph/0511246.
- [88] K. Kajantie et al. In: *Nucl. Phys.* B466 (1996), pp. 189–258. DOI: 10.1016/0550-3213(96)00052-1. arXiv: hep-lat/9510020 [hep-lat].
- [89] H. H. Patel and M. J. Ramsey-Musolf. In: *JHEP* 07 (2011), p. 029. DOI: 10.1007/JHEP07(2011)029. arXiv: 1101.4665 [hep-ph].
- [90] G. D. Moore. In: *Phys. Rev. D* 59 (1999), p. 014503. DOI: 10.1103/PhysRevD.59.014503. arXiv: hep-ph/9805264.
- [91] J. Löfgren et al. In: *Phys. Rev. Lett.* 130.25 (2023), p. 251801. DOI: 10.1103/PhysRevLett.130.251801. arXiv: 2112.05472 [hep-ph].
- [92] O. Gould and T. V. I. Tenkanen. In: *JHEP* 06 (2021), p. 069. DOI: 10.1007/JHEP06(2021)069. arXiv: 2104.04399 [hep-ph].
- [93] L. Niemi and T. V. I. Tenkanen. In: *Phys. Rev. D* 111.7 (2025), p. 075034. DOI: 10.1103/PhysRevD.111.075034. arXiv: 2408.15912 [hep-ph].
- [94] N. Turok and J. Zadrozny. In: *Phys. Rev. Lett.* 65 (1990), pp. 2331–2334. DOI: 10.1103/PhysRevLett.65.2331.
- [95] E. H. Fradkin and S. H. Shenker. In: *Phys. Rev. D* 19 (1979), pp. 3682–3697. DOI: 10.1103/PhysRevD.19.3682.
- [96] S. Elitzur. In: *Phys. Rev. D* 12 (1975), pp. 3978–3982. DOI: 10.1103/PhysRevD.12.3978.
- [97] P. H. Damgaard and U. M. Heller. In: *Phys. Lett. B* 164 (1985), pp. 121–126. DOI: 10.1016/0370-2693(85)90044-9.
- [98] H. G. Dosch et al. In: *Phys. Lett. B* 365 (1996), pp. 213–218. DOI: 10.1016/0370-2693(95)01269-9. arXiv: hep-ph/9509352.
- [99] C. Lee, V. Cirigliano, and M. J. Ramsey-Musolf. In: *Phys. Rev. D* 71 (2005), p. 075010. DOI: 10.1103/PhysRevD.71.075010. arXiv: hep-ph/0412354.
- [100] D. Bodeker et al. In: *JHEP* 02 (2005), p. 026. DOI: 10.1088/1126-6708/2005/02/026. arXiv: hep-ph/0412366.
- [101] V. Cirigliano et al. In: *Phys. Rev. D* 73 (2006), p. 115009. DOI: 10.1103/PhysRevD.73.115009. arXiv: hep-ph/0603058.
- [102] L. Fromme and S. J. Huber. In: *JHEP* 03 (2007), p. 049. DOI: 10.1088/1126-6708/2007/03/049. arXiv: hep-ph/0604159.

- [103] L. Fromme, S. J. Huber, and M. Seniuch. In: *JHEP* 11 (2006), p. 038. DOI: 10.1088/1126-6708/2006/11/038. arXiv: hep-ph/0605242.
- [104] V. Cirigliano et al. In: *Phys. Rev. D* 81 (2010), p. 103503. DOI: 10.1103/PhysRevD.81.103503. arXiv: 0912.3523 [hep-ph].
- [105] V. Cirigliano, C. Lee, and S. Tulin. In: *Phys. Rev. D* 84 (2011), p. 056006. DOI: 10.1103/PhysRevD.84.056006. arXiv: 1106.0747 [hep-ph].
- [106] T. Konstandin. In: *Phys. Usp.* 56 (2013), pp. 747–771. DOI: 10.3367/UFNe.0183.201308a.0785. arXiv: 1302.6713 [hep-ph].
- [107] M. Postma, J. van de Vis, and G. White. In: *JHEP* 12 (2022), p. 121. DOI: 10.1007/JHEP12(2022)121. arXiv: 2206.01120 [hep-ph].
- [108] H. Jukkala. PhD thesis. Jyväskylä U, Jyväskylä U., 2022. arXiv: 2211.11785 [hep-ph].
- [109] K. Kainulainen and N. Venkatesan. In: *JCAP* 08 (2024), p. 058. DOI: 10.1088/1475-7516/2024/08/058. arXiv: 2407.13639 [hep-ph].
- [110] Y.-Z. Li, M. J. Ramsey-Musolf, and J.-H. Yu. In: (Apr. 2024). arXiv: 2404.19197 [hep-ph].
- [111] G. 't Hooft. In: *Phys. Rev. Lett.* 37 (1976). Ed. by M. A. Shifman, pp. 8–11. DOI: 10.1103/PhysRevLett.37.8.
- [112] G. D. Moore. In: *Phys. Rev. D* 62 (2000), p. 085011. DOI: 10.1103/PhysRevD.62.085011. arXiv: hep-ph/0001216.
- [113] G. D. Moore. In: *Phys. Lett. B* 439 (1998), pp. 357–365. DOI: 10.1016/S0370-2693(98)01009-0. arXiv: hep-ph/9801204.
- [114] S. Y. Khlebnikov and M. E. Shaposhnikov. In: *Nucl. Phys. B* 308 (1988), pp. 885–912. DOI: 10.1016/0550-3213(88)90133-2.
- [115] M. Quiros. In: *ICTP Summer School in High-Energy Physics and Cosmology*. Jan. 1999, pp. 187–259. arXiv: hep-ph/9901312.
- [116] D. Bodeker, G. D. Moore, and K. Rummukainen. In: *Phys. Rev. D* 61 (2000), p. 056003. DOI: 10.1103/PhysRevD.61.056003. arXiv: hep-ph/9907545.
- [117] A. D. Linde. In: *Phys. Lett.* 96B (1980), pp. 289–292. DOI: 10.1016/0370-2693(80)90769-8.
- [118] M. E. Shaposhnikov. In: *Phys. Lett. B* 316 (1993), pp. 112–120. DOI: 10.1016/0370-2693(93)90666-6. arXiv: hep-ph/9306296.
- [119] E. Braaten. In: *Phys. Rev. Lett.* 74 (1995), pp. 2164–2167. DOI: 10.1103/PhysRevLett.74.2164. arXiv: hep-ph/9409434.

- [120] H. G. Dosch et al. In: *Nucl. Phys. B* 507 (1997), pp. 519–546. DOI: 10.1016/S0550-3213(97)00439-2. arXiv: hep-ph/9612450.
- [121] F. R. Klinkhamer. In: *Nucl. Phys. B* 410 (1993), pp. 343–354. DOI: 10.1016/0550-3213(93)90437-T. arXiv: hep-ph/9306295.
- [122] T. Akiba, H. Kikuchi, and T. Yanagida. In: *Phys. Rev. D* 38 (1988), pp. 1937–1941. DOI: 10.1103/PhysRevD.38.1937.
- [123] G. 't Hooft. In: *Phys. Rev. D* 14 (1976). Ed. by M. A. Shifman. [Erratum: Phys.Rev.D 18, 2199 (1978)], pp. 3432–3450. DOI: 10.1103/PhysRevD.14.3432.
- [124] P. B. Arnold and L. D. McLerran. In: *Phys. Rev. D* 36 (1987), p. 581. DOI: 10.1103/PhysRevD.36.581.
- [125] P. B. Arnold and L. D. McLerran. In: *Phys. Rev. D* 37 (1988), p. 1020. DOI: 10.1103/PhysRevD.37.1020.
- [126] L. Carson and L. D. McLerran. In: *Phys. Rev. D* 41 (1990), p. 647. DOI: 10.1103/PhysRevD.41.647.
- [127] L. Carson et al. In: *Phys. Rev. D* 42 (1990), pp. 2127–2143. DOI: 10.1103/PhysRevD.42.2127.
- [128] J. Baacke and S. Junker. In: *Mod. Phys. Lett. A* 8 (1993), pp. 2869–2874. DOI: 10.1142/S0217732393003251. arXiv: hep-ph/9306307.
- [129] J. Baacke and S. Junker. In: *Phys. Rev. D* 49 (1994), pp. 2055–2073. DOI: 10.1103/PhysRevD.49.2055. arXiv: hep-ph/9308310.
- [130] J. Baacke and S. Junker. In: *Phys. Rev. D* 50 (1994), pp. 4227–4228. DOI: 10.1103/PhysRevD.50.4227. arXiv: hep-th/9402078.
- [131] P. B. Arnold and O. Espinosa. In: *Phys. Rev. D* 47 (1993). [Erratum: Phys.Rev.D 50, 6662 (1994)], p. 3546. DOI: 10.1103/PhysRevD.47.3546. arXiv: hep-ph/9212235.
- [132] K. Farakos et al. In: *Nucl. Phys. B* 425 (1994), pp. 67–109. DOI: 10.1016/0550-3213(94)90173-2. arXiv: hep-ph/9404201 [hep-ph].
- [133] P. H. Ginsparg. In: *Nucl. Phys. B* 170 (1980), pp. 388–408. DOI: 10.1016/0550-3213(80)90418-6.
- [134] T. Appelquist and R. D. Pisarski. In: *Phys. Rev. D* 23 (1981), p. 2305. DOI: 10.1103/PhysRevD.23.2305.
- [135] S. Nadkarni. In: *Phys. Rev. D* 27 (1983), p. 917. DOI: 10.1103/PhysRevD.27.917.
- [136] N. P. Landsman. In: *Nucl. Phys. B* 322 (1989), pp. 498–530. DOI: 10.1016/0550-3213(89)90424-0.

- [137] T. Matsubara. In: *Prog. Theor. Phys.* 14 (1955), pp. 351–378. DOI: 10.1143/PTP.14.351.
- [138] J. Hirvonen. In: (May 2022). arXiv: 2205.02687 [hep-ph].
- [139] G. D. Moore. In: *Phys. Rev. D* 53 (1996), pp. 5906–5917. DOI: 10.1103/PhysRevD.53.5906. arXiv: hep-ph/9508405.
- [140] A. Ekstedt, P. Schicho, and T. V. I. Tenkanen. In: *Phys. Rev. D* 110.9 (2024), p. 096006. DOI: 10.1103/PhysRevD.110.096006. arXiv: 2405.18349 [hep-ph].
- [141] D. J. Gross, R. D. Pisarski, and L. G. Yaffe. In: *Rev. Mod. Phys.* 53 (1981), p. 43. DOI: 10.1103/RevModPhys.53.43.
- [142] K. Kajantie, K. Rummukainen, and M. E. Shaposhnikov. In: *Nucl. Phys. B* 407 (1993), pp. 356–372. DOI: 10.1016/0550-3213(93)90062-T. arXiv: hep-ph/9305345.
- [143] K. Farakos et al. In: *Phys. Lett. B* 336 (1994), pp. 494–501. DOI: 10.1016/0370-2693(94)90563-0. arXiv: hep-ph/9405234.
- [144] K. Farakos et al. In: *Nucl. Phys. B* 442 (1995), pp. 317–363. DOI: 10.1016/0550-3213(95)80129-4. arXiv: hep-lat/9412091 [hep-lat].
- [145] K. Rummukainen et al. In: *Nucl. Phys. B* 532 (1998), pp. 283–314. DOI: 10.1016/S0550-3213(98)00494-5. arXiv: hep-lat/9805013.
- [146] D. Y. Grigoriev and V. A. Rubakov. In: *Nucl. Phys. B* 299 (1988), pp. 67–78. DOI: 10.1016/0550-3213(88)90466-X.
- [147] D. Y. Grigoriev, V. A. Rubakov, and M. E. Shaposhnikov. In: *Nucl. Phys. B* 326 (1989), pp. 737–757. DOI: 10.1016/0550-3213(89)90553-1.
- [148] D. Y. Grigoriev, V. A. Rubakov, and M. E. Shaposhnikov. In: *Phys. Lett. B* 216 (1989), pp. 172–176. DOI: 10.1016/0370-2693(89)91390-7.
- [149] J. Ambjorn et al. In: *Nucl. Phys. B* 353 (1991), pp. 346–378. DOI: 10.1016/0550-3213(91)90341-T.
- [150] J. Ambjorn et al. In: *Phys. Lett. B* 244 (1990), pp. 479–487. DOI: 10.1016/0370-2693(90)90350-F.
- [151] J. Ambjorn and A. Krasnitz. In: *Phys. Lett. B* 362 (1995), pp. 97–104. DOI: 10.1016/0370-2693(95)01157-L. arXiv: hep-ph/9508202.
- [152] W.-H. Tang and J. Smit. In: *Nucl. Phys. B* 482 (1996), pp. 265–285. DOI: 10.1016/S0550-3213(96)00481-6. arXiv: hep-lat/9605016.
- [153] J. Ambjorn and A. Krasnitz. In: *Nucl. Phys. B* 506 (1997), pp. 387–403. DOI: 10.1016/S0550-3213(97)00524-5. arXiv: hep-ph/9705380.

- [154] G. D. Moore and N. Turok. In: *Phys. Rev. D* 56 (1997), pp. 6533–6546. DOI: 10.1103/PhysRevD.56.6533. arXiv: hep-ph/9703266.
- [155] D. Bodeker, L. D. McLerran, and A. V. Smilga. In: *Phys. Rev. D* 52 (1995), pp. 4675–4690. DOI: 10.1103/PhysRevD.52.4675. arXiv: hep-th/9504123.
- [156] P. B. Arnold, D. Son, and L. G. Yaffe. In: *Phys. Rev. D* 55 (1997), pp. 6264–6273. DOI: 10.1103/PhysRevD.55.6264. arXiv: hep-ph/9609481.
- [157] E. Braaten and R. D. Pisarski. In: *Nucl. Phys. B* 337 (1990), pp. 569–634. DOI: 10.1016/0550-3213(90)90508-B.
- [158] J. Frenkel and J. C. Taylor. In: *Nucl. Phys. B* 334 (1990), pp. 199–216. DOI: 10.1016/0550-3213(90)90661-V.
- [159] E. Braaten and R. D. Pisarski. In: *Phys. Rev. D* 45.6 (1992), R1827. DOI: 10.1103/PhysRevD.45.R1827.
- [160] A. Ekstedt. In: *JHEP* 06 (2023), p. 135. DOI: 10.1007/JHEP06(2023)135. arXiv: 2302.04894 [hep-ph].
- [161] A. Ekstedt. In: (Apr. 2023). arXiv: 2304.09255 [hep-ph].
- [162] G. D. Moore, C.-r. Hu, and B. Muller. In: *Phys. Rev. D* 58 (1998), p. 045001. DOI: 10.1103/PhysRevD.58.045001. arXiv: hep-ph/9710436.
- [163] D. Bodeker. In: *Phys. Lett. B* 426 (1998), pp. 351–360. DOI: 10.1016/S0370-2693(98)00279-2. arXiv: hep-ph/9801430.
- [164] M. Eriksson and M. Laine. In: *JCAP* 06 (2024), p. 016. DOI: 10.1088/1475-7516/2024/06/016. arXiv: 2404.06116 [hep-ph].
- [165] P. B. Arnold, D. T. Son, and L. G. Yaffe. In: *Phys. Rev. D* 59 (1999), p. 105020. DOI: 10.1103/PhysRevD.59.105020. arXiv: hep-ph/9810216.
- [166] P. B. Arnold and L. G. Yaffe. In: *Phys. Rev. D* 62 (2000), p. 125013. DOI: 10.1103/PhysRevD.62.125013. arXiv: hep-ph/9912305.
- [167] P. B. Arnold and L. G. Yaffe. In: *Phys. Rev. D* 62 (2000), p. 125014. DOI: 10.1103/PhysRevD.62.125014. arXiv: hep-ph/9912306.
- [168] D. Bodeker. In: *Nucl. Phys. B* 559 (1999), pp. 502–538. DOI: 10.1016/S0550-3213(99)00435-6. arXiv: hep-ph/9905239.
- [169] D. Bodeker. In: *Nucl. Phys. B* 647 (2002), pp. 512–538. DOI: 10.1016/S0550-3213(02)00841-6. arXiv: hep-ph/0205202.
- [170] G. D. Moore. In: *Nucl. Phys. B* 568 (2000), pp. 367–404. DOI: 10.1016/S0550-3213(99)00746-4. arXiv: hep-ph/9810313.

- [171] G. D. Moore, K. Rummukainen, and A. Tranberg. In: *JHEP* 04 (2001), p. 017. DOI: 10.1088/1126-6708/2001/04/017. arXiv: hep-lat/0103036.
- [172] M. D’Onofrio, K. Rummukainen, and A. Tranberg. In: *JHEP* 08 (2012), p. 123. DOI: 10.1007/JHEP08(2012)123. arXiv: 1207.0685 [hep-ph].
- [173] M. D’Onofrio, K. Rummukainen, and A. Tranberg. In: *Phys. Rev. Lett.* 113.14 (2014), p. 141602. DOI: 10.1103/PhysRevLett.113.141602. arXiv: 1404.3565 [hep-ph].
- [174] J. Annala and K. Rummukainen. In: *Phys. Rev. D* 107.7 (2023), p. 073006. DOI: 10.1103/PhysRevD.107.073006. arXiv: 2301.08626 [hep-ph].
- [175] G. D. Moore and K. Rummukainen. In: *Phys. Rev. D* 61 (2000), p. 105008. DOI: 10.1103/PhysRevD.61.105008. arXiv: hep-ph/9906259.
- [176] G. D. Moore and M. Tassler. In: *JHEP* 02 (2011), p. 105. DOI: 10.1007/JHEP02(2011)105. arXiv: 1011.1167 [hep-ph].
- [177] L. Altenkort et al. In: *Phys. Rev. D* 103.11 (2021), p. 114513. DOI: 10.1103/PhysRevD.103.114513. arXiv: 2012.08279 [hep-lat].
- [178] A. Strumia and N. Tetradis. In: *Nucl. Phys. B* 542 (1999), pp. 719–741. DOI: 10.1016/S0550-3213(98)00804-9. arXiv: hep-ph/9806453.
- [179] D. Croon et al. In: *JHEP* 04 (2021), p. 055. DOI: 10.1007/JHEP04(2021)055. arXiv: 2009.10080 [hep-ph].
- [180] C. Wainwright, S. Profumo, and M. J. Ramsey-Musolf. In: *Phys. Rev. D* 84 (2011), p. 023521. DOI: 10.1103/PhysRevD.84.023521. arXiv: 1104.5487 [hep-ph].
- [181] M. Garny and T. Konstandin. In: *JHEP* 07 (2012), p. 189. DOI: 10.1007/JHEP07(2012)189. arXiv: 1205.3392 [hep-ph].
- [182] C.-W. Chiang and E. Senaha. In: *Phys. Lett. B* 774 (2017), pp. 489–493. DOI: 10.1016/j.physletb.2017.09.064. arXiv: 1707.06765 [hep-ph].
- [183] H. H. Patel and M. J. Ramsey-Musolf. In: *Phys. Rev. D* 88 (2013), p. 035013. DOI: 10.1103/PhysRevD.88.035013. arXiv: 1212.5652 [hep-ph].
- [184] S. Profumo et al. In: *Phys. Rev. D* 91.3 (2015), p. 035018. DOI: 10.1103/PhysRevD.91.035018. arXiv: 1407.5342 [hep-ph].
- [185] W. Chao. In: *Phys. Rev. D* 92.1 (2015), p. 015025. DOI: 10.1103/PhysRevD.92.015025. arXiv: 1412.3823 [hep-ph].
- [186] N. Blinov et al. In: *Phys. Rev. D* 92.3 (2015), p. 035012. DOI: 10.1103/PhysRevD.92.035012. arXiv: 1504.05195 [hep-ph].
- [187] A. V. Kotwal et al. In: *Phys. Rev. D* 94.3 (2016), p. 035022. DOI: 10.1103/PhysRevD.94.035022. arXiv: 1605.06123 [hep-ph].

- [188] C.-W. Chiang, M. J. Ramsey-Musolf, and E. Senaha. In: *Phys. Rev. D* 97.1 (2018), p. 015005. DOI: 10.1103/PhysRevD.97.015005. arXiv: 1707.09960 [hep-ph].
- [189] C.-W. Chiang, Y.-T. Li, and E. Senaha. In: *Phys. Lett. B* 789 (2019), pp. 154–159. DOI: 10.1016/j.physletb.2018.12.017. arXiv: 1808.01098 [hep-ph].
- [190] J. Kozaczuk. In: *JHEP* 10 (2015), p. 135. DOI: 10.1007/JHEP10(2015)135. arXiv: 1506.04741 [hep-ph].
- [191] W. Chao, H.-K. Guo, and J. Shu. In: *JCAP* 09 (2017), p. 009. DOI: 10.1088/1475-7516/2017/09/009. arXiv: 1702.02698 [hep-ph].
- [192] C.-Y. Chen, J. Kozaczuk, and I. M. Lewis. In: *JHEP* 08 (2017), p. 096. DOI: 10.1007/JHEP08(2017)096. arXiv: 1704.05844 [hep-ph].
- [193] Z. Kang, P. Ko, and T. Matsui. In: *JHEP* 02 (2018), p. 115. DOI: 10.1007/JHEP02(2018)115. arXiv: 1706.09721 [hep-ph].
- [194] A. Alves et al. In: *JHEP* 04 (2019), p. 052. DOI: 10.1007/JHEP04(2019)052. arXiv: 1812.09333 [hep-ph].
- [195] R. Zhou, L. Bian, and H.-K. Guo. In: *Phys. Rev. D* 101.9 (2020), p. 091903. DOI: 10.1103/PhysRevD.101.091903. arXiv: 1910.00234 [hep-ph].
- [196] J. Kozaczuk, M. J. Ramsey-Musolf, and J. Shelton. In: *Phys. Rev. D* 101.11 (2020), p. 115035. DOI: 10.1103/PhysRevD.101.115035. arXiv: 1911.10210 [hep-ph].
- [197] W. Zhang et al. In: *JHEP* 12 (2023), p. 018. DOI: 10.1007/JHEP12(2023)018. arXiv: 2303.03612 [hep-ph].
- [198] W. Zhang et al. In: *JHEP* 01 (2024), p. 051. DOI: 10.1007/JHEP01(2024)051. arXiv: 2307.01615 [hep-ph].
- [199] P. Schicho, T. V. I. Tenkanen, and G. White. In: *JHEP* 11 (2022), p. 047. DOI: 10.1007/JHEP11(2022)047. arXiv: 2203.04284 [hep-ph].
- [200] O. Gould. In: *JHEP* 04 (2021), p. 057. DOI: 10.1007/JHEP04(2021)057. arXiv: 2101.05528 [hep-ph].
- [201] A. Ekstedt and J. Löfgren. In: *JHEP* 12 (2020), p. 136. DOI: 10.1007/JHEP12(2020)136. arXiv: 2006.12614 [hep-ph].
- [202] L. Niemi et al. In: *Phys. Rev. Lett.* 126.17 (2021), p. 171802. DOI: 10.1103/PhysRevLett.126.171802. arXiv: 2005.11332 [hep-ph].
- [203] H. A. Kramers. In: *Physica* 7 (1940), pp. 284–304. DOI: 10.1016/S0031-8914(40)90098-2.
- [204] J. S. Langer. In: *Annals Phys.* 54 (1969), pp. 258–275. DOI: 10.1016/0003-4916(69)90153-5.

- [205] J. S. Langer. In: *Physica* 73.1 (1974), pp. 61–72. DOI: 10.1016/0031-8914(74)90226-2.
- [206] A. D. Linde. In: *Phys. Lett. B* 100 (1981), pp. 37–40. DOI: 10.1016/0370-2693(81)90281-1.
- [207] A. D. Linde. In: *Nucl. Phys. B* 216 (1983). [Erratum: Nucl.Phys.B 223, 544 (1983)], p. 421. DOI: 10.1016/0550-3213(83)90072-X.
- [208] J. Baacke and K. Heitmann. In: *Phys. Rev. D* 60 (1999), p. 105037. DOI: 10.1103/PhysRevD.60.105037. arXiv: hep-th/9905201.
- [209] A. Ekstedt. In: *Eur. Phys. J. C* 82.2 (2022), p. 173. DOI: 10.1140/epjc/s10052-022-10130-5. arXiv: 2104.11804 [hep-ph].
- [210] A. Ekstedt. In: *JHEP* 08 (2022), p. 115. DOI: 10.1007/JHEP08(2022)115. arXiv: 2201.07331 [hep-ph].
- [211] A. Ekstedt. In: *Phys. Rev. D* 106.9 (2022), p. 095026. DOI: 10.1103/PhysRevD.106.095026. arXiv: 2205.05145 [hep-ph].
- [212] A. Ekstedt, O. Gould, and J. Hirvonen. In: *JHEP* 12 (2023), p. 056. DOI: 10.1007/JHEP12(2023)056. arXiv: 2308.15652 [hep-ph].
- [213] J. Hirvonen. In: (Mar. 2024). arXiv: 2403.07987 [hep-ph].
- [214] O. Gould, A. Kormu, and D. J. Weir. In: *Phys. Rev. D* 111.5 (2025), p. L051901. DOI: 10.1103/PhysRevD.111.L051901. arXiv: 2404.01876 [hep-th].
- [215] J. Hällfors and K. Rummukainen. In: (Feb. 2025). arXiv: 2502.14610 [hep-lat].
- [216] M. Chala et al. In: *JHEP* 10 (2024), p. 025. DOI: 10.1007/JHEP10(2024)025. arXiv: 2406.02667 [hep-ph].
- [217] F. Bernardo et al. In: (Mar. 2025). arXiv: 2503.18904 [hep-ph].
- [218] M. Chala and G. Guedes. In: (Mar. 2025). arXiv: 2503.20016 [hep-ph].
- [219] M. Chala, L. Gil, and Z. Ren. In: (May 2025). arXiv: 2505.14335 [hep-ph].
- [220] A. Ekstedt, P. Schicho, and T. V. I. Tenkanen. In: *Comput. Phys. Commun.* 288 (2023), p. 108725. DOI: 10.1016/j.cpc.2023.108725. arXiv: 2205.08815 [hep-ph].
- [221] M. Laine and A. Vuorinen. Vol. 925. Springer, 2016. DOI: 10.1007/978-3-319-31933-9. arXiv: 1701.01554 [hep-ph].
- [222] K. Kajantie et al. In: *Phys. Lett. B* 423 (1998), pp. 137–144. DOI: 10.1016/S0370-2693(97)01584-0. arXiv: hep-ph/9710538.
- [223] M. Kierkla et al. In: *JHEP* 02 (2024), p. 234. DOI: 10.1007/JHEP02(2024)234. arXiv: 2312.12413 [hep-ph].

- [224] J. E. Camargo-Molina, R. Enberg, and J. Löfgren. In: *JHEP* 10 (2021), p. 127. DOI: 10.1007/JHEP10(2021)127. arXiv: 2103.14022 [hep-ph].
- [225] K. Kajantie et al. In: *Nucl. Phys. B* 493 (1997), pp. 413–438. DOI: 10.1016/S0550-3213(97)00164-8. arXiv: hep-lat/9612006.
- [226] K. Kajantie et al. In: *Nucl. Phys. B* 520 (1998), pp. 345–381. DOI: 10.1016/S0550-3213(98)00064-9. arXiv: hep-lat/9711048.
- [227] K. Kajantie et al. In: *Nucl. Phys. B* 503 (1997), pp. 357–384. DOI: 10.1016/S0550-3213(97)00425-2. arXiv: hep-ph/9704416.
- [228] O. Gould and C. Xie. In: *JHEP* 12 (2023), p. 049. DOI: 10.1007/JHEP12(2023)049. arXiv: 2310.02308 [hep-ph].
- [229] J. Annala, K. Rummukainen, and T. V. Tenkanen. In preparation. 2025.
- [230] A. Gynther and M. Vepsalainen. In: *JHEP* 03 (2006), p. 011. DOI: 10.1088/1126-6708/2006/03/011. arXiv: hep-ph/0512177.
- [231] M. Laine and M. Meyer. In: *JCAP* 07 (2015), p. 035. DOI: 10.1088/1475-7516/2015/07/035. arXiv: 1503.04935 [hep-ph].
- [232] F. R. Klinkhamer and R. Laterveer. In: *Z. Phys. C* 53 (1992), pp. 247–252. DOI: 10.1007/BF01597560.
- [233] R. M. Fonseca. In: *Comput. Phys. Commun.* 267 (2021), p. 108085. DOI: 10.1016/j.cpc.2021.108085. arXiv: 2011.01764 [hep-th].
- [234] L. Niemi, P. Schicho, and T. V. I. Tenkanen. In: *Phys. Rev. D* 103.11 (2021). [Erratum: *Phys.Rev.D* 109, 039902 (2024)], p. 115035. DOI: 10.1103/PhysRevD.103.115035. arXiv: 2103.07467 [hep-ph].
- [235] W. Buchmuller and Z. Fodor. In: *Phys. Lett. B* 331 (1994), pp. 124–130. DOI: 10.1016/0370-2693(94)90952-0. arXiv: hep-ph/9403388.
- [236] M. C. A. York and G. D. Moore. In: *JHEP* 10 (2014), p. 105. DOI: 10.1007/JHEP10(2014)105. arXiv: 1407.3816 [hep-ph].
- [237] A. Hart et al. In: *Phys. Lett. B* 396 (1997), pp. 217–224. DOI: 10.1016/S0370-2693(97)00104-4. arXiv: hep-lat/9612021.
- [238] K. Kajantie et al. In: *JHEP* 11 (1998), p. 011. DOI: 10.1088/1126-6708/1998/11/011. arXiv: hep-lat/9811004.
- [239] L. Niemi et al. In: *JHEP* 02 (2023), p. 212. DOI: 10.1007/JHEP02(2023)212. arXiv: 2206.14487 [hep-lat].
- [240] G. Catumba et al. In: *Phys. Rev. Res.* 6.4 (2024), p. 043172. DOI: 10.1103/PhysRevResearch.6.043172. arXiv: 2407.15422 [hep-lat].

- [241] C. Bonati, A. Pelissetto, and E. Vicari. In: (Oct. 2024). arXiv: 2410.05823 [cond-mat.stat-mech].
- [242] M. Kierkla et al. In: (Mar. 2025). arXiv: 2503.13597 [hep-ph].
- [243] S. Y. Khlebnikov and M. E. Shaposhnikov. In: *Phys. Lett. B* 387 (1996), pp. 817–822. DOI: 10.1016/0370-2693(96)01116-1. arXiv: hep-ph/9607386.
- [244] G. Barenboim and J. Rasero. In: *JHEP* 07 (2012), p. 028. DOI: 10.1007/JHEP07(2012)028. arXiv: 1202.6070 [hep-ph].
- [245] T. V. I. Tenkanen and J. van de Vis. In: *JHEP* 08 (2022), p. 302. DOI: 10.1007/JHEP08(2022)302. arXiv: 2206.01130 [hep-ph].
- [246] O. Gould et al. In: *Phys. Rev. D* 100.11 (2019), p. 115024. DOI: 10.1103/PhysRevD.100.115024. arXiv: 1903.11604 [hep-ph].
- [247] L. Niemi et al. In: *Phys. Rev. D* 100.3 (2019), p. 035002. DOI: 10.1103/PhysRevD.100.035002. arXiv: 1802.10500 [hep-ph].
- [248] L. S. Friedrich et al. In: (Mar. 2022). arXiv: 2203.05889 [hep-ph].
- [249] Q.-H. Cao et al. In: *Phys. Rev. D* 111.9 (2025), p. 095003. DOI: 10.1103/PhysRevD.111.095003. arXiv: 2212.07756 [hep-ph].
- [250] L. Niemi. MA thesis. U. Helsinki (main), Apr. 2018.
- [251] J. O. Andersen et al. In: *Phys. Rev. Lett.* 121.19 (2018), p. 191802. DOI: 10.1103/PhysRevLett.121.191802. arXiv: 1711.09849 [hep-ph].
- [252] T. Gorda et al. In: *JHEP* 02 (2019), p. 081. DOI: 10.1007/JHEP02(2019)081. arXiv: 1802.05056 [hep-ph].
- [253] K. Kainulainen et al. In: *JHEP* 06 (2019), p. 075. DOI: 10.1007/JHEP06(2019)075. arXiv: 1904.01329 [hep-ph].
- [254] L. Niemi, M. J. Ramsey-Musolf, and G. Xia. In: *Phys. Rev. D* 110.11 (2024), p. 115016. DOI: 10.1103/PhysRevD.110.115016. arXiv: 2405.01191 [hep-ph].
- [255] R. Qin and L. Bian. In: *Phys. Rev. D* 111.5 (2025), p. L051702. DOI: 10.1103/PhysRevD.111.L051702. arXiv: 2408.09677 [hep-ph].
- [256] M. Carena, M. Quiros, and C. E. M. Wagner. In: *Phys. Lett. B* 380 (1996), pp. 81–91. DOI: 10.1016/0370-2693(96)00475-3. arXiv: hep-ph/9603420.
- [257] D. Bodeker et al. In: *Nucl. Phys. B* 497 (1997), pp. 387–414. DOI: 10.1016/S0550-3213(97)00252-6. arXiv: hep-ph/9612364.
- [258] S. J. Huber and M. G. Schmidt. In: *Nucl. Phys. B* 606 (2001), pp. 183–230. DOI: 10.1016/S0550-3213(01)00250-4. arXiv: hep-ph/0003122.
- [259] C. Grojean, G. Servant, and J. D. Wells. In: *Phys. Rev. D* 71 (2005), p. 036001. DOI: 10.1103/PhysRevD.71.036001. arXiv: hep-ph/0407019.

- [260] A. Menon, D. E. Morrissey, and C. E. M. Wagner. In: *Phys. Rev. D* 70 (2004), p. 035005. DOI: 10.1103/PhysRevD.70.035005. arXiv: hep-ph/0404184.
- [261] C. Delaunay, C. Grojean, and J. D. Wells. In: *JHEP* 04 (2008), p. 029. DOI: 10.1088/1126-6708/2008/04/029. arXiv: 0711.2511 [hep-ph].
- [262] J. R. Espinosa and M. Quiros. In: *Phys. Rev. D* 76 (2007), p. 076004. DOI: 10.1103/PhysRevD.76.076004. arXiv: hep-ph/0701145.
- [263] S. Profumo, M. J. Ramsey-Musolf, and G. Shaughnessy. In: *JHEP* 08 (2007), p. 010. DOI: 10.1088/1126-6708/2007/08/010. arXiv: 0705.2425 [hep-ph].
- [264] V. Barger et al. In: *Phys. Rev. D* 79 (2009), p. 015018. DOI: 10.1103/PhysRevD.79.015018. arXiv: 0811.0393 [hep-ph].
- [265] J. R. Espinosa et al. In: *Phys. Rev. D* 78 (2008), p. 123528. DOI: 10.1103/PhysRevD.78.123528. arXiv: 0809.3215 [hep-ph].
- [266] K. Funakubo and E. Senaha. In: *Phys. Rev. D* 79 (2009), p. 115024. DOI: 10.1103/PhysRevD.79.115024. arXiv: 0905.2022 [hep-ph].
- [267] J. R. Espinosa, T. Konstandin, and F. Riva. In: *Nucl. Phys. B* 854 (2012), pp. 592–630. DOI: 10.1016/j.nuclphysb.2011.09.010. arXiv: 1107.5441 [hep-ph].
- [268] J. M. Cline et al. In: *Phys. Rev. D* 88 (2013). [Erratum: Phys.Rev.D 92, 039906 (2015)], p. 055025. DOI: 10.1103/PhysRevD.88.055025. arXiv: 1306.4710 [hep-ph].
- [269] G. C. Dorsch et al. In: *Phys. Rev. Lett.* 113.21 (2014), p. 211802. DOI: 10.1103/PhysRevLett.113.211802. arXiv: 1405.5537 [hep-ph].
- [270] D. Curtin, P. Meade, and C.-T. Yu. In: *JHEP* 11 (2014), p. 127. DOI: 10.1007/JHEP11(2014)127. arXiv: 1409.0005 [hep-ph].
- [271] P. Basler et al. In: *JHEP* 02 (2017), p. 121. DOI: 10.1007/JHEP02(2017)121. arXiv: 1612.04086 [hep-ph].
- [272] G. C. Dorsch et al. In: *JCAP* 05 (2017), p. 052. DOI: 10.1088/1475-7516/2017/05/052. arXiv: 1611.05874 [hep-ph].
- [273] A. Beniwal et al. In: *JHEP* 08 (2017), p. 108. DOI: 10.1007/JHEP08(2017)108. arXiv: 1702.06124 [hep-ph].
- [274] S. Bruggisser et al. In: *JHEP* 12 (2018), p. 099. DOI: 10.1007/JHEP12(2018)099. arXiv: 1804.07314 [hep-ph].
- [275] J. M. Cline et al. In: *Phys. Rev. D* 103.12 (2021), p. 123529. DOI: 10.1103/PhysRevD.103.123529. arXiv: 2102.12490 [hep-ph].
- [276] M. Laine. In: *Phys. Rev. D* 51 (1995), pp. 4525–4532. DOI: 10.1103/PhysRevD.51.4525. arXiv: hep-ph/9411252.

- [277] N. K. Nielsen. In: *Nucl. Phys. B* 101 (1975), pp. 173–188. DOI: 10.1016/0550-3213(75)90301-6.
- [278] R. Fukuda and T. Kugo. In: *Phys. Rev. D* 13 (1976), p. 3469. DOI: 10.1103/PhysRevD.13.3469.
- [279] M. Laine, G. Nardini, and K. Rummukainen. In: *JCAP* 01 (2013), p. 011. DOI: 10.1088/1475-7516/2013/01/011. arXiv: 1211.7344 [hep-ph].
- [280] W. Buchmuller, Z. Fodor, and A. Hebecker. In: *Nucl. Phys. B* 447 (1995), pp. 317–339. DOI: 10.1016/0550-3213(95)00254-P. arXiv: hep-ph/9502321.
- [281] A. K. Rajantie. In: *Nucl. Phys. B* 480 (1996). [Erratum: Nucl.Phys.B 513, 761–762 (1998)], pp. 729–752. DOI: 10.1016/S0550-3213(96)00474-9. arXiv: hep-ph/9606216.
- [282] M. Laine and M. Losada. In: *Nucl. Phys. B* 582 (2000), pp. 277–295. DOI: 10.1016/S0550-3213(00)00298-4. arXiv: hep-ph/0003111.
- [283] M. Laine, M. Meyer, and G. Nardini. In: *Nucl. Phys. B* 920 (2017), pp. 565–600. DOI: 10.1016/j.nuclphysb.2017.04.023. arXiv: 1702.07479 [hep-ph].
- [284] M. A. Bezuglov and A. I. Onishchenko. In: *Phys. Lett. B* 788 (2019), pp. 122–130. DOI: 10.1016/j.physletb.2018.11.005. arXiv: 1805.06482 [hep-ph].
- [285] A. Dashko and A. Ekstedt. In: *JHEP* 03 (2025), p. 024. DOI: 10.1007/JHEP03(2025)024. arXiv: 2411.05075 [hep-ph].
- [286] M. J. Ramsey-Musolf, T. V. I. Tenkanen, and V. Q. Tran. In: (Sept. 2024). arXiv: 2409.17554 [hep-ph].
- [287] O. Gould and P. M. Saffin. In: *JHEP* 03 (2025), p. 105. DOI: 10.1007/JHEP03(2025)105. arXiv: 2411.08951 [hep-ph].
- [288] A. Ekstedt et al. In: (Nov. 2024). arXiv: 2411.04970 [hep-ph].
- [289] T. Brauner et al. In: *JHEP* 03 (2017), p. 007. DOI: 10.1007/JHEP03(2017)007. arXiv: 1609.06230 [hep-ph].
- [290] P. M. Schicho, T. V. I. Tenkanen, and J. Österman. In: *JHEP* 06 (2021), p. 130. DOI: 10.1007/JHEP06(2021)130. arXiv: 2102.11145 [hep-ph].